MODEL-BASED FEEDBACK CONTROL: EFFECT OF CONSTRAINTS ON CONTROLLER STRUCTURE IN THREE CASE STUDIES

A Dissertation

Presented to

the Faculty of the Department of Chemical and Biomolecular Engineering

University of Houston

In Partial Fulfillment

of the Requirements for the Degree

Doctor of Philosophy

In Chemical Engineering

by

Ajay Pratap Singh

May 2012

Dedicated

to

my parents for their love and support.

ACKNOWLEDGEMENTS

I would like to thanks my adviser Dr. Michael Nikolaou. It was his strong support and motivation which kept me always excited and enthusiastic toward my research work. Without his guidance and patience this work would not have been possible. His guidance has helped me to develop as an independent researcher, a better speaker and technical writer.

I would also like to thanks my thesis committee members, Dr D.J. Economou, Dr. Michael P. Harold, Dr. Karolos Grigoriadis and Dr. David H. Papell for their suggestions.

I would like to dedicate my dissertation to my parents and sisters; Seema Dee, Neeta Dee, Sangeeta Dee (*Mann*), Bhawna & Neelam (*Gudia, motu, gude singh*) and Rajesh *Jijaji*. I am blessed with their love, care and support which has always inspired me and kept me motivated towards my research work.

I have been very lucky to have wonderful friends around me during my PhD. Anupam (*Babban*), Kshitij (*Kmo*), Ashu (*Dad*), and Ashu (*Lala*) & Garima deserve my special thanks with whom I spent most of the time during my PhD period and without their presence life in Houston would not be that exciting, joyful and memorial.

I would like to mention my thanks to all of my friends: Sameer & Helly, Ashok & Kantaji, Saurabh, Divesh, Ratandeep, Avinash, Charu, Teja, Rahul jain / Kumar, Pranit, Pratik, Srimoyee, Aaditya, Pankaj Singh / Kumar, Robin, Illa, Manoj, Yogendra.

The financial support from Bayer foundation and Bayer Technology Services is gratefully acknowledged. I would like to express my gratitude to Rich Guhl, Stephen Hua, Pratik Misra and Samrat Mukherjee for their support and guidance during my internship work and PhD work as well.

MODEL-BASED FEEDBACK CONTROL: EFFECT OF CONSTRAINTS ON CONTROLLER STRUCTURE IN THREE CASE STUDIES

An Abstract

of a

Dissertation

Presented to

the Faculty of the Department of Chemical and Biomolecular Engineering

University of Houston

In Partial Fulfillment

of the Requirements for the Degree

Doctor of Philosophy

In Chemical Engineering

by

Ajay Pratap Singh

May 2012

ABSTRACT

In the first section, focus is an instance of the problem, in which the steady-state gain sign may change as a result of large unmeasured external disturbances entering a process with input multiplicities. The conventional approach to design a linear controller for a nonlinear system recommends that the controller must be tuned sluggishly. However, such a recommendation resulted in the instability of closed loop. To explain and anticipate closed-loop behavior a theoretical analysis based on nonlinear operator theory is used to provide controller design guidelines. Moreover, it has been demonstrated that linear control can be effective for a wide range of operating conditions, if designed correctly. Numerical simulations using a dynamic model calibrated on plant (industrial NOx reduction unit) data are used to illustrate the proposed controller design approach.

The second section proposes a novel, simple and effective scheme to debottleneck level control in a system of three tanks in series. Level control often involves two conflicting issues, rejection of disturbance and the minimization of outlet flow variations. Normally, the level controller is intentionally designed to response sluggishly to reduce flow oscillations in downstream. However, constraints in level variations restrict sluggish tuning of level controller. The proposed scheme translates system of tanks in seris; from multiple, single input single output into a single system of multiple inputs multiple outputs. Feedback controls based on a linear PI controller, are used and generalized tuning charts are prepared. Further, the performance of the proposed control structure is compared to the control structures derived from numerical optimization.

In the last section, the model predictive control concept has been proposed to design an optimal central bank interest rate. The optimization problem which relies on dynamic programming technique can only produce numbers but cannot provide interest rate rules. A multiparametric model predictive control framework is employed to derive rules for central bank interest rates bounded by zero. It has been found that rules are actually piecewise linear, finite in number and follow the celebrated *Taylor-rule* forms (Taylor 1993). Rules with or without inertia are included in the derivation. The proposed approach is illustrated through simulations on US economy data.

TABLE OF CONTENTS

LIST OF FIGURES

LIST OF TABLES

CHAPTER 1

INTRODUCTION

Automatic system control is considered to be one of the most successful milestones for the engineering community in the last few decades. Whether it is a chemical plant, an aerospace industry, an automobile or oil-gas industry; control theory has played a significant role in achieving strict quality control, environmental and safety regulations and over all better economics of processes. Over time control theory has become mature enough entailing conventional fixed linear and nonlinear control, adaptive control and advanced control schemes such as model predictive control (MPC). Increase in the computational power computer aided process control has become a practical and useful tool to design the control structure and perform rigorous analysis for large scale industrial processes. This research work focuses on model-based feedback control structure design in the presence of implicit or explict process constraints. In general processes are subject to various constraints due to limitations on output process variables to achieve desired performance and physical limitations on input variables. Controller structure design is get affected by these process constraints. This dissertation presents three case studies from real life problems and demonstrates how computer aided process control can be used in synthesis of control structure which helps to achieve the desired control objective. In particular this research work focuses on:

1. Control of a process with unmeasured disturbances that change its steady-state gain sign,
2. Debottlenecking level control for tanks in series,

3. Design of optimal rules for central bank interest rate subject to zero lower bound.

The following sections present a brief overview and literature review for each of these problems.

1.1 Control of a process with unmeasured disturbances that change its steady-state gain sign

Control design has been well studied in literature for nonlinear systems within chemical engineering and other disciplines. Obvious reason is that nearly all processes involve systems which are inherently nonlinear in nature. The design of a controller for nonlinear system has always raised a basic question; whether to use a linear controller or a nonlinear controller. Both have their own advantages and disadvantages. Linear control is simple in design and requires low implementation and maintenance costs. Many times the linear feedback controller works very well for nonlinear processes, especially in the cases when closed loop operates very near to the steady state or disturbances are not large in magnitude. Several industrial applications of linear controllers have been implemented for various nonlinear processes (Nikolaou 1997; Qin and Badgwell 2000). However, linear control has limited application due to the assumption of closed-loop process being linear for all operating conditions. Hence nonlinear control becomes necessary for processes where linearity of closed loop is no longer valid. Such processes are also quite common (Sistu and Bequette 1995; Chidambaram and Reddy 1996; Qin and Badgwell 2000; Golbert and Lewin 2004).

One example of nonlinear system is a process which is subject to reversal of steady-state gain sign (SSGS). In this work focus is an industrial situation (Singh and Nikolaou 2009), where the SSGS of a controlled process may change as a result of a large unmeasured input disturbance. Such instances of SSGS reversal have also been reported (Karra and Karim 2010). These situations are results of input-multiplicity (same output for different inputs) exhibited by this system. Systems displaying such behavior have been studied extensively (see, for example, (Razon and Schmitz 1987; Pearson 2003) and references therein). Control of systems involving input-multiplicities can raise stability issues or push the system to less desirable operating conditions (Koppel 1982; Dash and Koppel 1989). A number of studies have focused on eliminating input-multiplicity (Balakotaiah and Luss 1985; Ma, Valdes-Gonzalez et al. 2010), to remedy possible control problems. However, this option is not available when the underlying process dynamics inherently entail input multiplicity, hence SSGS reversal. As a solution to this problem nonlinear model predictive control has also been proposed (Sistu and Bequette 1995), while nonlinear PI controller is designed by (Chidambaram and Reddy 1996). Before, one decides to go for the development of nonlinear controller for any nonlinear process; one must carefully examine the possibility of linear control and its advantage over nonlinear control. The basic question that one can ask,

> *"What are the limits of disturbances or operating range for which simple linear control delivers satisfactory results for given nonlinear process?"*

This question is not new to control design and to answer this; various conventional and unique approaches have been adopted in literature in recent years. These approaches have developed various nonlinearity measurement methods to capture the inherent nonlinearity of a process in a single parameter for its use in control design. (Desoer and Wang 1980) has defined nonlinearity of process as a difference of open loop nonlinear and linear process, but they were not concerned for nonlinearity calculation rather than its definition. (Nikolaou 1993; Allgöwer 1996; Helbig, Marquardt et al. 2000) proposed nonlinearity measurement calculation for open-loop over different operating ranges. The basic idea behind all of these approaches is that if a nonlinear open loop system is not far away from a linearized system, than the probability of corresponding closed loop being stable is quite high and vice-versa. However, an open loop nonlinearity measurement cannot guarantee closed-loop stability in general.

The researchers, (Eker and Nikolaou 2000; Nikolaou and Misra 2003) have proposed a general theoretical framework to quantify nonlinearity of closed loop and anticipate closed-loop behavior. The calculation for the bounds of closed-loop nonlinearity is presented in terms of open loop process nonlinearity and the IMC (Vidyasagar 1985) based feedback controller. However, in their work process model was assumed to have an output disturbance model which basically cannot account for the input disturbances. Due to this limitation of the model their technique is only applicable to capture robustness issue fairly well. The closed-loop behavior for processes having SSGS reversal which is due to an input disturbance cannot be explained. The present research work extends their approach for analyzing closed-loop stability with input disturbance model. A theoretical analysis based on nonlinear operator theory is used to provide controller design guidelines and hence generalizing the stability theorem developed in (Eker and Nikolaou 2000; Nikolaou and Misra 2003).

The operator based analysis resulted in stability criterion which is a variant of small gain theorem (Desoer and Vidyasagar 1975) but is more meaningful in context to industrial applications. To explain the closed-loop behavior on the basis of stability theorem, computer-aided calculations are performed based on a plant model calibrated for an actual industrial process. The analysis provides the basis for controller design and finally control scheme was implemented in the plant (Bayer 2008).

1.2 Debottlenecking level control for tanks in series

Bottlenecking is a practical and serious issue in industries having continuous processes. As the throughput of the process increases over time to meet increased production rates, the same process may not be able to deliver desired performance. Many times it is possible to debottleneck the system by changing some of the process operating conditions or by simple modifications in the existing process. However, if a process requires significant changes with capital investment one must carefully explore if there exists any alternatives to debottleneck the system. In this work the focus is on debottlenecking of the level control problem for an industrial process (details are in chapter 3) which entails liquid-liquid extraction in three tanks in series (Figure 1.1)

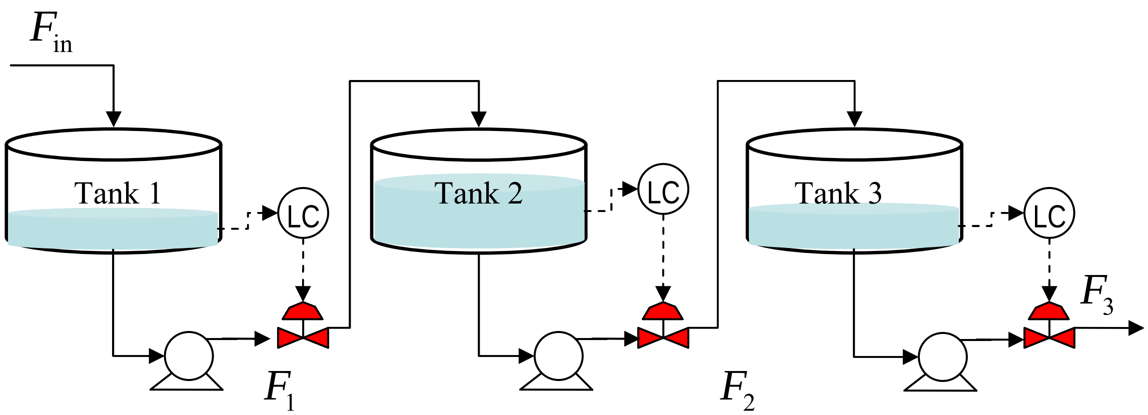

Figure 1.1. Level control of three tanks in series with conventional feedback control scheme.

Liquid level control of a tank system shown in Figure 1.1 has two competing control objectives to achieve. A) Minimize the change in the outlet flow rate F_3 in comparison to change in the inlet flow rate F_{in}, i.e., disturbance attenuation is required, and B) keeping the liquid levels in each tank much closer to the desired setpoint along with avoiding the violation of the minimum and maximum level constraints, i.e., tight level control is required. The first objective is important as it helps to filter the flow disturbances and disturbance attenuation will avoid upsetting the downstream process. The second objective is important to avoid overflow in a tank or in maintaining residence time constant in liquid-liquid extraction system (Singh and Nikolaou 2011). The aim is to design PI controllers to achieve the desired performance for step disturbances of known magnitude and sinusoidal disturbances of known amplitude and frequency content in the inlet flow rate F_{in}.

If tank does not have a large capacity as compared to the magnitude of flow disturbance present in F_{in}, both of these objectives will conflict with each other. One such scenario is shown in Figure 1.2 and Figure 1.3 for three tanks in series as shown in Figure 1.1 where three PI level controllers manipulate outlet flow rate of each tank for tight level control ($\pm 5\%$). It is clear that level fluctuations increase from tank 1 to 3, as do fluctuations in F_3 compared to F_{in}. Such a performance is not desirable as the closed-loop system is magnifying the magnitude of disturbance present in F_{in} and eventually results in downstream process experiencing a disturbance large in magnitude. Extensive trail-error method does not produce any tuning setting for PI controller which can produce desired performance (i.e., flow rate attenuations). This raises the question:

> *"Is there an alternative configuration of the three PI controllers that would provide satisfactory or better performance with appropriate tuning that would be relatively easy to determine?"*

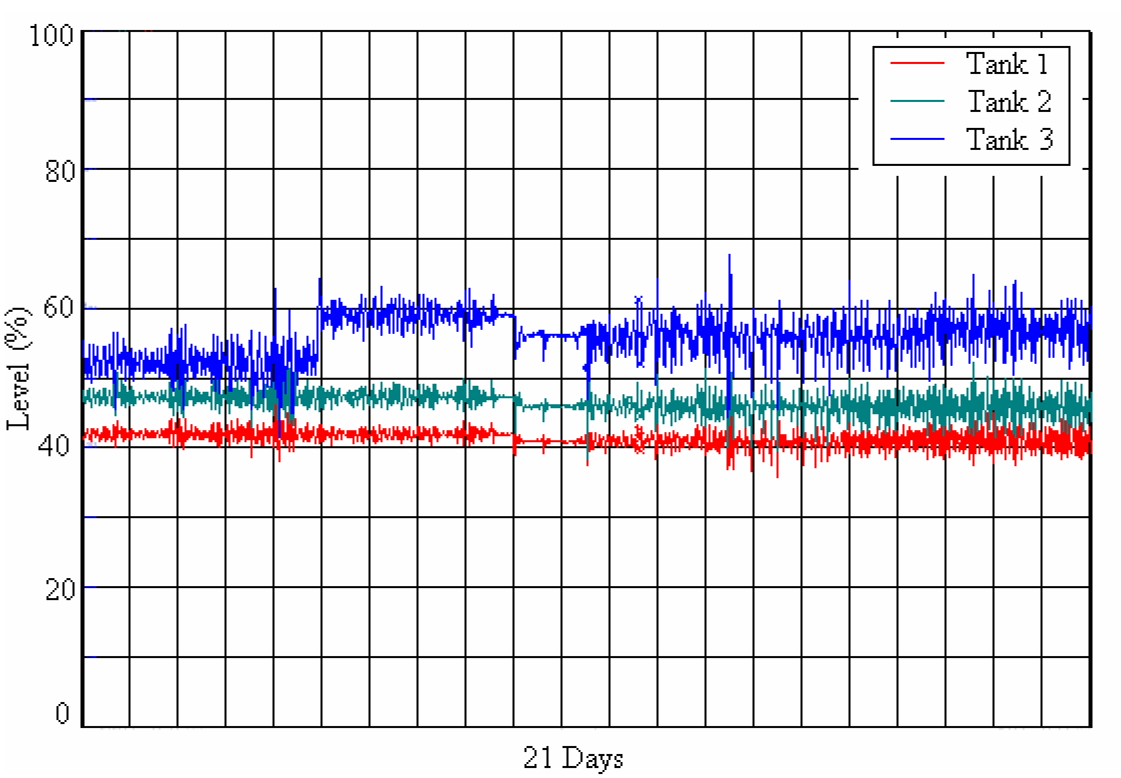

Figure 1.2. Level fluctuations (actual plant data).

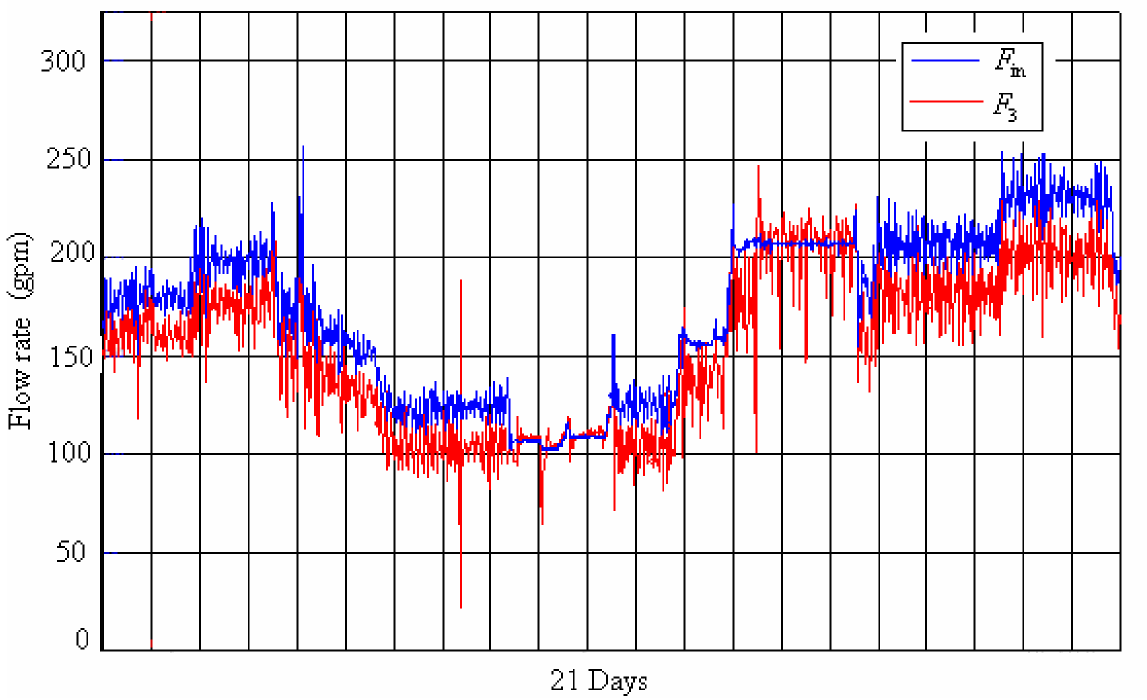

Figure 1.3. Flow rate variations for inlet F_{in} and outlet flow rate F_3 (actual plant data).

The answer to this question has not been well addressed. There are various control schemes in literature for the level control of a single tank but few have addressed liquid level control for tanks in series. The conventional approach proposes a design of feedback level controller for each tank by manipulating outlet flow rates of the corresponding tank. Feedback level controller is designed by specifying the maximum peak height in tank level and maximum rate of change in outlet for maximum inlet step disturbance (McDonald, McAvoy et al. 1986). The feedback control law can be designed by linear PI (Cheung and Luyben 1979) or nonlinear PI (Cheung and Luyben 1980) which provides fast action for large errors and slow action for small errors. (Rivera, Morari et al. 1986) have developed a P-only controller using internal model control (IMC) theory. (Shin, Lee et al. 2008) have proposed analytic design of an optimal PI controller. (Sbarbaro and Ortega 2007) have developed control design based on the mass balance approach. These controller designs are proposed for a single tank and similar design approach is adopted to tune all downstream tanks in series by mainly focusing on tight level control. To achieve flow rate attenuation, level controllers are intentionally detuned (McDonald, McAvoy et al. 1986).

Level control tuning can have various control issues when several cascaded tanks are considered as suggested by (Cheung and Luyben 1979) (especially in the case of nonlinear control or complex control laws). The problem becomes more complicated with the sinusoidal disturbance (as shown in Figure 1.2 and Figure 1.3). Another approach is to use a variant of linear feedback (discussed in chapter 3) and feedforward control scheme as suggested by (Luyben and Buckley 1977; Cheung and Luyben 1979) . In the feedforward configuration level remains almost unchanged and by proper feedback control tuning outlet flow rate can be made smooth. However, the feedforward scheme proposed in (Cheung and Luyben 1979) requires an additional measurement of inlet flow rates $F_{in}, F_1, F_2,\ F_3$ and this information may not be available always (Bayer 2008). Hence, for practical purposes it will be useful to improve the level control of tanks in series without using feedforward information.

In this work a design of feedback based control structure with tight level control is presented to gain maximum flow attenuation for sinusoidal disturbances and smooth change in flow rate for step disturbance. Model predictive control (MPC) scheme is a good candidate to design such controllers as it can handle constraints explicitly while achieving desired control objectives (Muske and Rawlings 1993; Edward P. Gatzke 2000). However, based on cost consideration this option was not explored in this study.

To debottleneck level control problem discussed above, a novel control scheme is proposed which entails multivariate control design. Control problem is solved for a system having three levels as control variable and three flow rates as manipulative variables. Simple generalized tuning rules for control synthesis are presented based on desired performance subjected to process constraints and disturbances. Finally, new control scheme was implemented in the plant (Bayer 2008).

1.3 Optimal rules for central bank interest rate subject to zero lower bound

The current US economics condition is the motivation for application of the control theory in economics. In recent years the US economy has suffered one of the largest recessions as shown in Figure 1.4. After the third quarter of year 2008 output gap (difference between real gross domestic product (GDP) to its potential GDP) has become highly negative and the central bank has pushed interest rate (federal fund rates at which banks and other depository institutions lend money to each other, usually on an overnight basis) to zero. This is the first time the US economy has got stuck to zero lower bound. The realization of zero lower bound (ZLB) was earlier considered as an academic or hypothetical case. However, now it has become a reality. Japan has been suffering from zero bound on interest rate from the last decade which has slowed down the economic growth of Japan (Figure 1.5). During the last recession, ZLB has constrained the ability of central banks to lower the interest rates below zero in many countries including the US and Japan. Interest rate is a primary channel to stabilize the economy and hence once it is constrained by the ZLB it impairs the monetary policy to stabilize output gap and inflation rate (Fuhrer and Madigan 1997; Reifschneider and Williams 2000; Williams 2009). Japan's economic data (Figure 1.5) reveals that the ZLB slows down the recovery of a weak economy. Now since the US economy is also facing similar weak economic conditions, the question arises how to modify interest rate rules to counter the effect of ZLB.

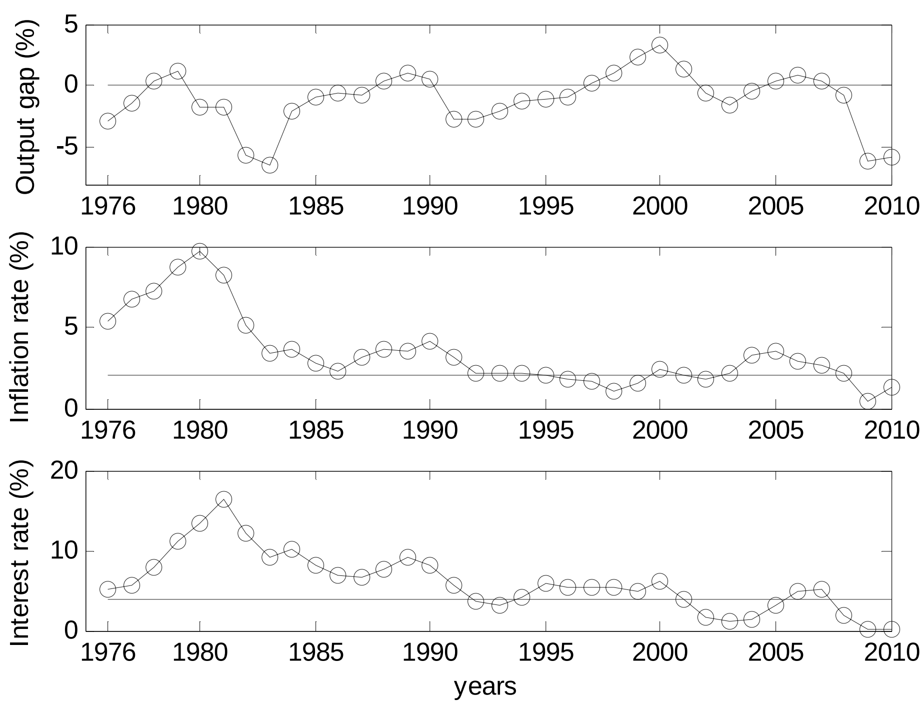

Figure 1.4. Revised data for US output gap, GDP deflator inflation rate and federal fund rates in annual percentage for year 1976-2010 (CBO 2011). Solid lines corresponds to equilibrium values for $y^* = 0, \pi^* = 2, i^* = 4$.

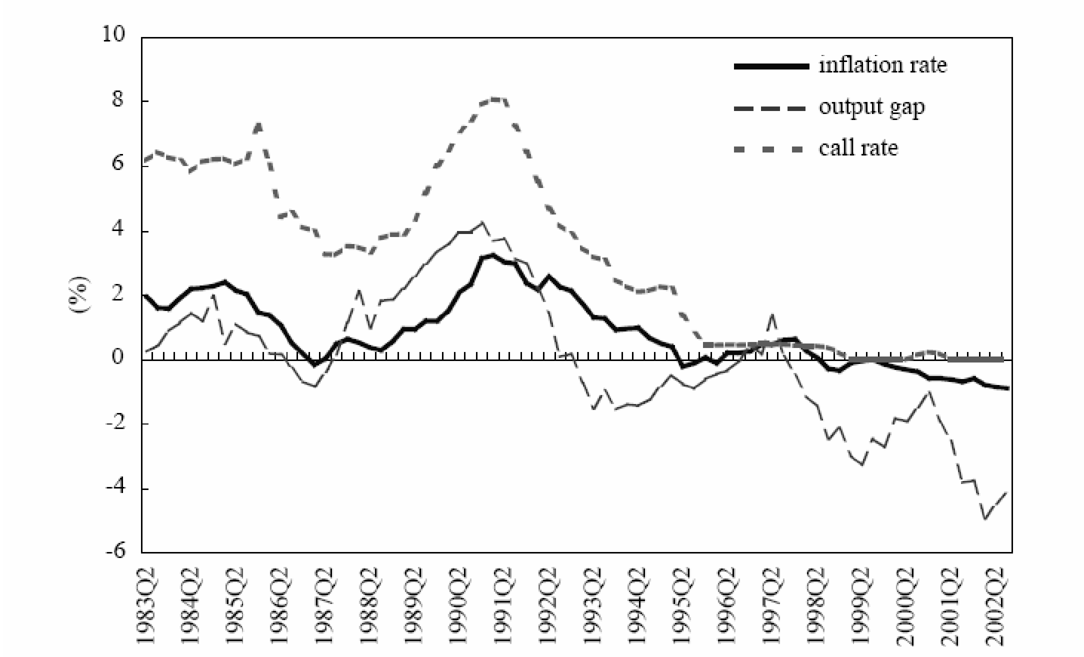

Figure 1.5. Inflation rate, output gap, and call rate (interest rate) for 1983:Q2–2002:Q3. Source (Kato and Nishiyama 2005).

1.3.1 Economy model

In a simple form economy is described by a linear relationship between GDP,inflation rate and interest rate (Ball 1999). A dynamic IS (Investment-saving relationship) or aggregate-spending equation:

$$y_{t+1} = \rho y_t - \xi\left(i_t - \pi_t\right) + e^{y}_{t+1}, \tag{1.1}$$

and an accelerationist Phillips curve:

$$\pi_{t+1} = \pi_t + \alpha y_t + e^{\pi}_{t+1}. \tag{1.2}$$

where output gap y at time t is defined as

$$y_{\mathrm{t}} = \left(\frac{\text{Real GDP}\big|_t - \text{Potential GDP}\big|_t}{\text{Potential GDP}\big|_t} \right) \times 100, \tag{1.3}$$

potential GDP refers to the highest level of real GDP that can be sustained over the long term and π represents inflation rate. There are two notions to measure inflation, 1) GDP deflator and 2) price index (consumer price index). In this context GDP deflator is used to measure the average inflation in time period t and $t-1$ and given by

$$\pi_{\mathrm{t}}=\left(\frac{\text{GDP Deflator}\big|_{t-1}-\text{GDP Deflator}\big|_{t}}{\text{GDP Deflator}\big|_{t}}\right)\times 100\,. \tag{1.4}$$

In eqns.(1.1) and (1.2), α and ξ are positive constants; $\rho\in[0,1)$; e_{t+1}^{y} and e_{t+1}^{π} are zero-mean white noise signals; and the sampling period (time interval from t to $t+1$) is one year. The shock e_{t+1}^{y} captures other influences on spending, such as consumer confidence and fiscal policy while the shock e_{t+1}^{π} is an inflation or 'supply'shock, arising for example from large changes in commodity prices.

1.3.2 Central bank interest rate rules

The best-known example of a proposed rule for setting the interest rates is proposed by John Taylor (Taylor 1993), both as a rough approximation of the way that interest rate rule had actually been implemented by the US Federal Reserve under Alan Greenspan's chairmanship, and as an optimal policy rule (on the basis of stochastic simulations using a number of economic models). According to the *Taylor rule*, interest rate i_t at time t is set as a linear function of measures of the current inflation rate and the current output gap and it is given by,

$$i_t=0.5(y_t-0)+1.5(\pi_t-2)+4\,. \tag{1.5}$$

Figure 1.6 represents closed-loop structure of economy with generalized Taylor rule for interest rate settings. Output gap and inflation rate are controller variable and interest rate is manipulating variable. The constants in Taylor's numerical specification indicate an implicit inflation target of 2% per annum and an estimate of the long-run real interest rate of 2% per annum as well, so that long-run average interest rate of 4%. In control settings setpoints are $y^* = 0$ and $\pi^* = 2\%$ for output gap and inflation rate respectively, while equilibrium interest rate is 4%. Clearly the Taylor rule in eqn. (1.5) belongs to P-controller.

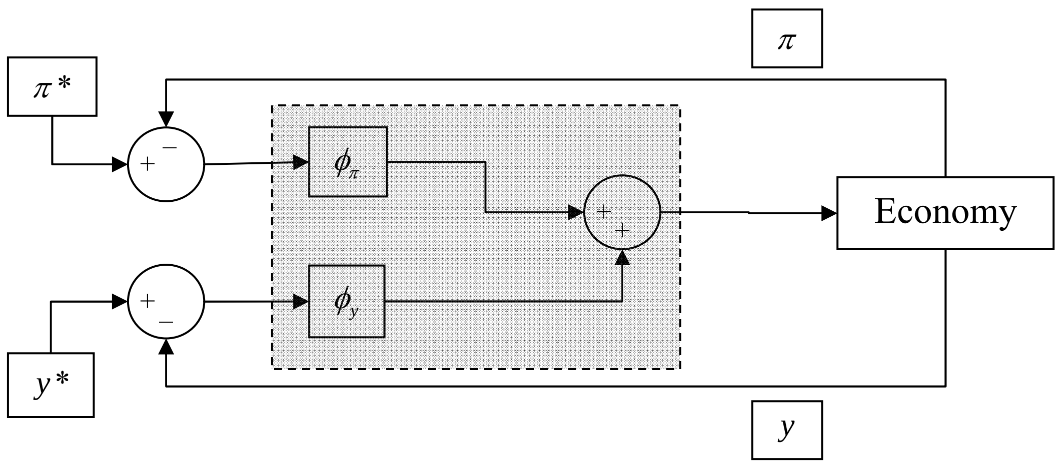

Figure 1.6. Closed-loop representation of economy with generalized Taylor rule. The shaded square represents feedback controller. In case of Taylor rule ϕ_π, ϕ_y are constant, 0.5 and 1.5 respectively.

The Taylor rule got much attention because it is a simple rule that prescribes how central bank should adjust its interest rate. Taylor has pointed that the central bank should raise its interest rate *more than one-for-one* with increase in inflation (i.e. $\phi_\pi > 1$). Later on this principle is known as the *Taylor principle* (Woodford 2001; Davig and Leeper 2007). After this celebrated rule, various versions of the Taylor rules have been proposed. Variants of the above basic Taylor rule have been studied in literature, such as rules with an inertia term containing i_{t-1} and/or with projected future values of π and y

in the right-hand side of eqn. (1.5) (Taylor and Williams 2010, and references therein). The stated objective for inertia-based policies is interest rate smoothing, to avoid large variations in interest rates and to produce robust policy rules (Goodfriend 1991; Woodford 1999; Orphanides and Williams 2007). Additional variants of the Taylor rule containing more lagged terms of i have also appeared (Judd and Rudebusch 1998; Clarida, Gali et al. 2000).

While the initial inspiration for the Taylor rule was based on fitting actual historical data, Taylor rules and some of its variants can be derived by the application of the optimization theory on a quadratic objective function, using a small-scale model of the economy to capture the effect of interest rate on inflation and output gap (Ball 1999; Orphanides and Wieland 2000; Giannoni and Woodford 2002; Orphanides 2003). Such derivations have mainly focused on the effect of the form of the quadratic objective function (terms included and values of weighting factors) on the resulting rule. This approach, however, has not been successful at producing a rigorous derivation of explicit Taylor rules when a zero lower bound (ZLB) on the interest rate is included in the optimization. Nevertheless, a number of approaches for determining an optimal interest rate subject to ZLB have been proposed, which can be broadly classified into two categories:

The first category includes explicit rules that rely on truncation to zero of an interest rate i_t^{TR} calculated by a Taylor rule (i.e., $i_t = \max[0, i_t^{\mathrm{TR}}]$), to ensure that a non-negative interest rate i_t is produced (Reifschneider and Williams 2000). Another commonly addressed rule is augmented Taylor rule (Reifschneider and Williams 2000) which suggests settings for interest rate:

$$
\begin{aligned}
i_t &= \max[0, i_t^{TR} - \alpha Z_t] \\
Z_t &= Z_{t-1} + \left(i_t - i_t^{TR}\right)
\end{aligned}, \tag{1.6}
$$

where $\alpha \in (0,1]$. There are several kinds of truncation rules proposed in literature and many of them can be found in (Williams 2006; Nakov 2008). The rationale behind approaches in this category relies on qualitative analysis of a ZLB-constrained quadratic optimization problem or on other qualitative analysis of optimal policy effects on inflation and output gap.

The second category does not produce explicit rules; rather, it employs numerical simulation, i.e., repeated numerical solution of a ZLB-constrained optimization problem, to determine the optimal values of interest rate for inflation and output gap values in a range of interest (Orphanides and Wieland 2000; Hunt and Laxton 2003; Jung, Teranishi et al. 2005; Kato and Nishiyama 2005; Adam and Billi 2007). Most studies in this category rely on a constrained dynamic programming formulation of the underlying optimization problem, whose explicit solution is hard to get. These simulation studies have revealed interesting facts that policies may become nonlinear and aggressive when interest rate approaches to ZLB.

The focus of this research work is a systemic derivation of optimal interest rate rules with ZLB constraint. The main issue addressed here is the effect of ZLB on the optimal interest rate determined by a central bank. The concept of multiparametric (mp) (Pistikopoulos, Dua et al. 2000) model predictive control (MPC) (Rawlings and Mayne 2009) is introduced to solve constrained optimization problem. Multiparametric model predictive control (mpMPC) framework allows the derivation of explicit feedback rules even when inequality constraints are present. Application of this framework to a simple model of the US economy produced a number of Taylor-like rules, depending on the form and parameter values in the objective function employed by MPC.

1.4 Objective of the research

In summary the present research work has three objectives:

a) Determination of general closed-loop stability condition using IMC based linear control for nonlinear process with input disturbance model,

b) Design of multivariate level control to debottleneck three tanks in series,

c) Determination of central bank optimal interest rate with zero lower bound using mpMPC framework.

The rest of this dissertation is organized as follows. In chapter 2 the design of a linear controller for a nonlinear industrial process is discussed. Chapter 3 entails the use of multivariate control to achieve desired control objectives while overcoming the bottlenecking issue in an industrial process. Chapter 4 extends the idea of MPC in economics and presents discussion on determination of the central bank's optimal interest rate to stabilize the US economy in presence of the ZLB. Chapter 5 has conclusions and suggestion for future work.

CHAPTER 2

CONTROL OF A PROCESS WITH UNMEASURED DISTURBANCES THAT CHANGE ITS STEADY-STATE GAIN SIGN

2.1 Introduction and motivation

The steady-state gain sign (SSGS) of a process under feedback control plays an important role for closed-loop robustness. For example, it is well known (Morari and Zafiriou 1989) that no controller with integral action can be designed that maintains robust closed-loop stability if the steady-state gain of a controlled process can take any value in a range exceeding $\pm 100\%$ of its nominal value, i.e., if the SSGS is not certain. The focus of this article is an industrial situation where the SSGS of a controlled process may change as a result of a large unmeasured disturbance. Such instances of SSGS reversal have also been reported elsewhere in literature (Karra and Karim 2010). The process under consideration here is a reactor in a NOx emissions treatment unit (Bayer 2008). The reactor reduces NOx by using CO generated from fuel-rich combustion of a mixture that contains natural gas (methane) as the primary fuel as well as hydrogen coming in significant amounts from upstream units (Figure 2.1).

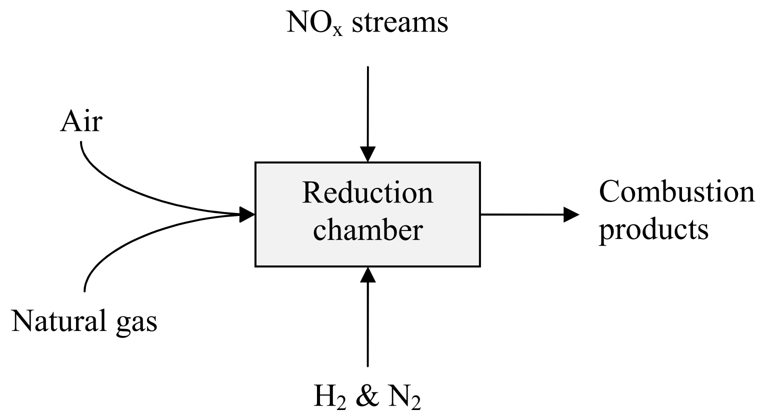

Figure 2.1. Schematic of NOx reduction process.

The amount of hydrogen fed to the reactor is an unmeasured disturbance, i.e., it may fluctuate significantly (e.g. it may experience large and sudden drops) and the fluctuations are not measured in real time, because of cost and instrument maintenance issues. To ensure proper operation (i.e., maintenance of the NOx reducing environment) of this reactor, its temperature is controlled by manipulating the flow rate of inlet air (denoted here as the corresponding amount of oxygen in the air). At normal operating conditions the combustion in the reactor is deliberately designed to be fuel-rich (the air-to-fuel ratio (AFR) is small) and hence the steady-state gain between inlet air (oxygen) flow rate and reactor temperature is positive, i.e., increasing air flow by a slight amount eventually causes temperature to increase. However, as already mentioned, the hydrogen flow rate may decrease considerably without warning, and, as a result, the AFR may increase to the point that the SSGS may be reversed. This is indicated by the simulation results shown in Figure 2.2 and Figure 2.3, as described in more detail in section 2.2.

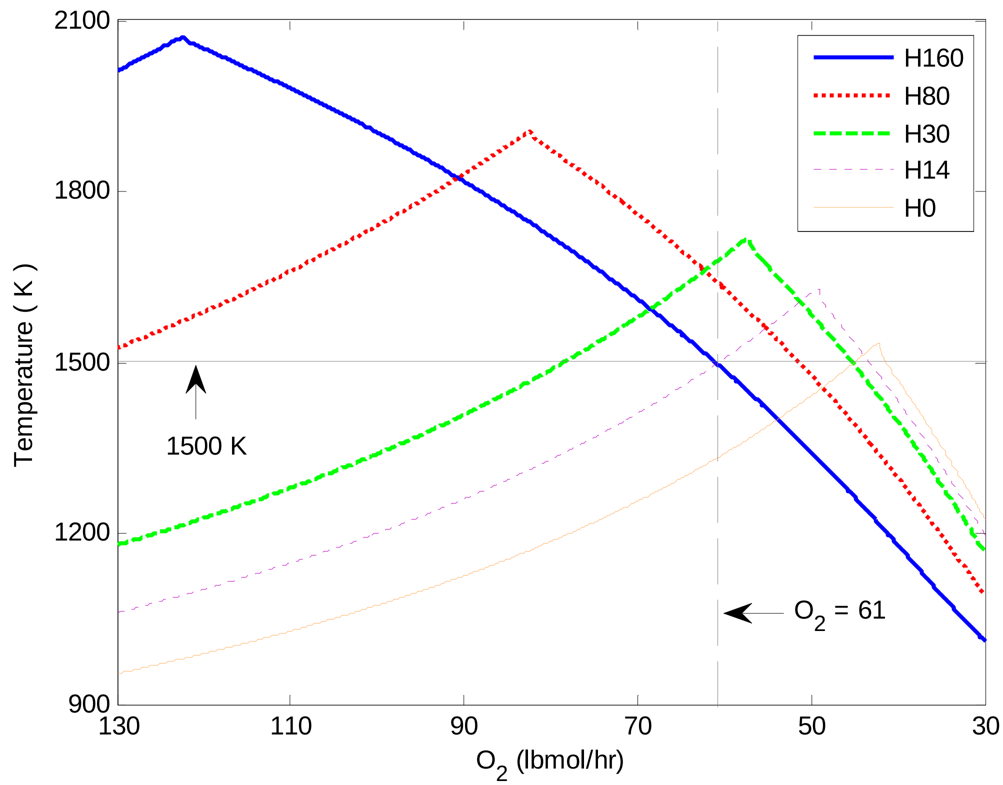

Figure 2.2. Steady–state temperature as a function of O_2 flow rate for different steady-state flow rates of H_2 below the normal operating value of 160 lbmol/hr. The slope of the corresponding curve, i.e., the SSGS, is reversed around the temperature peak, but the reversal point depends on the steady-state value of H_2 flow rate (Hx denotes hydrogen flow rate of x lbmol/hr).

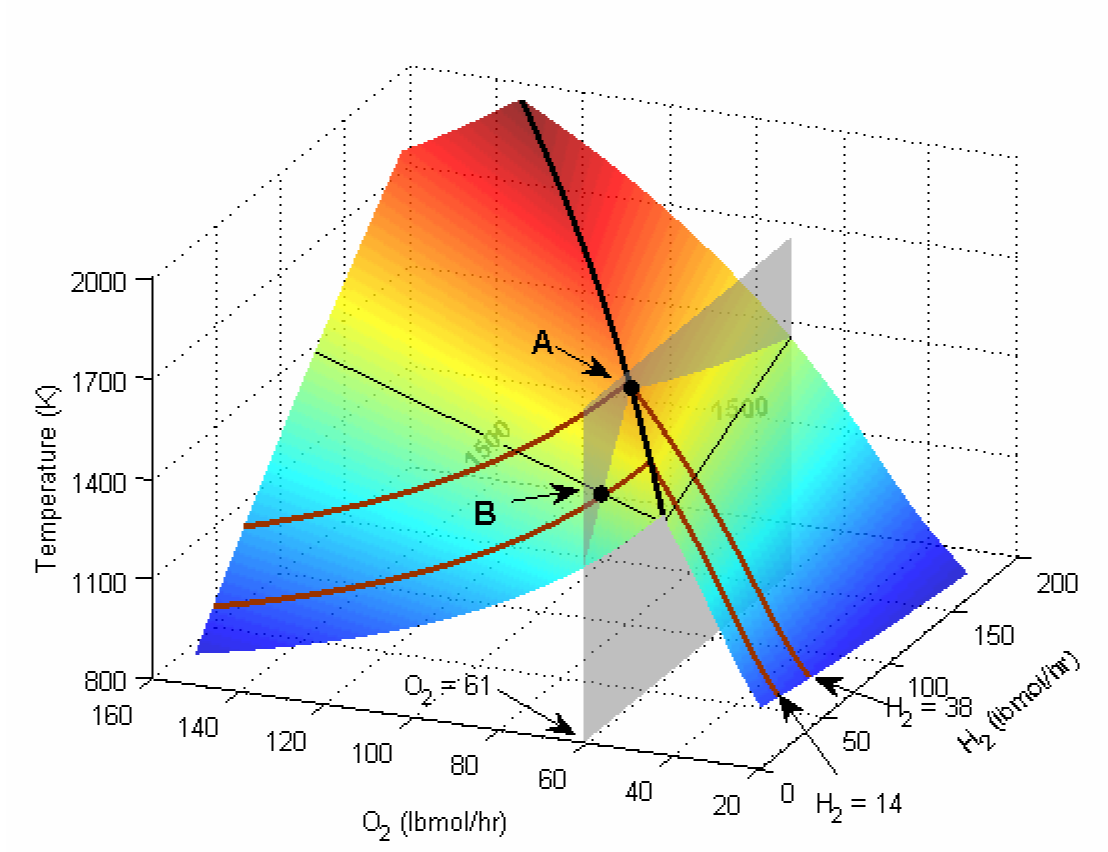

Figure 2.3. 3-D counterpart of Figure 2.2, showing the steady-state temperature of the CSTR for various combinations of the disturbance (H_2 flow rate) and manipulated input (O_2 flow rate).

The nonlinear nature of the process far from the normal operating point can be further visualized by observing the response of temperature to step changes of various magnitudes in either H_2 flow rate (Figure 2.4) or O_2 flow rate (Figure 2.5).

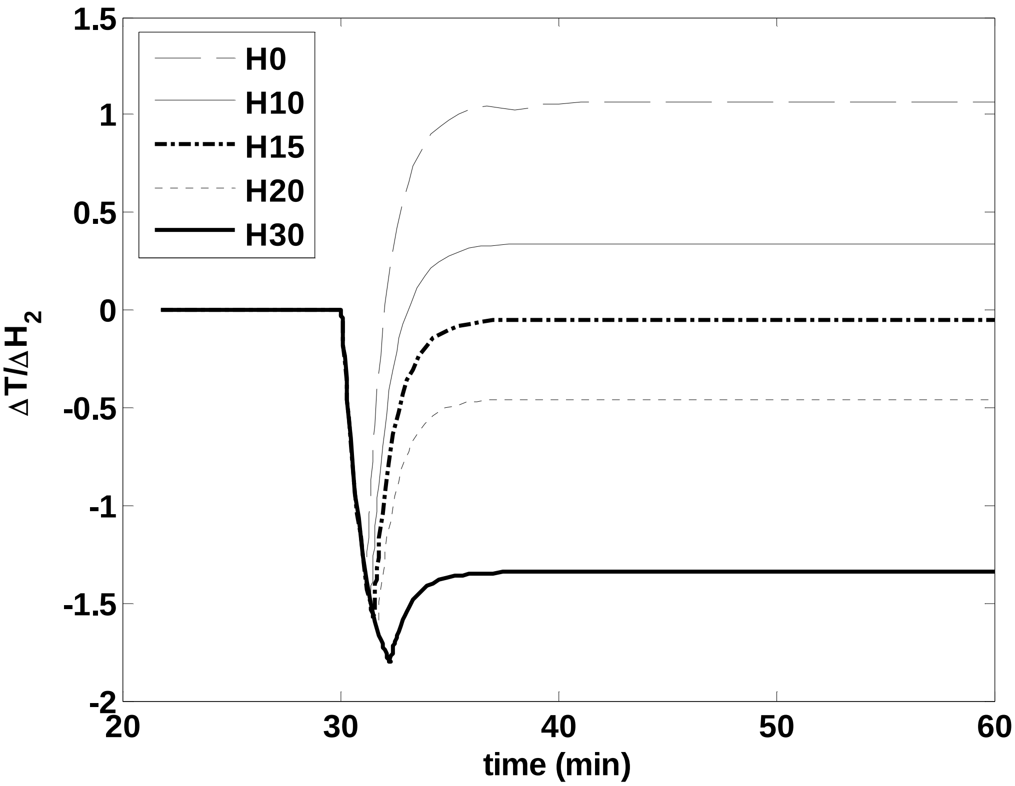

Figure 2.4. Temperature response to various step changes in H_2 flow rate below the normal operating value of 160 lbmol/hr at time 30 min (Hx denotes hydrogen flow rate of x lbmol/hr) for constant O_2=61 lbmol/hr. Δ stands for change from the initial steady state value.

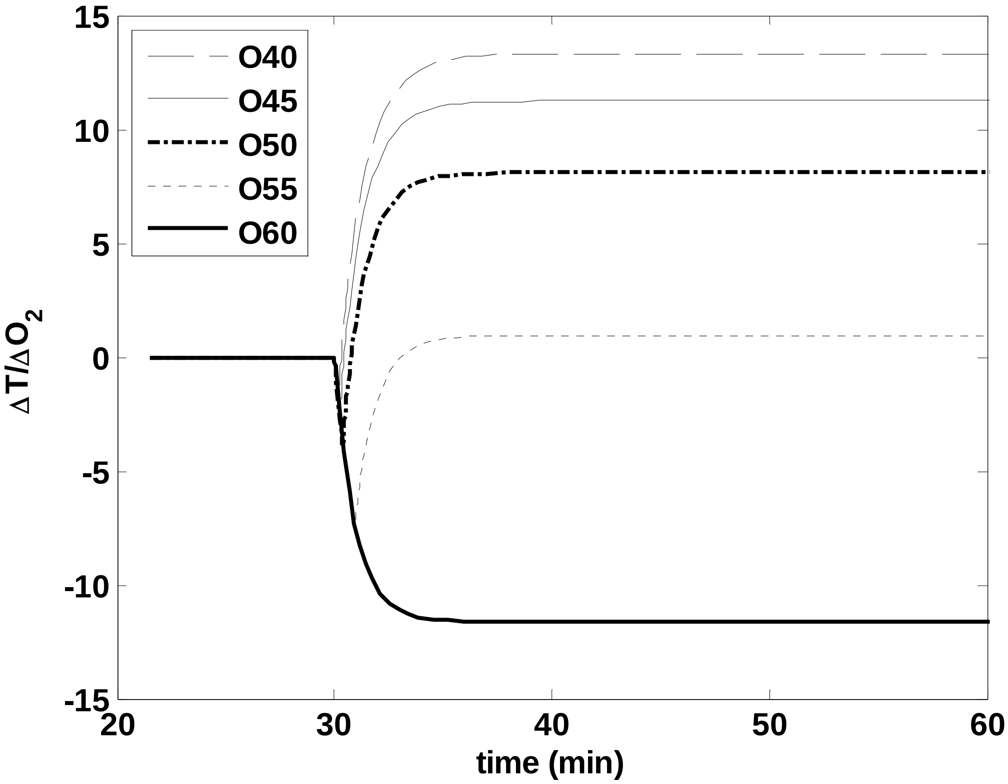

Figure 2.5. Temperature response to various step changes in O_2 flow rate (Ox denotes oxygen flow rate of x lbmol/hr) for constant H_2=30 lbmol/hr. Δ stands for change from the initial steady state value.

The manual feedback strategy, currently in use, can be summarized as follows: because at the normal operating point the AFR is low and consequently the SSGS is positive, the process operator controls temperature by increasing or decreasing the flow rate of the air, depending on whether the temperature is below or above its setpoint, respectively. If the temperature ever appears not to respond in the right direction, due to SSGS reversal because of large disturbances (large H_2 flow rate reduction), the operator reverses the feedback law (Bayer 2008). Clearly, operator experience on detecting the SSGS reversal is a key in this scheme for successful temperature control. However, this approach raises cost and performance concerns, because of potential inconsistencies from time to time and from operator to operator. To reliably replicate or improve the human operator strategy by an automatic controller, a number of questions must be answered, including the following:

- What are the limits of disturbances for which simple linear control delivers satisfactory results?
- Can better results be obtained by a control strategy that is not limited to simple linear control?

In this work we address mainly the first question and discuss the second one, with suggestions for further work. To motivate the approach, a series of closed-loop simulations are used to reveal interesting outcomes from various linear controllers and disturbance magnitudes for this process. The simulations involve a virtual process, calibrated on the real plant as outlined in section 2.2, and internal model control (IMC) feedback (Figure 2.6). The linear IMC is designed based on a linear model of the nonlinear process around the normal operating point (Table 2.1).

Table 2.1. Steady state values for process *N*

Variable	Steady-state value[1]
CH_4 flow rate	$N_{1,\text{inlet}} = 2.65$ mol/sec (21 lbmol/hr)
H_2 flow rate	$N_{2,\text{inlet}} = 20.2$ mol/sec (160 lbmol/hr)
O_2 flow rate	$N_{3,\text{inlet}} = 7.7$ mol/sec (61 lbmol/hr)
N_2 flow rate	$N_{7,\text{inlet}} = 51.0$ mol/sec (400 lbmol/hr)
Temperature	$T = 1500\,\text{K}$
Exit pressure	$P_{\text{exit}} = 90,000\,\text{Pa}$

[1]No product species is present in inlet flow.

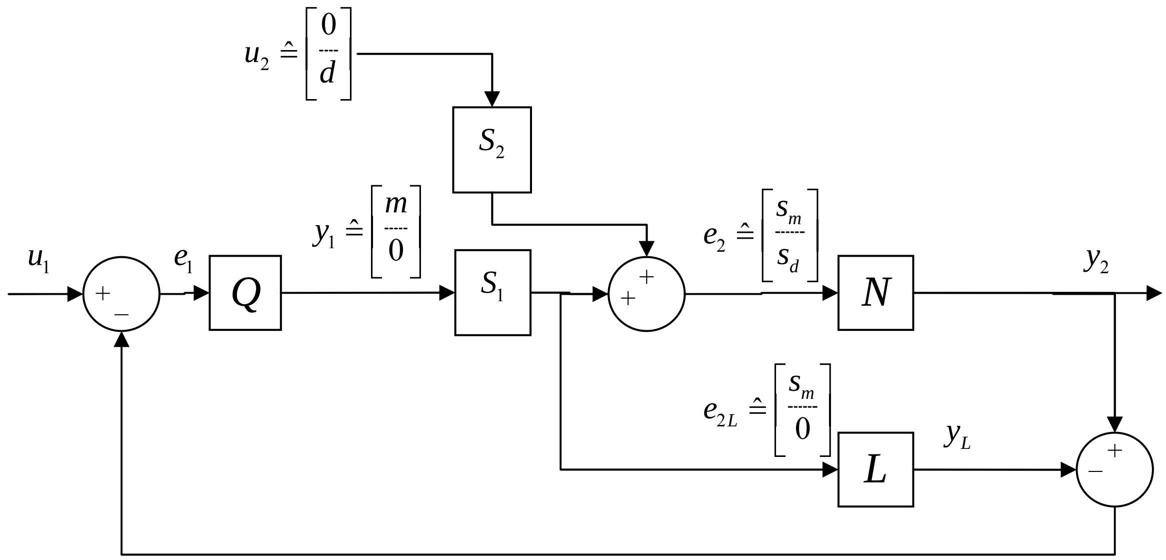

Figure 2.6. Closed-loop block diagram of IMC for the nonlinear process N. The saturation blocks S_1, S_2 place bounds on both manipulated inputs and input disturbances respectively (Morari and Zafiriou 1989). The block Q includes the IMC filter $F(s) = \frac{1}{\lambda s + 1}$ and the stable inverse of the linearized model L of N around the normal operating point.

The interesting result of these simulations is that a properly tuned IMC structure can deliver reasonable results over a wide operating range. However, tuning exhibits an interesting behavior, namely, closed-loop stability is achieved for tuning in a narrow range that is neither too aggressive nor too sluggish. While instability for overly aggressive tuning is expected and fairly well understood, instability due to sluggish tuning is entirely due to the nonlinear nature of the controlled process. Such behavior has been observed in other nonlinear systems as well (Stack and Doyle 1997; Eker and Nikolaou 2002).

In the remainder of the research work we provide a description of the process studied and the model developed for use as a virtual process. Next, we present computer simulations along with corroborating theory underlying the observed behavior. Finally, we identify opportunities for further development of alternative control strategies. Background material and details are provided in appendices.

2.2 Process description and control objective

The purpose of the reactor model is to serve as virtual process with enough qualitative accuracy, so that general trends from control action can be studied via computer simulation.

2.2.1 Dynamic model formulation

Combustion of natural gas or hydrogen has long been studied in literature, especially for internal combustion engines and industrial burners. A simplified low-dimension model for this process is developed below. The combustion process is modelled as a single continuous-flow stirred tank reactor (CSTR). All input streams are gaseous and reactions are in the gas phase. Hydrocarbon combustion chemistry entails thousands of free radical reactions (Tsang and Hampson 1986) involving many detailed kinetics mechanisms (Smith 1999; Konnov, Zhu et al. 2004), which complicate modelling. However, to predict temperature and some of the key component concentrations it is enough to rely on a set of just a few global reaction mechanisms (Jones and Lindstedt 1988; Kim 2008). We assume that combustion of hydrogen and methane follows the kinetics of such a set of four global reactions (Kim 2008):

$$CH_4 + 0.5O_2 \rightarrow CO + 2H_2, \tag{2.1}$$

$$CH_4 + H_2O \rightarrow CO + 3H_2, \tag{2.2}$$

$$CO + 0.5O_2 \rightarrow CO_2 , \tag{2.3}$$

$$H_2 + 0.5O_2 \rightarrow H_2O . \tag{2.4}$$

The rate expressions for these four reactions in a laboratory setting are given in Table 2.2. Assuming adiabatic conditions, ideal gases, constant heats of reaction (Table 2.3), and constant heat capacities (Table 2.4), standard mass and energy balances result in the following equations:

$$\frac{dc_k}{dt} = \frac{N_{k,\text{inlet}}}{V} - c_k \frac{F}{V} - \sum_{i=1}^{4} r_i \eta_{ki} , \quad k = 1,...,7 , \tag{2.5}$$

$$\frac{dT}{dt} = \frac{1}{\left(C_{P,\text{mix}} - c_{\text{mix}} R\right)} \left(\sum_{k=1}^{7} \left(\frac{C_{P,k} N_{k,\text{inlet}}}{V} \left(T_{\text{inlet}} - T\right) + RT \frac{dc_k}{dt} \right) + \sum_{i=1}^{4} r_i \Delta H_i \right), \tag{2.6}$$

$$P = c_{\text{mix}} RT , \tag{2.7}$$

where

$$F = K_v \sqrt{\frac{P - P_{\text{exit}}}{\rho_{\text{mix}}}} , \quad \rho_{\text{mix}} = \sum_{k=1}^{7} c_k M_k , \quad c_{\text{mix}} = \sum_{k=1}^{7} c_k , \quad C_{P,\text{mix}} = \sum_{k=1}^{7} C_{P,k} c_k , \tag{2.8}$$

$$r_i = K_i e^{-E_i/(RT)} \prod_{k=1}^{7} c_k^{\alpha_{ik}} . \tag{2.9}$$

Eqns. (2.5) through (2.6) are stiff. They are solved by the implicit method provided by Matlab®.

Table 2.2. Rate expressions for reactions (2.1)-(2.4)

Reaction	Rate Expression (mol/m^3-sec)	Rate constant
$r_1: CH_4 + 0.5O_2 \rightarrow CO + 2H_2$	$\frac{d[CH_4]}{dt} = -K_1[CH_4]^{0.5}[O_2]^{1.25}$	$K_1 = 2.47\times10^9 \exp(-15098/T)$
$r_2: CH_4 + H_2O \rightarrow CO + 3H_2$	$\frac{d[CH_4]}{dt} = -K_2[CH_4][H_2O]$	$K_2 = 3.1\times10^5 \exp(-15098/T)$
$r_3: CO + 0.5O_2 \rightarrow CO_2$	$\frac{d[CO]}{dt} = -K_3[CO][O_2]^{0.3}[H_2O]^{0.5}$	$K_3 = 9.95\times10^5 \exp(-8052/T)$
$r_4: H_2 + 0.5O_2 \rightarrow H_2O$	$\frac{d[H_2]}{dt} = -K_4[H_2][O_2]^{0.5}$	$K_4 = 2.5\times10^9 \exp(-17614/T)$

Table 2.3. Heat of reaction for reactions (2.1)-(2.4)

Reaction	r_1	r_2	r_3	r_4
Heat of Reaction[2] (ΔH) at 1500K [KJ/mol]	$\Delta H_1 = 43$	$\Delta H_2 = -226$	$\Delta H_3 = 280$	$\Delta H_4 = 249$

[2]Heat of reactions are positive for exotheric rections

Table 2.4. Molar mass and molar heat capacity of chemical species

Chemical species	CH_4	H_2	O_2	CO_2	CO	H_2O	N_2
Molar Mass [M] (kg/mol)	0.016	0.002	0.032	0.044	0.028	0.018	0.028
Molar Heat Capacity (C_P) at 1500K [J/mol-K]	86.9	32.3	36.5	58.0	34.9	47.0	34.67

2.2.2 Dynamic model calibration and linear model identification

The model described by the above eqns. (2.5)-(2.9) was calibrated using plant tests. The tests involved multiple step changes made successively on the air (O_2) flow rate and recording of the resulting temperature response. The collected data, shown in Figure 2.7.

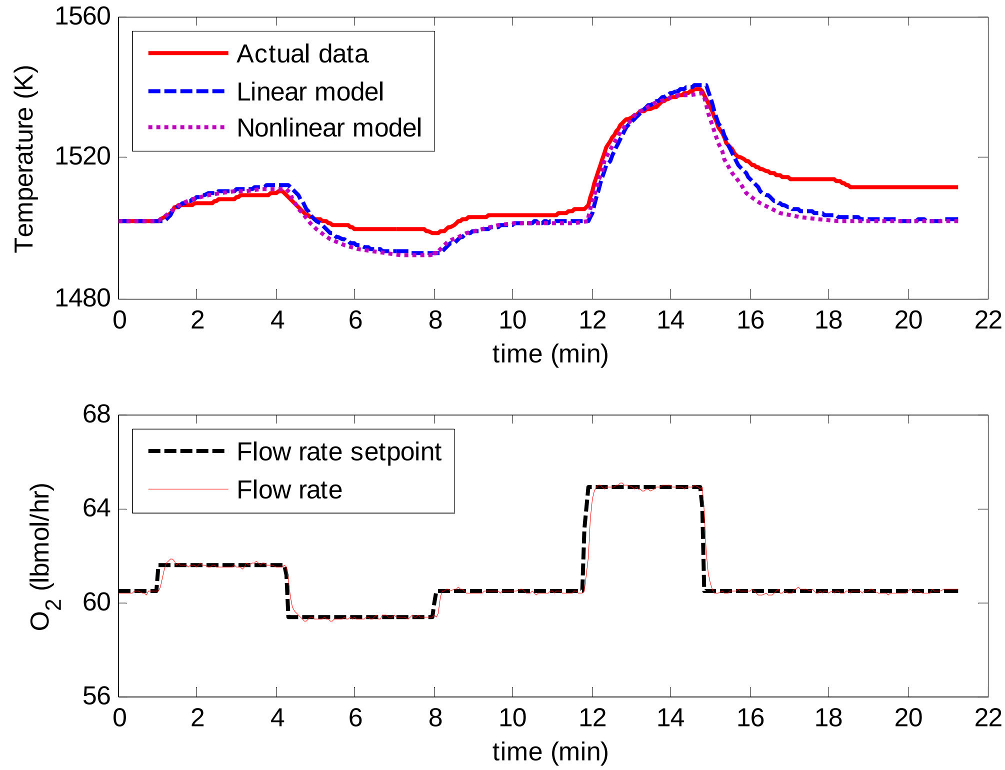

Figure 2.7. Plant tests for calibration of the dynamic model in eqns. (2.5)-(2.9) and of a linear first-order model $\frac{K}{\tau s+1}$. While some nonlinearity is evident in the response, it does not appear to be excessive.

The plant in Figure 2.7 were used in two ways.

- The apparent residence time in the nonlinear model was adjusted (by adjusting V), as shown in Table 2.5. All other parameters were kept at their literature values.

- A simple first-order model corresponding to the transfer functions

$$
\begin{aligned}
G_I(s) &= \frac{K}{\tau s+1} \\
G_L(s) &= \begin{bmatrix} \dfrac{K}{\tau s+1} & 0 \end{bmatrix},
\end{aligned}
\tag{2.10}
$$

was developed for use in IMC design. The resulting values for the gain, K, and time constant, τ, are shown in Table 2.5. It is fairly evident that the process behavior is fairly linear for the small range of inputs considered.

Table 2.5. Constants

Reactor Volume, V	475 m^3
Valve constant, K_V	0.06m^2
Gas constant, R	8.314 J/K-mol
Linear Process gain, K	$105\frac{\text{K}}{\text{mol/sec}}$
Linear Process time constant, τ	57 sec

2.2.3 Control objective and controllability

As pointed above, in order to reduce NOx from different waste streams feeding to the reactor, it is necessary to maintain temperature and operate under fuel-rich conditions. Indeed, low temperature would result in unburned fuel mixture as reaction rates would decrease, whereas at higher temperatures N_2 would be oxidized to NOx. The challenge is that the fuel is composed of both CH_4, which is manipulated, and H_2, which is a disturbance, and, as a result, H_2 also affects the concentration of CO, the NOx reducing agent. Because normal operating conditions are fuel-rich, decreasing the flow rate of H_2 to a small amount would increase temperature, hence the rate of reactions. Combustion would then be driven more towards completion, namely less CO would be produced, as shown in Figure 2.8, thus compromising NOx reduction. Consequently, for desired NOx reduction, temperature should be at a particular value (1500K in this case study) and the reactor should always be operated at reducing (i.e., fuel-rich) conditions.

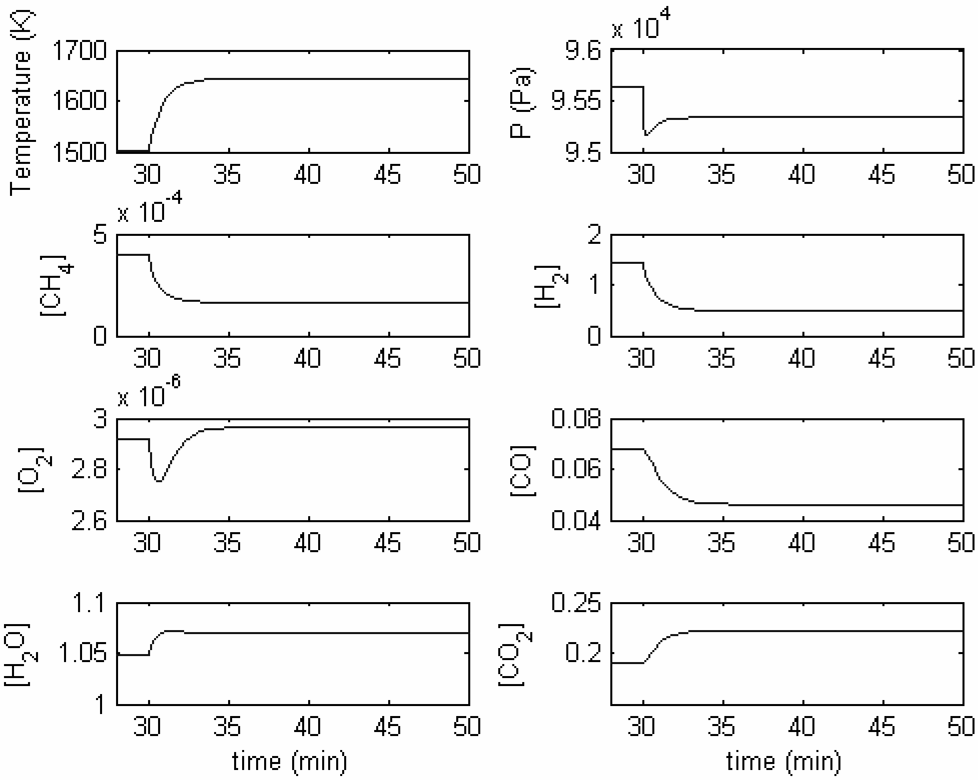

Figure 2.8. Open loop simulation for process N with decrease in H_2 flow by 50% (80 lbmol/hr) at time = 30 min. Species concentration denoted by [] are in mol/m^3.

Small to moderate perturbations in the flow rate of H_2 will not push the process towards fuel-lean conditions. Under these circumstances, fluctuations in temperature can be easily controlled by appropriate adjustment of air flow rate using a standard linear controller as discussed in section 2.4. However, due to changes in upstream processes, the H_2 flow rate may be reduced to very low values or even stopped. Such a disturbance is large in magnitude and usually remains constant for a long period compared to the reactor time constant. To understand the dynamics of such a scenario, corresponding simulations are shown in Figure 2.4 and Figure 2.5, which are in agreement with the steady-state behavior shown in Figure 2.2. These results also make clear the input-multiplicity (same output for different inputs) exhibited by this system.

2.2.4 IMC design

Figure 2.6 shows the IMC structure used for this system. Note that because of system nonlinearity, disturbances do not enter linearly as additive output disturbances, but as input disturbances, where the dimensions and structure of corresponding vectors and of the operators N (nonlinear plant), L (linear plant model), and Q (Youla-Kučera parameter of IMC (Vidyasagar 1985) have been adjusted accordingly for compatibility, as follows.

$$\begin{aligned} N:\ & e_2 \triangleq \begin{bmatrix} s_m \\ \hdashline s_d \end{bmatrix} \mapsto y_2 \\ L:\ & e_{2L} \triangleq \begin{bmatrix} s_m \\ \hdashline 0 \end{bmatrix} \mapsto y_L\ , \\ Q:\ & e_1 \mapsto y_1 \triangleq \begin{bmatrix} m \\ \hdashline 0 \end{bmatrix} \end{aligned} \tag{2.11}$$

where the vectors d, m, and y, represent the disturbance, manipulated input, and controlled output, respectively. The operators

$$S_1:\ \begin{bmatrix} m \\ \hdashline 0 \end{bmatrix} \mapsto \begin{bmatrix} s_m \\ \hdashline 0 \end{bmatrix}, \tag{2.12}$$

$$S_2:\ \mathrm{u}_2 \triangleq \begin{bmatrix} 0 \\ \hdashline d \end{bmatrix} \mapsto \begin{bmatrix} 0 \\ \hdashline s_d \end{bmatrix}, \tag{2.13}$$

denote diagonal saturation functions for the manipulated input (air or O_2 flow rate) and disturbance (H_2 flow rate) respectively. The values of saturation limits are shown in Table 2.6.

Table 2.6. Saturation limits

Process inputs	Upper limit	Lower limit
O_2 flow rate (lbmol/hr)	96	16
H_2 flow rate (lbmol/hr)	176	0

The idea behind the above representation is that disturbances do not enter the plant additively but nonlinearly, hence the composite vector e_2 in Figure 2.6, and that bounded values will be considered for both the manipulated input m, and for the disturbance d, hence the saturation blocks S_1, S_2.

The structure of the linear block Q, eqn. (2.11), is such that it generates signals only for the manipulated input vector m. That is, Q can be represented as

$$Q = \begin{bmatrix} q \\ \hdashline 0 \end{bmatrix} \Rightarrow y_1 = \begin{bmatrix} [qe_1] \\ \hdashline 0 \end{bmatrix}, \tag{2.14}$$

where q refers to the standard linear IMC parameter for stable square linear systems.

A brief background on corresponding operator theory and terms is provided in Appendix A. The linear model of eqn. (2.10) is used in IMC design, with $q = l^{-1}F$, where

$$G_F(s) = \frac{1}{\lambda s + 1}, \tag{2.15}$$

$$G_Q(s) = \begin{bmatrix} \dfrac{\tau s + 1}{K(\lambda s + 1)} \\ 0 \end{bmatrix}. \tag{2.16}$$

2.3 Simulation results

A number of simulations were conducted using the virtual plant described in sections 2.2.1 and 2.2.2 along with the controller designed in section 2.2.4. Two factors were varied in these simulations: The magnitude of the disturbance (H_2 flow rate) and controller tuning (value of IMC filter time constant λ, eqn. (2.15).

To make the simulations more realistic, measurement and actuator delays were accounted for in the simulations (but not explicitly used in controller design) by adding the transfer function

$$T_m(s) = \frac{e^{-6s}}{45s+1} T_a(s), \tag{2.17}$$

where T_m and T_a are measured and actual temperature of the reactor, respectively, and time constants are in seconds.

The results are summarized in Table 2.7, which indicates whether the observed closed-loop response was stable or unstable. Table 2.7 suggests that for overly aggressive control action, corresponding to very small values of λ, the closed loop is unstable, as can be observed in the simulations presented in Figure 2.9 through Figure 2.14. This kind of closed-loop behavior is well in line with what one would expect from feedback control of an open-loop stable process.

Table 2.7. Closed-loop simulation scenarios for steady deviations of H_2 flow rate from its steady-state value of 160 lbmol/hr and various values for the IMC tuning parameter λ

λ (sec)	H_2 (lbmol/hr)					
	176	80	30	10	5	0
5	Unstable	Unstable	Unstable	Unstable	Unstable	Unstable
10	Stable	Stable	Stable	Stable	Unstable	Unstable
50	Stable	Stable	Stable	Stable	Stable	Stable
105	Stable	Stable	Stable	Stable	Stable	Unstable
180	Stable	Stable	Stable	Stable	Unstable	Unstable
500	Stable	Stable	Stable	Unstable	Unstable	Unstable

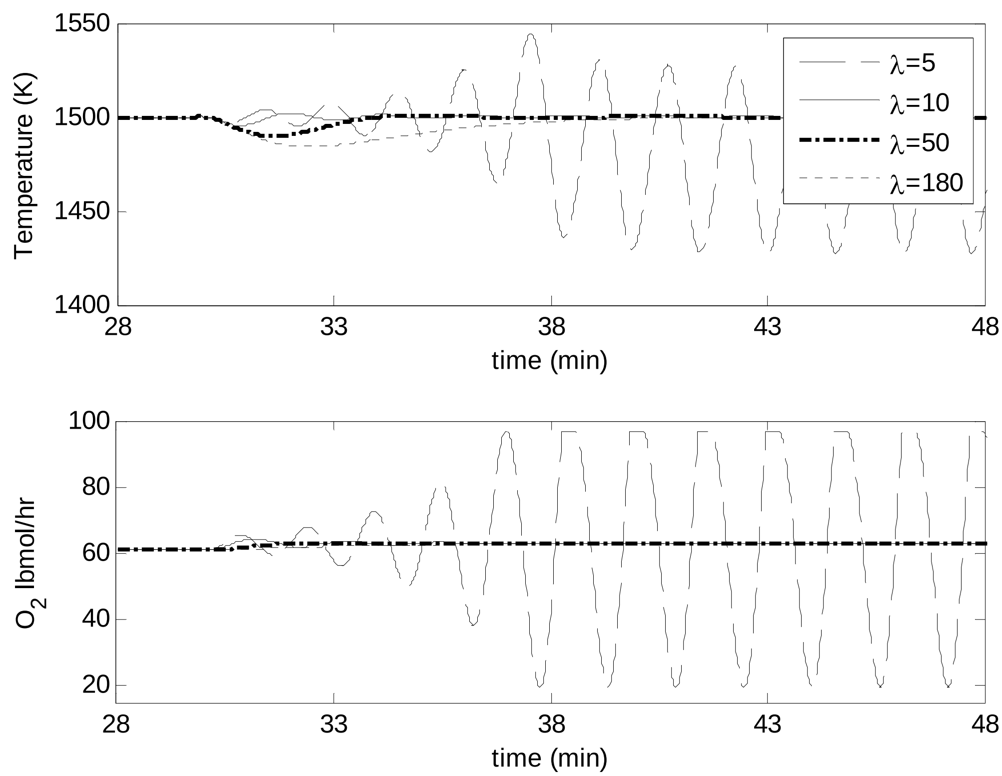

Figure 2.9. Closed loop responses when H_2 flow rate is increased to 176 lbmol/hr, namely +10% above its nominal value of 160 lbmol/hr at time 30 min. The IMC filter time constant takes values λ = 5, 10, 50, 180 sec.

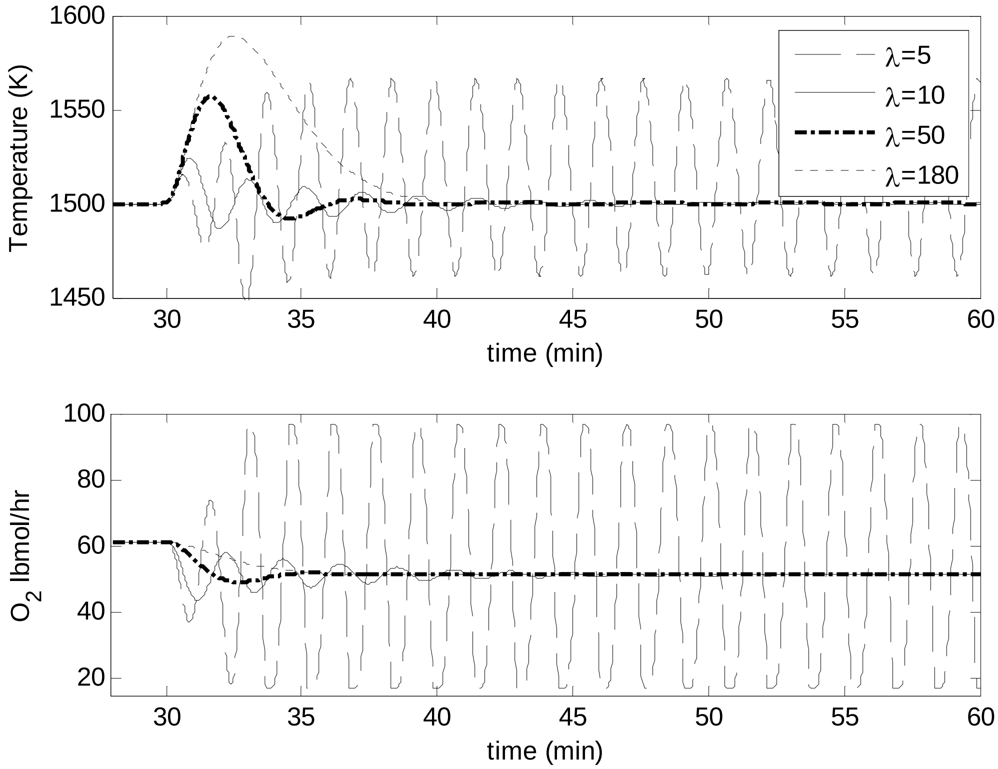

Figure 2.10. Closed loop responses when H_2 flow rate is reduced to 80 lbmol/hr, namely 50% of its nominal value of 160 lbmol/hr (d =-80 lbmol/hr) at time 30 min. The IMC filter time constant takes values λ = 5, 10, 50, 180 sec.

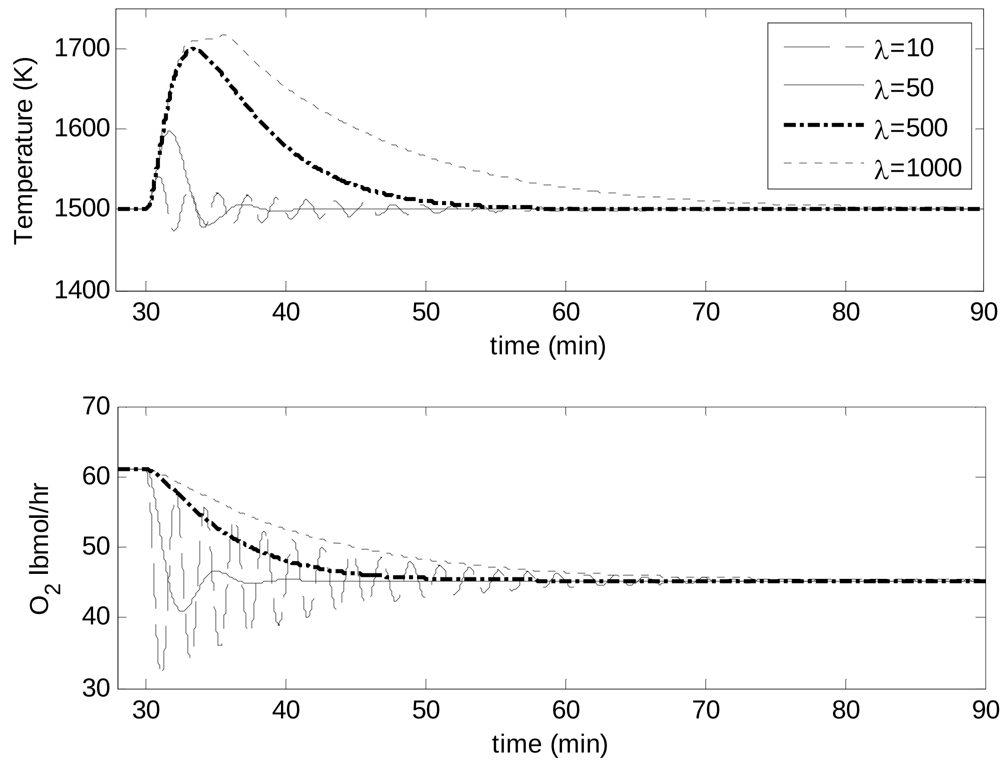

Figure 2.11. Closed loop responses when H_2 flow rate is reduced to 30 lbmol/hr, namely 81% of its nominal value of 160 lbmol/hr ($d =$-130 lbmol/hr) at time 30 min. The IMC filter time constant takes values λ = 10, 50,500, 1000 sec.

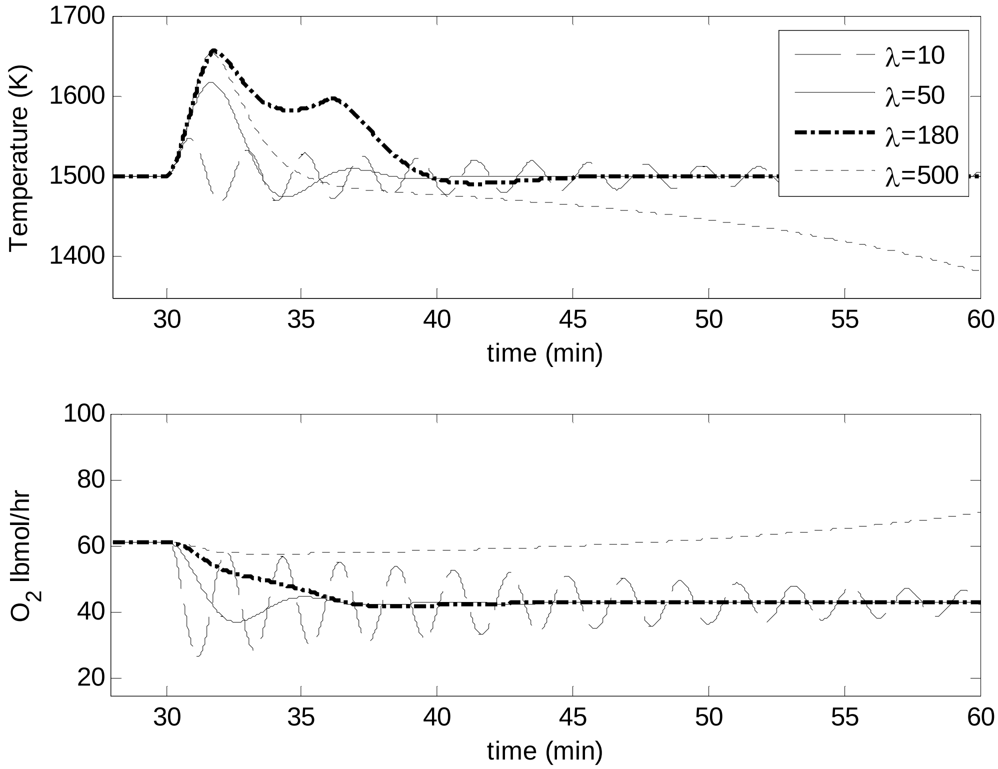

Figure 2.12. Closed loop temperature response when H_2 flow rate is reduced to 10 lbmol/hr (d =-150 lbmol/hr) from 160 lbmol/hr of its nominal value at time 30 min. The IMC filter time constant takes values λ = 10, 50, 180, 500 sec.

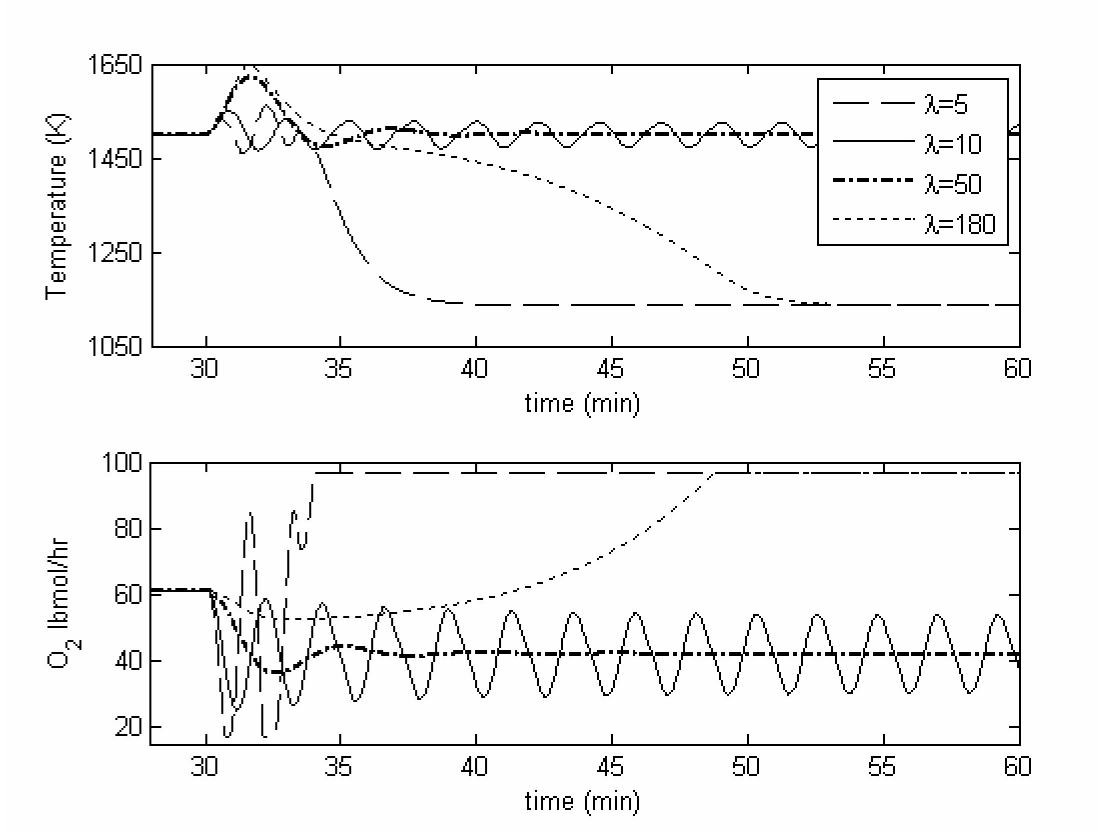

Figure 2.13. Closed loop temperature response when H_2 flow rate is reduced to 5 lbmol/hr from 160 lbmol/hr of its nominal value at time 30 min. The IMC filter time constant takes values $\lambda = 5, 10, 50, 180$ sec.

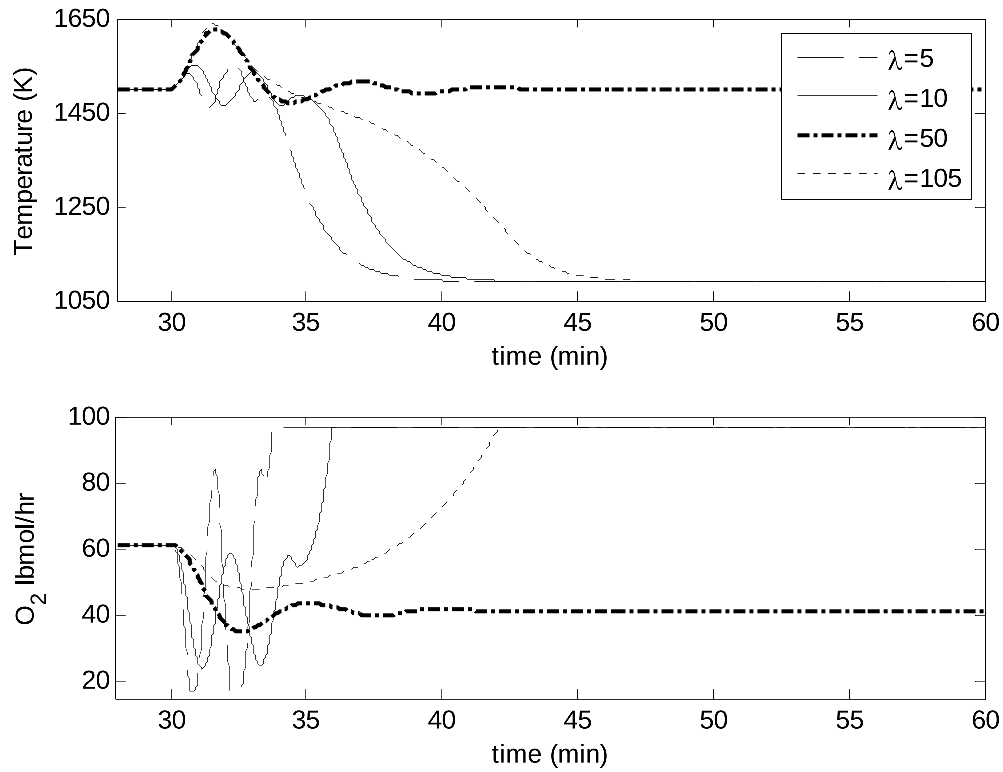

Figure 2.14. Closed-loop temperature response when H_2 flow rate is reduced to 0 lbmol/hr (d =-160 lbmol/hr) from 160 lbmol/hr of its nominal value at time 30 min. The IMC filter time constant takes values λ = 5, 10, 50, 105 sec.

More interesting is the behavior of the closed loop when control becomes very sluggish, for large values of λ, as can also be observed in the simulations presented in Figure 2.9 through Figure 2.14. While for small disturbances (values of H_2 flow rate near its steady-state value of 160 lbmol/hr) the closed loop becomes and remains stable as λ increases above a threshold, for larger disturbances (namely values of H_2 flow rate well below its steady-state value of 160 lbmol/hr, including zero flow rate) the closed loop becomes stable as λ increases above a threshold, but closed-loop stability is eventually lost as λ becomes very large. This behavior is clearly the result of process nonlinearity, and is analyzed in more detail in the next section. In the next section, we analyze the reasons underlying the observed behavior, in terms of a general framework that makes minimal assumptions about the nonlinear system at hand.

2.4 Analysis of simulation results

The observed closed-loop behavior for different combinations of (a) values of λ and (b) disturbance magnitudes is analyzed in terms of two approaches: An input-output approach that relies on a variant of the small-gain theorem over sets (Nikolaou and Manousiouthakis 1989), and a heuristic approach that capitalized on the particulars of the system at hand, as captured by the steady-state surface shown in Figure 2.2.

2.4.1 Input-output analysis of nonlinearity effect

Based on the preceding formulation of the feedback loop, the following variant of the small-gain theorem provides a sufficient condition for closed-loop stability. The value of the theorem is that it places a bound on an expression that entails the nonlinearity of the controlled process, $N-L$, and the controller design parameter Q. The idea is based on a basic result by Desoer and Liu (Desoer and Liu 1982) that has found a number of applications in literature (e.g. in (Eker and Nikolaou 2002)).

Theorem 1 – Small-gain theorem

If (a) the linear operators L, Q are stable; (b) the nonlinear operator N is incrementally stable over the set U corresponding to the saturation blocks S_1, S_2, i.e.

$$\|N\|_{\Delta U} < \infty , \tag{2.18}$$

with $U \hat{=} \{u \mid u = S_1 \begin{bmatrix} m \\ \hline 0 \end{bmatrix} + S_2 \begin{bmatrix} 0 \\ \hline d \end{bmatrix}\}$; and (c) the nonlinear operator $(N-L)S_1Q$ is stable with

$$\gamma \hat{=} \|(N-L)S_1Q\| < 1 , \tag{2.19}$$

then the closed-loop system shown in Figure 2.6 is finite-gain stable, i.e., there exist positive constants k_1, k_2, k_3, k_4 such that

$$\|e_1\| \le k_1 \|u_1\| + k_2 \|u_2\| , \tag{2.20}$$

and

$$\|e_2\| \le k_3 \|u_1\| + k_4 \|u_2\| . \tag{2.21}$$

Proof: See Appendix B.

The following remarks are in order:

- Theorem 1 is a general closed-loop stability theorem for any stable process, based on the IMC structure shown in Figure 2.6. Without loss of generality, the disturbance and manipulated input signals are combined in such a way that both of these signals can enter the process nonlinearly.

- Theorem 1 relies on the operator $\left(N-L\right)S_1Q$ having a small gain (namely operator norm less than one).
- It should be noted that the above version of the small-gain theorem is more useful than the classical version $\|NC\|\|F\|<1$, which involves a standard feedback loop with operators N,C (plant and controller, respectively) in the forward path and F in the feedback path (Khalil 2002). The reason is that the classical version is too conservative and will not include controllers with integral action, as $\|NC\|=\infty$ for such controllers.
- As is the case for the classical small-gain theorem, eqn. (2.19) is a sufficient but not necessary condition for closed-loop stability.
- The saturation blocks S_1,S_2 place natural bounds on manipulated inputs and disturbances.
- Theorem 1 does not require linearity of L, Q, or N. Similarly, the introduction of nonlinearity by the saturation blocks S_1,S_2 is not restrictive.
- For a stable process, eqn. (2.18) is trivially satisfied. Therefore, it is eqn. (2.19) which is essential for closed-loop stability.
- $\left\|\left(N-L\right)S_1Q\right\|$ is cumbersome to compute, an upper bound can be computed via approximation of $\left\|\left(N-L\right)S_1Q\right\|_\Delta$ using a linearization of the operator $(N-L)S_1Q$ around various steady states, following a procedure developed in (Nikolaou and Manousiouthakis 1989).
- Theorem 1 provides a useful assessment of how the magnitude of external disturbances affects closed-loop stability when linear control is used. Depending

on the saturation blocks S_1, S_2, i.e., the bounds on m, d (Figure 2.6), bounds on the signal y_1 can be established for a bounded-input-bounded-output stable closed loop. If S_1, S_2 are such that the resulting y_1 never reaches the saturation bounds in the block S_1, S_2, then that block can be removed, and the feedback controller is a standard linear IMC controller. The general finite-gain stability of the resulting closed loop can then be assessed based on whether

$$\left\|(N-L)Q\right\|_E < 1, \tag{2.22}$$

where the set E in the preceding inequality is defined as $E \triangleq \{e_1 \mid e_{1,\min} \le e_1 \le e_{1,\max}\}$ and its function is to ensure that the inequalities in eqn. (2.22) and (2.19) are compatible. Clearly, given a model L, the value of $\left\|(N-L)Q\right\|_E$ or $\left\|(N-L)Q\right\|_{\Delta E}$ depends on the set E, which in turn depends on (a) the bounds of the external disturbances and (b) the tuning of Q, i.e., the value of the time constant λ of the IMC filter, eqn. (2.16). Consequently, to assess the closed-loop stability resulting from a particular design (i.e.,choice of Q given L), one can use the following procedure.

a. For a choice of Q (value of the IMC filter tuning parameter λ) and E (bounds on e_1) evaluate $\left\|(N-L)Q\right\|_{\Delta E}$ using the procedure developed in (Nikolaou and Manousiouthakis 1989).

b. If $\left\|(N-L)Q\right\|_{\Delta E} < 1$, check whether the resulting closed loop produces signals e_1 within the set E for disturbances bounded by the saturation block S_2 (Figure 2.6).

c. If so, retain the above Q, as stabilizing. Otherwise discard it.

d. Repeat steps (a) through (c).

The results of $\left\|(N-L)Q\right\|_{\Delta E}$ computation are shown in Table 2.8, where the shaded areas correspond to $\left\|(N-L)Q\right\|_{\Delta E} > 1$. Table 2.9 shows the corresponding size of the set E over which the value of $\left\|(N-L)Q\right\|_{\Delta E}$ is calculated numerically as described above.

Table 2.8. Computation of $\left\|(N-L)Q\right\|_{\Delta E}$.

λ (sec)	H_2 (lbmol/hr)					
	176	80	30	10	5	0
5	1.09	1.12	1.15	1.90	1.95	1.95
10	0.91	0.95	0.97	0.99	1.02	1.94
50	0.48	0.55	0.61	0.64	0.68	0.89
105	0.29	0.36	0.45	0.50	0.60	1.94
180	0.21	0.25	0.28	0.37	1.91	1.92
500	0.09	0.11	0.15	1.75	1.75	1.75

Table 2.9. Computation of the bounds $e_{1,\min}$, $e_{1,\max}$ in the set
$E \triangleq \{e_1 \mid e_{1,\min} \le e_1(t) \le e_{1,\max}\}$

λ (sec)	H_2 flow rate (lbmol/hr)					
	176	80	30	10	5	0
5	-118, 179	-250, 54	-332, 0	-356, 790	-344, 836	-350, 883
10	0, 28	-148, 0	-253, 0	-301, 0	-318, 0	-329, 883
50	0, 29	-151, 0	-258, 0	-305, 0	-317, 0	-330, 0
105	0, 28	-152, 0	-263, 0	-319, 0	-313, 0	-215, 883
180	0, 27	-151, 0	-261, 0	-299, 0	-190, 836	-174, 883
500	0, 26	-148, 0	-263, 0	-170, 790	-159, 836	-150, 883

Comparison between Table 2.7 and Table 2.8 suggests that the values of the disturbance (H_2 flow rate) and λ for which the observed closed-loop response is stable correspond exactly to values of $\left\|\left(N-L\right)Q\right\|_{\Delta E}$ less than 1. This suggests that eqn. (2.19) is not conservative in this case. For H_2 flow rate = 176, 80 or 30 lbmol/hr (corresponding to changes of +10%, -50%, and -81% of the steady-state value of 160 lbmol/hr, respectively) the closed-loop is stable for large values of λ. However, for H_2 flow rate = 10, 5 or 0 lbmol/hr the closed-loop is not stable for large enough λ (Figure 2.12- Figure 2.14). It is clear that for $\lambda = 50$ the closed loop is stable for any step disturbances in the range considered. As expected, in all cases of an unstable closed loop, the size of set E is larger than in cases corresponding to stable closed loop.

2.4.2 Time-domain nonlinearity analysis

To understand the behavior of the closed loop when feedback control turns from aggressive to sluggish (λ increases) it is useful to point out the following features in the steady-state surface shown in Figure 2.3.

a. For each value of H_2 flow rate, there are clearly two values of O_2 flow rate that result in the same steady-state temperature (input multiplicity).
b. Constant-temperature lines at 1500K confirm that there are two values possible for O_2 flow rate that result in the same temperature, of which only one is acceptable, as discussed in the section 2.2.3.
c. The vertical plane going through O_2 = 61 lbmol/hr makes it clear that if the H_2 flow rate is reduced up to a value of 38 lbmol/hr and no feedback action is taken, then the corresponding steady-state temperature will reach higher values. The SSGS will remain positive for all of these steady states. Further reduction of the H_2 flow rate will result in steady-state temperature values lower than the peak

reached at H_2 = 38 lbmol/hr. The corresponding SSGS will now be negative. Figure 2.2 represents this observation as well.

d. The vertical plane going through H_2 = 14 lbmol/hr suggests that for values of the H_2 flow rate higher than that, the two resulting steady-state values of the O_2 flow rate are to the left and to the right of the nominal steady-state value of O_2 = 61 lbmol/hr. However, for values of the H_2 flow rate below 14 lbmol/hr, *both* of the two resulting steady-state values of the O_2 flow rate are *lower* than the nominal steady-state value of O_2 = 61 lbmol/hr. Figure 2.2 represents this observation as well.

The following connections can be made between the above observations and closed-loop stability.

- For step disturbances corresponding to H_2 flow rate reduction from 160 to 38 lbmol/hr, the SSGS remains positive, so instability due to SSGS reversal is not an issue. Whatever instability is observed is simply due to overly aggressive control action, well in line with expectations based on linear control theory. If the controller is made sluggish enough (λ made large enough), stability is maintained, as shown in Table 2.8.
- For step disturbances corresponding to H_2 flow rate reduction below 38 lbmol/hr but above 14 lbmol/hr, the SSGS turns negative, so instability due to SSGS reversal might be expected to be an issue. However, this issue is avoided in closed-loop operation, because the corresponding O_2 flow rate is monotonically (however slowly) reduced towards a new steady-state value *below* rather than above 61 lbmol/hr, as suggested by the above feature (c) and (d). Closed-loop

simulations in Figure 2.11 confirm this. Again, whatever instability is observed is simply due to overly aggressive control action (λ too small), as shown in Table 2.8.

- For steps disturbances corresponding to H_2 flow rate reduction below 14 lbmol/hr down to 0, the SSGS is again negative, so instability due to SSGS reversal might be an issue. Indeed, because there are now *two* possible steady-state values of the O_2 flow rate *below* the nominal steady-state value of 61 lbmol/hr as suggested by the above feature (d) (cf. Figure 2.2), the controller must push the O_2 flow rate towards the *smaller* of the two possible values. If the controller is not aggressive enough (i.e.,if λ is too large), then the O_2 flow rate may approach the *larger* of the two possible steady-states, around which the SSGS is negative, resulting in closed-loop instability with escape of temperature from its setpoint. Lowering the value of λ makes the controller aggressive enough for the closed loop to be stable, before instability is reached again for overly aggressive control action (λ too small). The resulting closed loop behavior for this case is shown in Figure 2.12 through Figure 2.14. Figure 2.15 shows the instantaneous steady-state gain of the controlled process linearized around the closed-loop trajectories (measurement delay is not considered in the closed loop) shown in Figure 2.16 when $\lambda = 105$ and for $\lambda = 50$ for H_2 flow reduced to 0. It can be observed that for $\lambda = 105$ the instantaneous SSGS is reversed while for $\lambda = 50$ it remains positive, which helps make the connection between the observed closed-loop instability and stability, respectively.

- The closed-loop behavior of the preceding three paragraphs is also shown in the phase-plane plot of Figure 2.16. (again, measurement delays are neglected.)

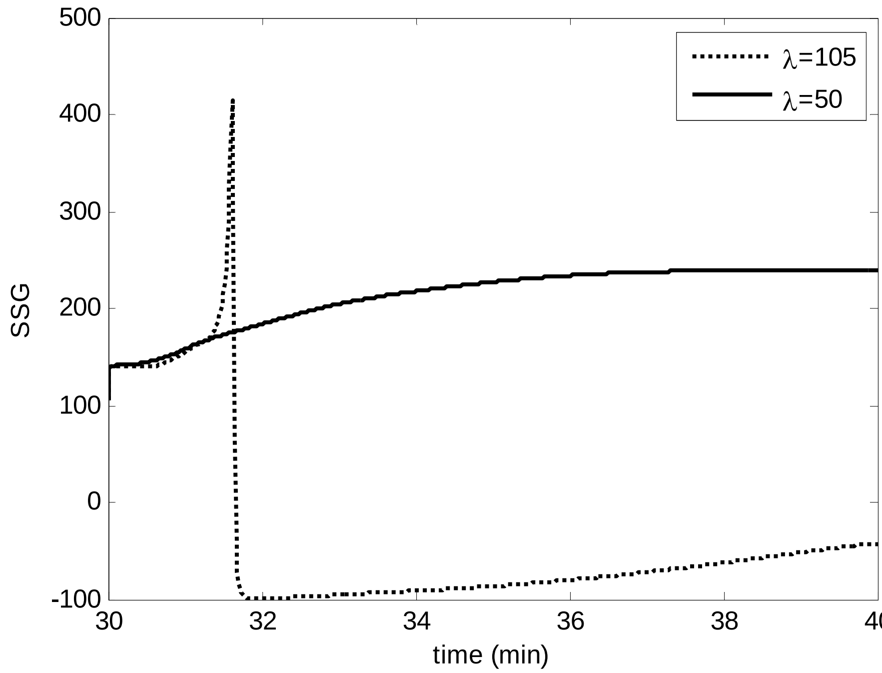

Figure 2.15. Steady-state gain (SSG) for closed-loop trajectories when H_2 flow rate is reduced to 0 lbmol/hr (d =-160 lbmol/hr) from 160 lbmol/hr of its nominal value at time 30 min. The IMC filter time constant takes values λ =50,105 sec. No measurement delay is considered in the closed loop.

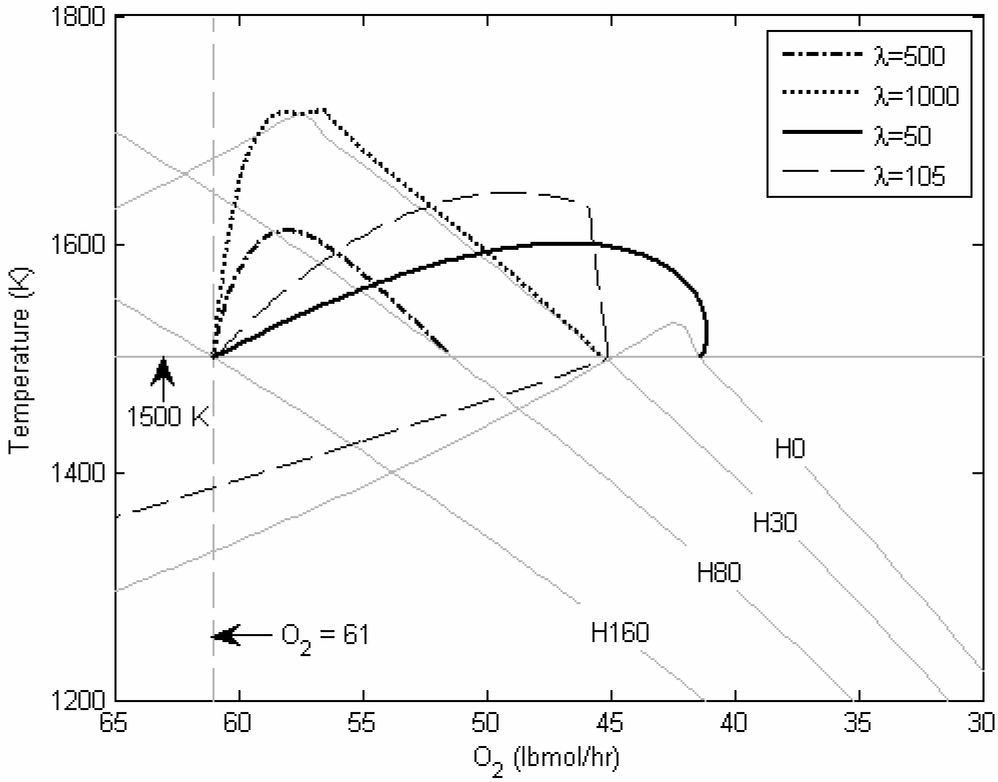

Figure 2.16. Closed-loop temperature response in phase-plane, when H_2 flow rate is reduced to 80, 30 and 0 lbmol/hr from 160 lbmol/hr of its nominal value for different values of λ. The gray lines represent steady-state values, cf. Figure 2.2. (Hx denotes hydrogen flow rate of x lbmol/hr). No measurement delay is considered in the closed loop.

Finally, Figure 2.17 shows the real part of the eigenvalues for the instantaneously linearized closed-loop when H_2 is reduced to 0 and $\lambda = 105$ (Figure 2.16). It can be seen that after 32 min the closed-loop is not stable as the real part of last eigenvalue becomes positive. Similar analysis is performed for $\lambda = 50$ and Figure 2.18 shows that the real part of all closed-loop eigenvalues is always negative, corroborating the observed closed-loop stability. Of course, it should be reminded that stability analysis via eigenvalue loci is not conclusive for linear *time-varying* systems, in that bounds on the rate of change of the corresponding linearized dynamics must be ensured for stability results to be conclusive; however, for many practical applications such analysis has been found to be useful (Vidyasagar 1993).

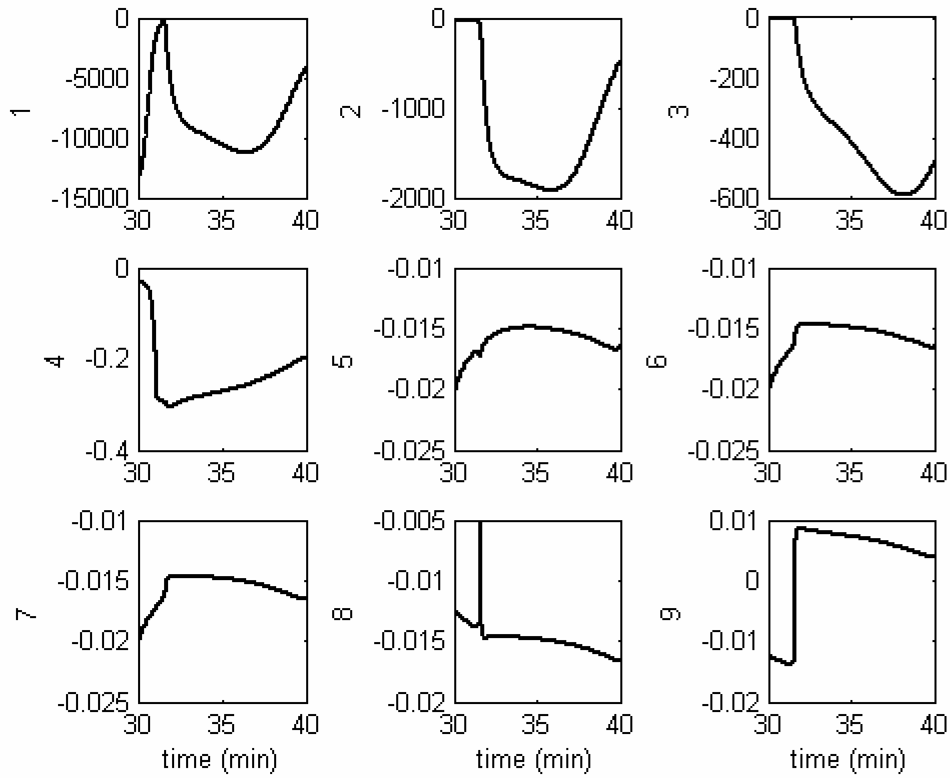

Figure 2.17. Closed-loop eigenvalues when H_2 flow rate is reduced to 0 lbmol/hr (d =-160 lbmol/hr) from 160 lbmol/hr of its nominal value at time 30 min. The IMC filter time constant takes value λ=105 sec. No measurement delay is considered in the closed loop.

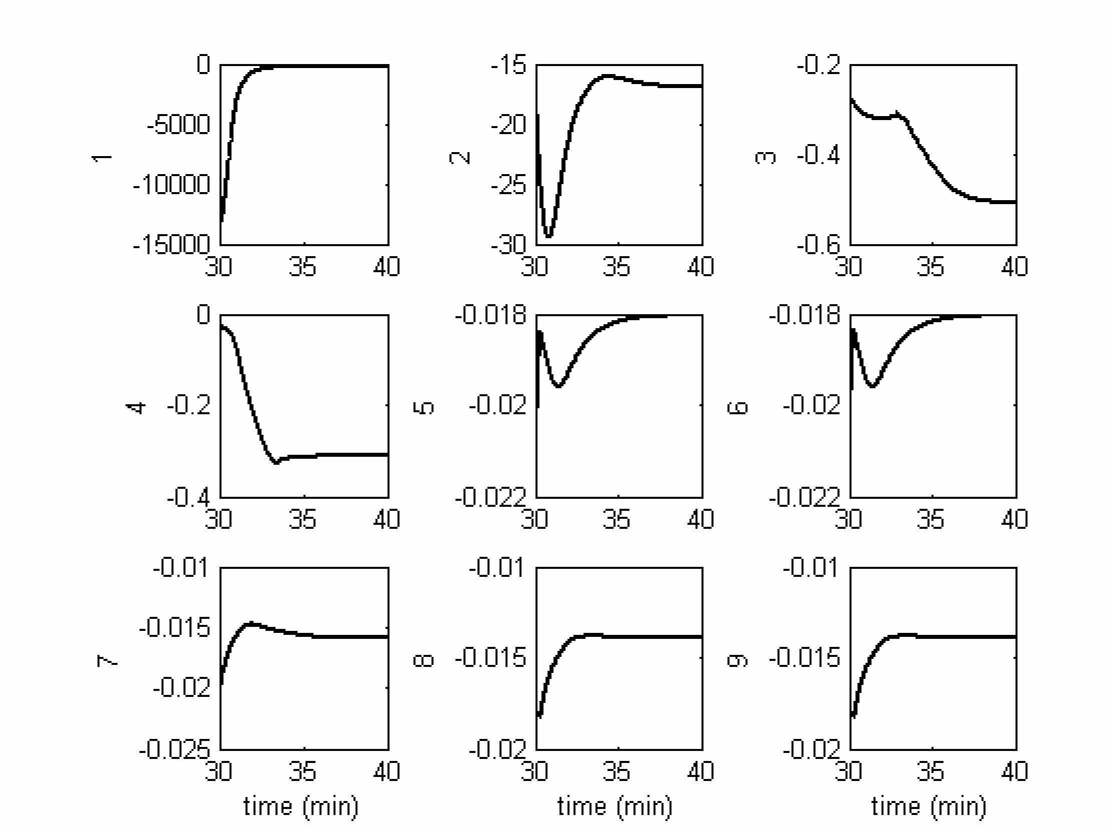

Figure 2.18. Closed-loop eigenvalues when H_2 flow rate is reduced to 0 lbmol/hr (d =-160 lbmol/hr) from 160 lbmol/hr of its nominal value at time 30 min. The IMC filter time constant takes value $\lambda = 50$ sec. No measurement delay is considered in the closed loop.

2.5 Conclusions

A computer simulation study was presented for control of an industrial process that shows interesting dynamic behavior, in that its SSGS may change as a result of external disturbances. Simulation results were supported by a version of the small gain theorem (Theorem 1), proven here for the particular problem setting. The associated stability criterion relies on a variant of the small-gain theorem (eqn. (2.19)) for which a computational approach was presented. Analysis based on a simplified first-principles model calibrated on plant data provided useful insight into controller design.

The simulations and analysis showed interesting closed-loop behavior, summarized as follows: For disturbances up to a certain magnitude, closed-loop stability is ensured if the controller is made sluggish enough. However, if disturbances exceed that magnitude, nonlinearity becomes so strong that instability ensues if the controller becomes too sluggish. It was found that a single linear controller can ensure universal stability over the entire range of anticipated disturbance magnitudes (corresponding to $\lambda = 50$ in Table 2.7). If a more narrow range of disturbances is anticipated, then the controller can be tuned more aggressively (e.g., $\lambda = 10$ for disturbances corresponding to H_2 flow rate no less than 5 lbmol/hr, Table 2.7).

CHAPTER 3

DEBOTTLENECKING LEVEL CONTROL FOR TANKS IN SERIES

3.1 Introduction

Motivation for this work is provided by a liquid-liquid extraction system that is part of an industrial process. The unit entails three tanks in series with a typical set of three feedback control loops (Figure 3.1). Smooth operation of this system requires that the outlet flow rate F_3 should fluctuate as little as possible in the presence of significant fluctuations in the feed flow rate F_{in}, to avoid upsetting the downstream process (a distillation unit). At the same time, the level of the liquid in each tank must be maintained at a setpoint, so that the contact time for the extraction in each tank can remain at a desired value. Unfortunately, these requirements conflict with each other. Indeed, control of the level in tank #3 at its setpoint would require manipulation of the flow rate F_3, which might induce undesired fluctuations on F_3. On the other hand, if the flow rate F_3 were kept at fixed value, only two manipulated inputs, F_1 and F_2, would be left for control of the three liquid levels, which would also be inadequate. Consequently, manipulation of the flow rate F_3 should remain available but fluctuations on F_3 should be avoided.

Within the above context, three PI controllers were tuned for the actual process by trial and error (section 3.2.4), and found to perform satisfactorily for a period of time. As the throughput of the process increased over time, to meet increased production rates, the three PI controllers were retuned by trial and error, to account for the altered dynamics of the process (decreased time constants). The results from this heuristic re-tuning were satisfactory. However, as throughput kept increasing, a value of F_{in} was eventually

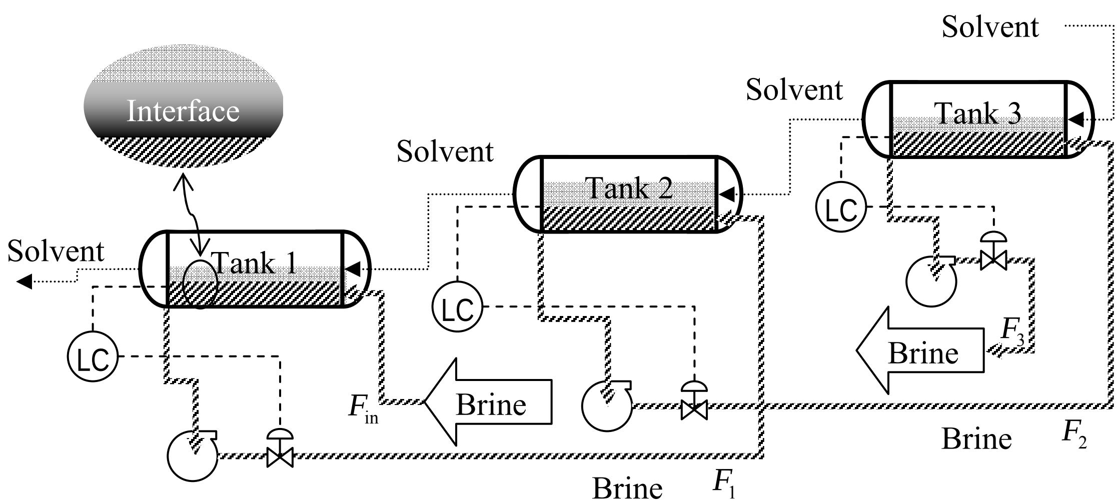

Figure 3.1. Three tanks in series with feedback control scheme. The solvent flow rate does not affect liquid interface level dynamics, as it is practically constant. The brine flow rate F_{in} is a major disturbance with significant fluctuations. The manipulated inputs are the three intermediate flow rates F_1, F_2, F_3. The compositions of the solvent and brine streams remain constant over time.

reached for which performance became unacceptable, manifest as excessive fluctuations on all three levels L_1, L_2, L_3 (Figure 1.2) and on the outlet flow rate, F_3 (Figure 1.3). In fact, it is evident from inspection of Figure 1.2 and Figure 1.3 that level fluctuations increase from tank 1 to 3, as do fluctuations in F_3 compared to F_{in}. After extensive trial-and-error simulations, no PI tuning could be found for the existing control structure to reduce these fluctuations. This raised the following questions.

- What was the underlying reason for the control system's unsatisfactory performance?
- Could it be that the extensive trial-and-error simulations missed controller tuning values that could provide satisfactory closed-loop performance, or can one reasonably infer that no such tuning exists?
- Regardless of the answer to the above question, is there an alternative configuration of the three PI controllers that would provide satisfactory or better performance with appropriate tuning that would be relatively easy to determine?
- Under what general conditions can the previous questions be answered?

It should be mentioned that solutions involving either process redesign (using bigger tanks to increase residence time and reduce oscillations as a result) or employment of an advanced control system (such as model predictive control) were deemed undesirable, based on cost considerations.

The aim of this research work is to provide an answer to the questions raised above within the outlined context. Specifically, in the following section we demonstrate the debottlenecking issue via computer simulation. Section 3.3 describes the proposed control scheme along with a theoretical justification and various tuning rules. Section 3.7 compares the control system design approach proposed here to a standard alternative based on numerical optimization. Section 3.8 illustrates the performance of the proposed scheme based on simulations that employ a model calibrated on the actual plant. Section 3.9 explores the effects of augmenting the proposed solution by adding feedforward control action to the proposed feedback scheme. Finally, a summary is presented in section 3.10.

3.2 Motivation

3.2.1 System description

The system under consideration is shown in Figure 3.1. The process involves liquid-liquid extraction in 3 tanks in series. The purpose of this process is to extract impurities present in the brine solution using a solvent. The brine is pumped from one tank to another while solvent flow is gravity driven. Both brine and solvent solutions are well mixed at the inlet. Brine, being heavier than the solvent settles at the bottom of each tank, while the solvent settles on top of the brine, with an interface forming in between. The tank volumes are such that enough residence time should be available for the two phases to separate. The interface level in each tank is measured in real time. It is assumed that liquid levels in each tank are always higher than the position of the outlet opening, to maintain continuous flow in the process.

3.2.2 System model

The three-tank system shown in Figure 3.1 (or its simplified formFigure 1.1) is modeled by standard mass balance equations for each tank.

$$\begin{aligned} A_1 \frac{d\Delta L_1}{dt} &= \Delta F_{\text{in}} - \Delta F_1 \\ A_2 \frac{d\Delta L_2}{dt} &= \Delta F_1 - \Delta F_2 \\ A_3 \frac{d\Delta L_3}{dt} &= \Delta F_2 - \Delta F_3 \end{aligned} \tag{3.1}$$

where L_i, A_i and F_i for $i = 1,2,3$ represent interface level, cross sectional area and outlet flow rate in each tank, respectively; and Δ represents deviation from steady-state corresponding to given setpoint. The solvent flow rates in eqn. (3.1) do not affect the interface level, as the solvent is lighter than the brine and hence the interface level depends only on the brine flow rate. Also, solvent rates are assumed to be practically constant. Steady-state and parameter values are shown in Table 3.1.

Table 3.1. Tank model parameters and constraints for case-1

A [m^2]	F_0 [gpm]	u_{step} [gpm]	$a_{F_{in}}$ [gpm]	$\Delta L_i^{max} = -\Delta L_i^{min}$ [%]	H [m]	Time period of disturbances [hr]
16.72	300	50	50	5	2	1-3

3.2.3 Control objectives

Two forms of the disturbance F_{in} are considered: A step of magnitude less than 17% of F_{in} and a sinusoidal disturbance of period 1-3 hours having amplitude less than 17% of F_{in}. These disturbances are due to operating practices of the upstream process feeding the brine to the extraction process.

The three levels L_i must be controlled at their respective setpoints, which remain constant. The liquid levels must also satisfy the constraints

$$\Delta L_i^{min} \le \Delta L_i \le \Delta L_i^{max}, \quad i = 1,2,3, \tag{3.2}$$

where ΔL_i^{min} and ΔL_i^{max} are $\pm 5\%$ away from corresponding setpoints, respectively. Such tight control of interface level is important as significant change in the residence time will affect the overall efficiency of the extraction process. In addition,

1) the flow rate F_3 must respond to sinusoidal disturbances in F_{in} with an amplitude ratio no higher than 1 and,
2) in case of step disturbance, the flow rate F_3 should be manipulated smoothly to avoid unwanted oscillations (i.e., avoidance of under damped tuning of level controller). Explicitly closed-loop damping factor ξ is constrained by $0.5 \le \xi \le 2$ as suggested in (Shin, Lee et al. 2008) to avoid severe oscillation in closed loop or very slow response.

In case constraints for both the three levels L_i and the outlet flow rate F_3 can be satisfied simultaneously when disturbances are sinusoidal, the controllers can be tuned to minimize fluctuations in F_3, to prevent upsetting the downstream process.

3.2.4 Inadequacy of conventional control

A conventional control scheme is considered with

$$\Delta F_i(s) = K_i(s)(\Delta L_i^{\text{SP}} - \Delta L_i(s)), \tag{3.3}$$

where $K_i(s)$, $i = 1,2,3$ represents a PI controller for tank 1, 2 and 3, respectively.

Consider the case when the three-tank system is subject to a step disturbance of magnitude 25 gpm and sinusoidal disturbance of period 3 hours of amplitude 25 gpm in F_{in}. A simple trial-and-error approach is adapted to tune the three PI controllers for satisfaction of the constraints in eqn. (3.2) and minimization of flow variation in F_3. The trial-and-error approach entails these steps:

- Consider the tuning of first level controller based on step disturbance so that level constraint in eqn. (3.2) is satisfied for the first tank for critically damped closed loop. This tuning setting works as first guess.
- Change the integral time and the gain of level controller to minimize the amplitude ratio of F_3 to F_{in}. While manipulating tuning parameters level constraints should be satisfied for both step and sinusoidal disturbances.
- Consider the same tuning parameter settings for second level controller as a start point and change the integral time and the gain to minimize flow fluctuations in F_2 while satisfying level constraint.
- Consider the second controller's tuning parameter settings as a start point and change the integral time and the gain to minimize flow fluctuations in F_3 while satisfying level constraint.

Controllers are designed based on above mentioned procedure and closed-loop response is shown in Figure 3.2. It is evident that this particular tuning performs well. Both the level and flow variations are decreasing with down stream tanks. The amplitude ratio is 63% (Figure 3.3) for sinusoidal disturbance of period 3 hours. The frequency response of the closed-loop transfer function between three levels to ΔF_{in} is shown in Figure 3.3. It is clear that even if the sinusoidal frequency is changed to higher or lower values controller performance is satisfactory as levels satisfy eqn. (3.2) and amplitude ratio is less than 1.

Now consider a case when the magnitude of step disturbance and amplitude of sinusoidal disturbance is increased to 50 gpm. The same approach is adopted to re-tune the controllers. However, in this case the amplitude ratio is found to be greater than 1 for sinusoidal disturbance of period 3 hours. The frequency response for the closed loop transfer function between three levels to ΔF_{in} in Figure 3.4 suggests that any disturbance which has period greater than 3 hours will not have flow attenuation. It is clear that the increase in the magnitude of disturbance has left fewer margins to attenuate the outlet flow rate with tight level control. This situation is the same as observed in actual plant Figure 1.2, Figure 1.3. Therefore, conventional feedback scheme is not able to perform well and hence advanced or multivariate control design is required.

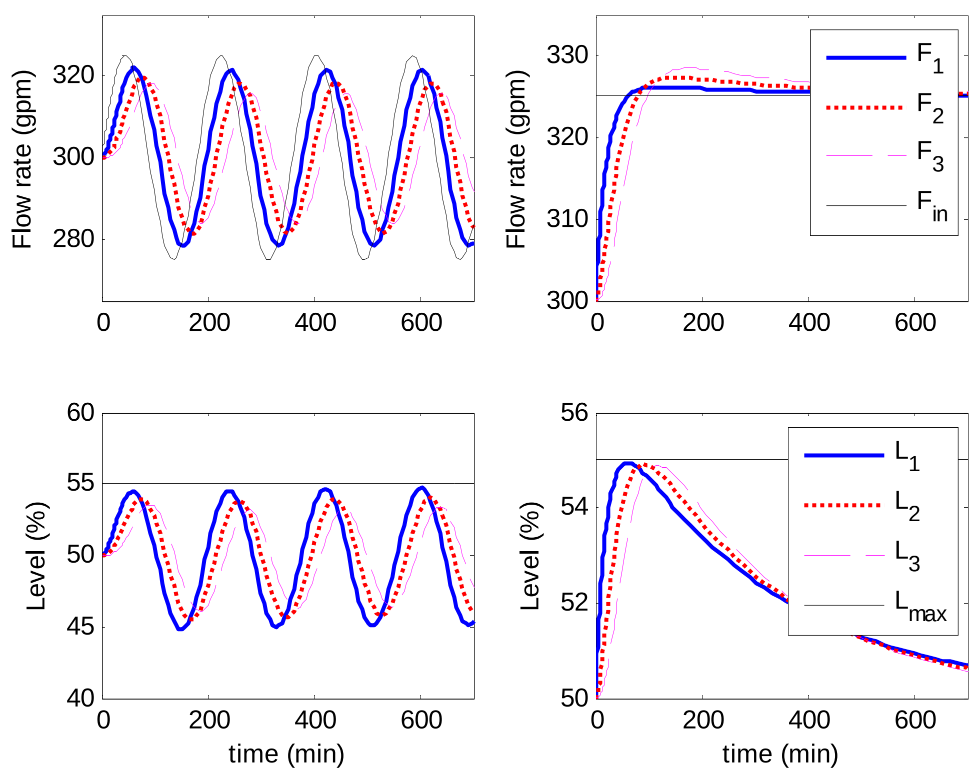

Figure 3.2. Disturbance rejection of sinusoidal and step disturbances of magnitude 25 gpm by the PI controllers $K_c\left(1+\frac{1}{\tau_I s}\right)$ with $K_{c,1}=-0.014\frac{\Delta F_1[m^3/s]}{\Delta L_1}$, $\tau_{I,1}=333\,\mathrm{min}$, $K_{c,2}=-0.0141\frac{\Delta F_2[m^3/\mathrm{sec}]}{\Delta L_2}$, $\tau_{I,2}=323\,\mathrm{min}$, $K_{c,3}=-0.0144\frac{\Delta F_3[m^3/s]}{\Delta L_3}$, $\tau_{I,3}=317\,\mathrm{min}$, around the steady state $F_{\mathrm{in,ss}}=F_{1,\mathrm{ss}}=F_{2,\mathrm{ss}}=F_{3,\mathrm{ss}}=25$ gpm.

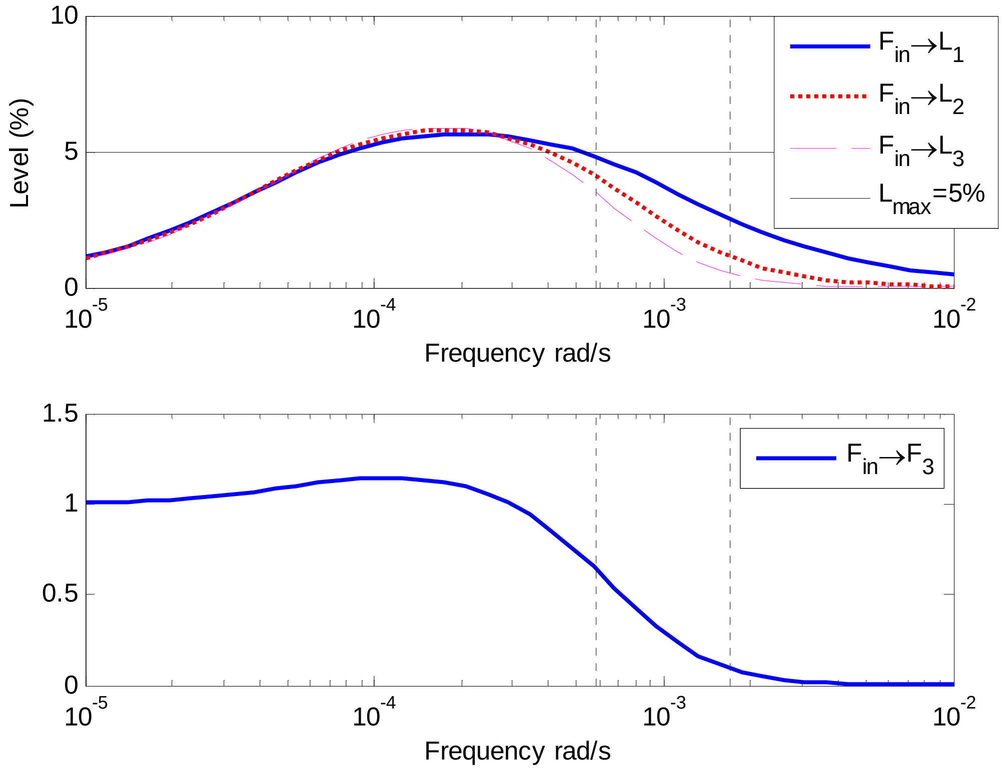

Figure 3.3. Amplitude ratio for the closed-loop transfer functions between F_{in} and L_1, L_2, L_3 (top) and between F_{in} and F_3 (bottom) around the steady state $F_{\text{in,ss}} = F_{1,\text{ss}} = F_{2,\text{ss}} = F_{3,\text{ss}} = 25$ gpm. Region between vertical dotted lines represents frequencies of period 3 hr to 1 hr.

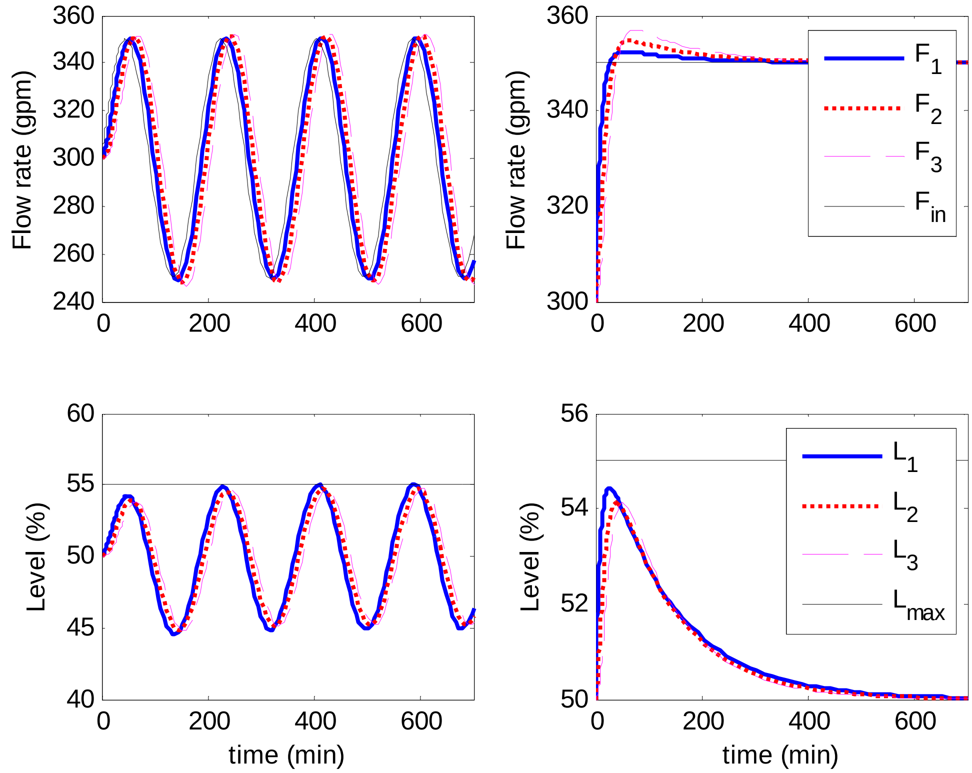

Figure 3.4. Disturbance rejection of sinusoidal and step disturbances of magnitude 50 gpm by the PI controllers $K_c\left(1+\dfrac{1}{\tau_I s}\right)$ **with** $K_{c,1}=-0.031\dfrac{\Delta F_1[m^3/\mathrm{s}]}{\Delta L_1}$**,** $\tau_{I,1}=143\,\mathrm{min}$**,** $K_{c,2}=-0.0334\dfrac{\Delta F_2[m^3/\mathrm{s}]}{\Delta L_2}$**,** $\tau_{I,2}=138\,\mathrm{min}$**,** $K_{c,3}=-0.034\dfrac{\Delta F_3[m^3/\mathrm{s}]}{\Delta L_3}$**,** $\tau_{I,3}=136\,\mathrm{min}$ **, around the steady state** $F_{in,ss}=F_{1,ss}=F_{2,ss}=F_{3,ss}=300$ **gpm. The amplitudes of flow rate variations are increasing with downstream tank.**

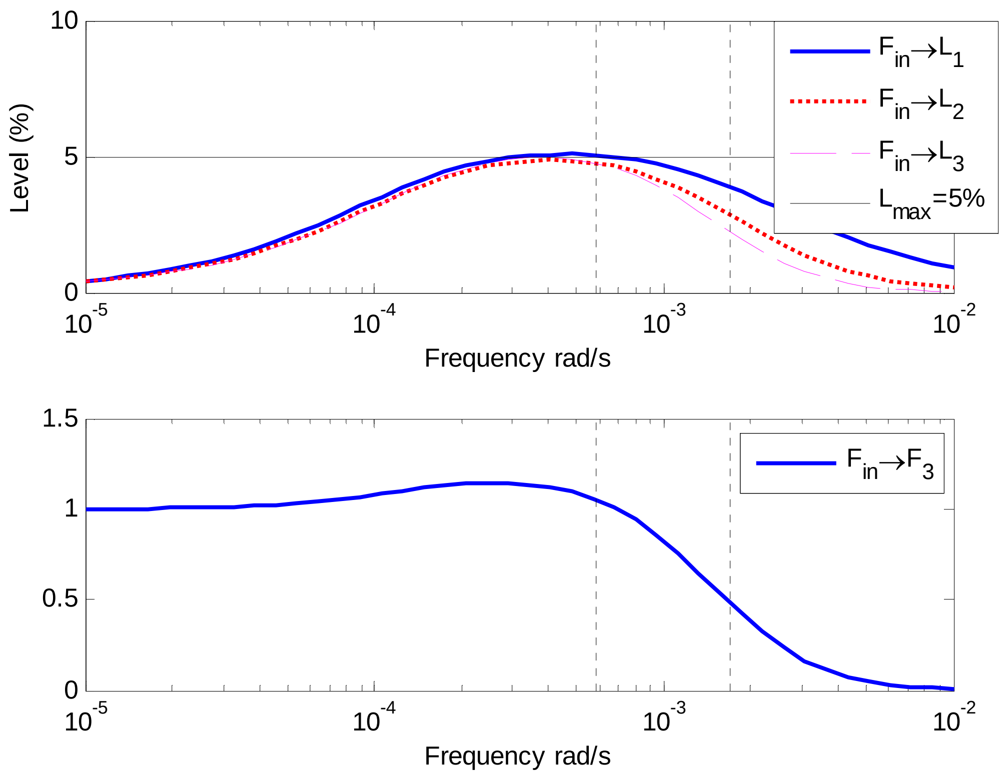

Figure 3.5. Amplitude ratio for the closed-loop transfer functions between F_{in} and L_1, L_2, L_3 (top) and between F_{in} and F_3 (bottom) around the steady state $F_{\text{in,ss}} = F_{1,\text{ss}} = F_{2,\text{ss}} = F_{3,\text{ss}} = 50$ gpm. Region between vertical dotted lines represents frequencies of period 3 hr to 1 hr.

3.3 Control scheme and controller synthesis

Before we proceed with presenting the development of an alternative control configuration we emphasize the setting of the problem, namely no feed flow rate measurements are available to be used for feedforward control (quite common specially in case of surge tanks) (Bayer 2008); levels are the only available measurements; the existing hardware can do simple calculations such as adding signals or multiplying by a constant, but not full multivariable control calculations and even less so constrained model predictive control calculations.

The justification for the development of the proposed control structure is as follows. What forces F_3 to fluctuate is feedback controller response to fluctuations in F_2 caused by fluctuations in F_1, which are in turn caused by fluctuations in the external process disturbance F_{in}. If the controllers in tanks #1 and #2 are tuned overly aggressively, then the fluctuations in F_1 and F_2 are going to be roughly comparable to fluctuations in the disturbance F_{in} (see Appendix C). Consequently, the third tank is going to experience a disturbance F_2 comparable (at least in high-frequency content) to F_{in}. How much F_3 will fluctuate depends on the tuning of the corresponding controller, which must be aggressive enough, to ensure that the level in the third tank stays within its bounds $\Delta L_{\min}$ and $\Delta L_{\max}$. If the capacity of the third tank were increased (by increasing A_3), then the corresponding controller could be tuned less aggressively, thus mitigating the fluctuations in F_3. Unfortunately, that could not be an option. However, the process controlled by the third controller can be made to appear to have higher capacity by considering all three tanks as one, and using the weighted average of the three tank levels $\left(Y_1Y_2\Delta L_1 + Y_2\Delta L_2 + \Delta L_3\right)/3$ as the controlled variable for the third controller. The first two controllers, then, can be used to ensure that the weighted levels of all three tanks behave as a whole, namely that $\Delta L_2 - Y_1\Delta L_1$ and $\Delta L_3 - Y_2\Delta L_2$ remain close to zero. The proposed control scheme is shown in Figure 3.6.

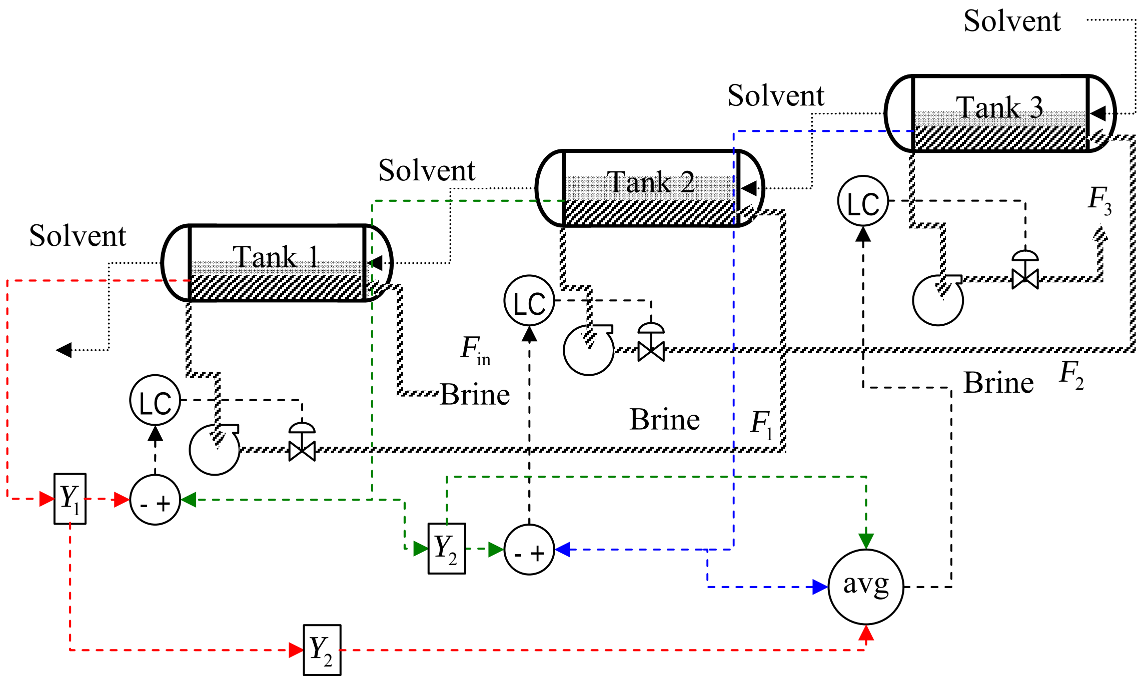

Figure 3.6. Proposed control scheme for three tanks in series.

After normalizing the levels as

$$\Delta\tilde{L}_i \mathrel{\hat{=}} X_i \Delta L_i\,,\; i = 1,2,3\,, \tag{3.4}$$

where

$$X_i \mathrel{\hat{=}} \frac{A_i}{A_3}\,,\; i = 1,2,3\,. \tag{3.5}$$

New control variables can be defined as

$$\mathbf{\Delta L'} = \mathbf{M}\Delta\tilde{\mathbf{L}}\,, \tag{3.6}$$

where

$$\mathbf{M} = \begin{bmatrix} -Y_1 & 1 & 0 \\ 0 & -Y_2 & 1 \\ \dfrac{Y_1 Y_2}{3} & \dfrac{Y_2}{3} & \dfrac{1}{3} \end{bmatrix}, \tag{3.7}$$

$\tilde{\mathbf{L}} \triangleq \begin{bmatrix} \tilde{L}_1 & \tilde{L}_2 & \tilde{L}_3 \end{bmatrix}^T$ and $\mathbf{L}' \triangleq \begin{bmatrix} L_1' & L_2' & L_3' \end{bmatrix}^T$.

Based on which the process model becomes

$$\begin{bmatrix} \Delta L_1'(s) \\ \Delta L_2'(s) \\ \Delta L_3'(s) \end{bmatrix} = \frac{1}{A_3 s}\left(\begin{bmatrix} 1+Y_1 & -1 & 0 \\ -Y_2 & 1+Y_2 & -1 \\ \frac{Y_2 - Y_1 Y_2}{3} & \frac{1-Y_2}{3} & -\frac{1}{3} \end{bmatrix} \begin{bmatrix} \Delta F_1(s) \\ \Delta F_2(s) \\ \Delta F_3(s) \end{bmatrix} + \begin{bmatrix} -Y_1 \\ 0 \\ \frac{Y_1 Y_2}{3} \end{bmatrix} \Delta F_{\text{in}}(s) \right), \tag{3.8}$$

and the original constraints in eqn. (3.2) become

$$\begin{aligned} X_1 \Delta L_1^{\min} &\le \frac{-\Delta L_2' + 3\Delta L_3' - 2\Delta L_1' Y_2}{3 Y_1 Y_2} \le X_1 \Delta L_1^{\max} \\ X_2 \Delta L_2^{\min} &\le \frac{-\Delta L_2' + 3\Delta L_3' + \Delta L_1' Y_2}{3 Y_2} \le X_2 \Delta L_2^{\max} \\ \Delta L_3^{\min} &\le \frac{2\Delta L_2' + 3\Delta L_3' + \Delta L_1' Y_2}{3} \le \Delta L_3^{\max} \end{aligned} . \tag{3.9}$$

The corresponding controller design will result in

$$\Delta F_i = K_i \Delta L_i', \text{ for } i = 1,2,3 . \tag{3.10}$$

For tight control of new control variables L_1', L_2' near their respective setpoints $\Delta L_{1,\text{SP}}' = \Delta L_{2,\text{SP}}' = 0$, the dynamics of 3 tank system is determined by eqn. (3.8) which yields

$$\Delta L_3'(s) = \frac{1}{\eta A_3 s}\left(\Delta F_{\text{in}}(s) - \Delta F_3(s)\right), \tag{3.11}$$

where

$$\eta = \frac{1 + Y_1 + Y_1 Y_2}{Y_1 Y_2} . \tag{3.12}$$

Similarly, for tight control of L_1' and L_2' near zero the constraints in eqn. (3.9) reduce to a constraint on L_3' alone, namely

$$\begin{aligned}&\max_{i=1,2,3}\left(Y_1Y_2X_1\Delta L_1^{\min}, Y_2X_2\Delta L_2^{\min}, \Delta L_3^{\min}\right) \le \Delta L_3' \\ &\le \min_{i=1,2,3}\left(Y_1Y_2X_1\Delta L_1^{\max}, Y_2X_2\Delta L_2^{\max}, \Delta L_3^{\max}\right)\end{aligned} . \tag{3.13}$$

The preceding discussion suggests a transformed control problem, as follows.

- *Controlled output variables*: Eqns. (3.6)-(3.7).
- *Manipulated input variables*: F_1, F_2, F_3.
- *Setpoints*:

$$\begin{aligned} L'_{1,\mathrm{SP}} &= 0 \\ L'_{2,\mathrm{SP}} &= 0 \\ L'_{3,\mathrm{SP}} &= L_{3,\mathrm{SP}} \end{aligned} \tag{3.14}$$

- *Constraints*: Eqn. (3.13).
- *Process model*: Eqn. (3.8), simplified as eqn. (3.11).

Remarks

1. If weights Y_1 and Y_2 are chosen based on the ratio of maximum capacity of adjacent tanks and given by

$$Y_1 \triangleq \frac{A_2\Delta L_2^{\max}}{A_1\Delta L_1^{\max}} = \frac{X_2\Delta L_2^{\max}}{X_1\Delta L_1^{\max}}, \tag{3.15}$$

$$Y_2 \triangleq \frac{A_3\Delta L_3^{\max}}{A_2\Delta L_2^{\max}} = \frac{\Delta L_3^{\max}}{X_2\Delta L_2^{\max}}, \tag{3.16}$$

eqns.(3.13) reduces to single linear constraint

$$\Delta L_3^{\min} \le \Delta L_3' \le \Delta L_3^{\max} . \tag{3.17}$$

In this way the three-tank control problem has been reduced to two fairly decoupled problems:

- Control of the "level" $\Delta L_3'$ of a "single tank" with capacity ηA_3 subject to constraint on $\Delta L_3'$ similar to the constraints on the original level ΔL_3.
- Tight control of the relative level differences $\Delta L_1'$ and $\Delta L_2'$.

The average level controller is the slowest controller in all three controllers and will govern the overall performance of closed loop.

2. Eqn. (3.12) suggests that the value of η is always great than 1 and hence satisfaction of the constraints on $\Delta L_3'$ in eqn. (3.17) can be achieved by using less aggressive manipulation of F_3 in comparison to the original control scheme shown Figure 1.1, resulting in improved closed-loop performance. Eqn. (3.11) indicates that if identical tanks are configured as proposed scheme, system of tanks in series will have η times more volume to reject the same disturbance than conventional scheme.

3. In general, equation similar to eqn. (3.11) can be derived for N tanks in series and corresponding η can be given by,

$$\eta = \frac{1 + Y_1 + Y_1Y_2 + Y_1Y_2Y_3 + ... + Y_1Y_2.....Y_{N-1}Y_N}{Y_1Y_2.....Y_{N-1}Y_N}, \tag{3.18}$$

where

$$Y_i \triangleq \frac{A_3 \Delta L_3^{\max}}{A_2 \Delta L_2^{\max}} = \frac{X_{i+1} \Delta L_{i+1}^{\max}}{X_i \Delta L_i^{\max}} \text{ for } i = 1, 2 \ldots, N-1. \tag{3.19}$$

3.4 Average level controller design

The closed-loop system expressed by eqns. (3.8) and (3.10) is a set of linear equations and can be solved for exact solution to find corresponding controllers which satisfy eqn. (3.9). However, analytic solution to these equations is complex and hence the derivation of tuning rules from the exact solution to eqn. (8) and (10) is not trivial. However as shown above that the closed loop described by of eqns. (3.8) and (3.10) is approximated by eqns. (3.11),(3.12), with single constraint given by eqn. (3.17). Hence an approximate solution can easily be found which can be used for controller tuning. Since, the set point of $L_3'^{sp}$ is constant, and $\Delta L_3' \approx \Delta L_3$ (tight control of L_1' and L_2'), eqn. (3.11) and eqn. (3.10) yields

$$\Delta L_3(s) \approx \frac{\Delta F_{\mathrm{in}}(s)}{\left(\eta A s + K_3(s)\right)}. \tag{3.20}$$

Considering the feedback control law is given by the PI controller

$$K_i(s) = K_{c,i} + \frac{K_{c,i}}{s\tau_{\mathrm{I},i}}, \tag{3.21}$$

the closed-loop transfer function is given as

$$L_3(s) \approx \frac{\Delta F_{\mathrm{in}}(s)}{\left(\eta A s + K_{c,3} + \dfrac{K_{c,3}}{s\tau_{\mathrm{I},3}}\right)}. \tag{3.22}$$

The dynamics of eqn. (3.22) is second order and will result in either over damped, critical damped or under damped closed loop based on damping factor ξ defined by

$$\xi = \frac{1}{2}\sqrt{\frac{\tau_{\mathrm{I},3} K_{c,3}}{\eta A}}. \tag{3.23}$$

3.5 Controller design criteria

3.5.1 Step disturbance

In case of step input, $\Delta F_{\text{in}}(s) = u_{\text{step}} \cdot \frac{1}{s}$ and using eqn. (3.22) the level of tank 3 is given as

$$\gamma_{\text{step}} \Delta L_{\text{step}}(s) = \frac{1}{\left(s + \frac{1}{\tau_{\text{H}}} + \frac{1}{s\tau_{\text{H}}\tau_{\text{I},3}}\right)s}, \tag{3.24}$$

where

$$\Delta L_{\text{step}} = \frac{100 * L_3}{H_3}, \tag{3.25}$$

$$\tau_{\text{H}} = \frac{\eta A}{K_{c,3}}, \tag{3.26}$$

$$\gamma_{\text{step}} = \frac{\eta \tau_{\text{V}}}{u_{\text{step}} \cdot 100 / F_0}, \tag{3.27}$$

$$\tau_{\text{V}} = \frac{AH}{F_0}, \tag{3.28}$$

$$\xi = \frac{1}{2}\sqrt{\frac{\tau_{\text{I},3}}{\tau_{\text{H}}}}. \tag{3.29}$$

H is the height of tank, F_0 is nominal feed flow rate, τ_{V} is total hold up time of the tank. ΔL_{step} is the % deviation of level in tank 3. Eqn. (3.24) is used to plot maximum value of $\gamma_{\text{step}} \Delta L_{\text{step}}$ ($\gamma_{\text{step}} \Delta L_{\text{step}}^{\max}$) as a function of tuning parameters τ_{H} and $\tau_{\text{I},3}$ for a step change in feed of magnitude u_{step} and resulting plot is used as a tuning chart (Figure 3.7). Using eqn.(3.29), damping factor ξ is also plotted in Figure 3.7 as a function of τ_{H} and $\tau_{\text{I},3}$.

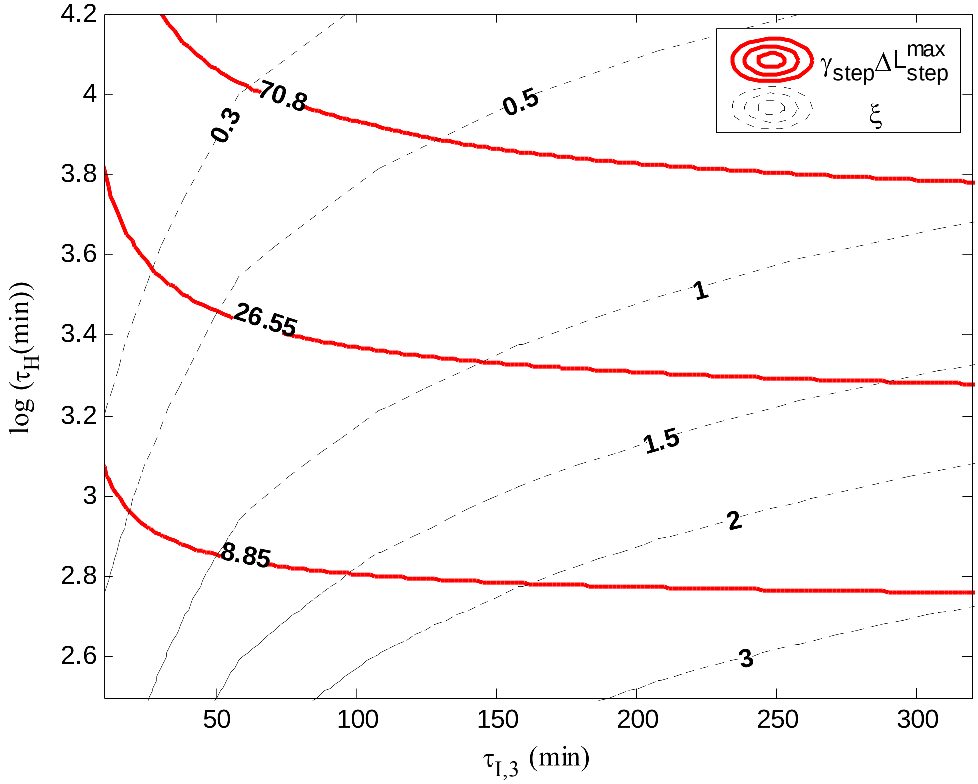

Figure 3.7. Average controller tuning chart for step change in flow rate.

3.5.2 Sinusoidal disturbance

For the sinusoidal disturbance of angular frequency ω, $F_{\text{in}}(s) = a_{F_{\text{in}}} \cdot \dfrac{\omega}{s^2+\omega^2}$ and using eqn. (3.22), level variation of tank 3 is given as

$$\gamma_{\text{sine}} \Delta L_{\text{sine}}(s) \approx \frac{1}{\left(s + \dfrac{1}{\tau_{\text{H}}} + \dfrac{1}{s\tau_{\text{H}}\tau_{\text{I}_3}}\right)} \frac{\omega}{s^2+\omega^2}, \tag{3.30}$$

where

$$\gamma_{\text{sine}} = \frac{\eta\tau_{\text{V}}}{a_{F_{\text{in}}} \cdot 100/F_0} \tag{3.31}$$

ΔL_{sine} is % deviation in level of tank 3 for sinusoidal disturbance of amplitude $a_{F_{\text{in}}}$ and angular frequency ω. For a given ω ΔL_{sine} is a function of tuning parameters and this equation can be used to generate a tuning chart (Figure 3.8) for maximum deviation $\Delta L_{\text{sine}}^{\max}$ in tank level for a given tuning parameter (τ_{H} and $\tau_{\text{I,3}}$). ξ is also plotted in Figure 3.8. In case of sinusoidal disturbance it is less likely to be the case of disturbance of only one particular frequency perturbing the system. Hence one need to generate charts for all frequencies of interest. This may be a cumbersome process, however, tuning parameters can be chosen for worst case frequency for which level deviation is the maximum at steady state. Eqn. (3.30) when solved for steady state yields

$$\gamma_{\text{sine}} \Delta L_{\text{sine}}^{SS} = \frac{1}{\left(\left(\omega - \frac{1}{\omega \tau_{\text{H}} \tau_{\text{I}_3}} \right)^2 + \left(\frac{1}{\tau_{\text{H}}} \right)^2 \right)^{1/2}}, \tag{3.32}$$

where $\Delta L_{\text{sine}}^{ss}$ is % deviation in level at steady state for disturbance of angular frequency ω. The worst case frequency can be calculated by maximization of eqn. (3.32) It is clear from eqn. (3.32) that for particular pair of tuning parameters ($\tau_{\text{H}}, \tau_{\text{I,3}}$) there exists an angular frequency ω_0 for which $\Delta L_{\text{sine}}^{SS}$ is maximum. This angular frequency is given by,

$$\omega_0 = \frac{1}{2\xi \tau_{\text{H}}}, \tag{3.33}$$

and corresponding maximum level variation is geiven by

$$\gamma_{\text{sine}} \Delta L_{\text{sine}}^{SS}(\omega_0) = \tau_{\text{H}} . \tag{3.34}$$

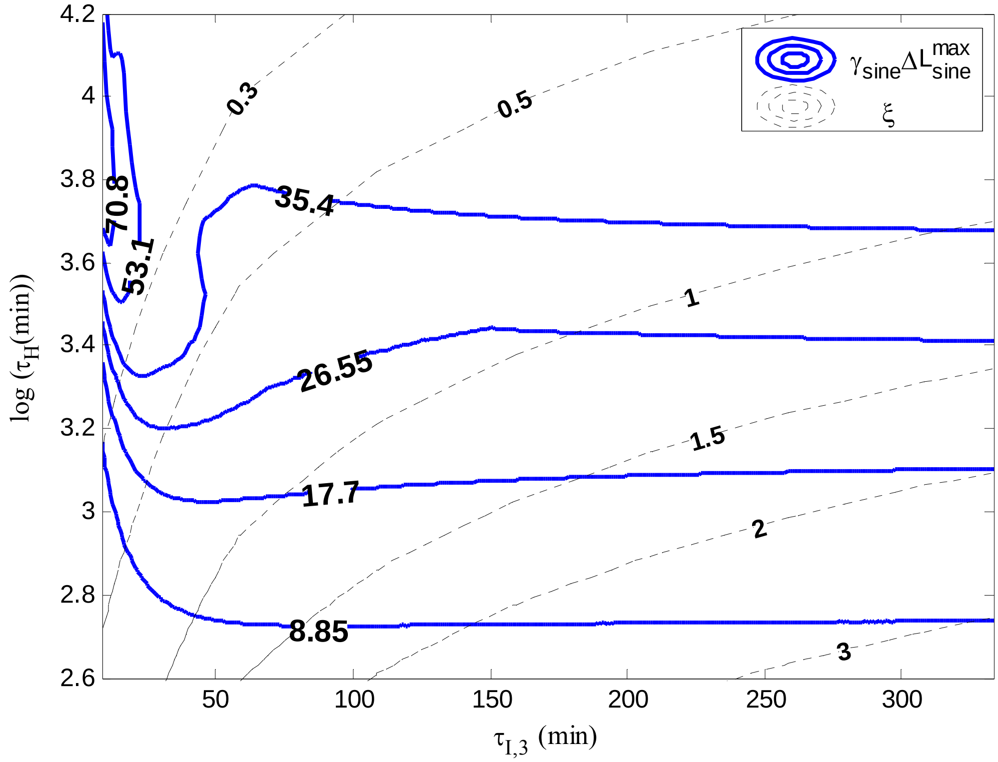

Figure 3.8. Average controller tuning chart for sinusoidal disturbance.

A general procedure to choose tuning parameter in case of both step and sinusoidal disturbance are listed as,

1. Choose controller tuning parameters (τ_H , $\tau_{I,3}$) based on step disturbance criteria (i.e.,use Figure 3.7)
2. Find the value of ω_0 using eqn.(3.33). If the $\omega_0 < \omega_{min} < \omega_{max}$, then ω_{min} (disturbance of maximum time period) will be considered as worst case frequency. If $\omega_0 > \omega_{min} > \omega_{max}$ (disturbance of minimum time period) will be considered as worst case frequency. Otherwise ω_0 will be worst frequency.
3. For the worst case frequency, calculate $\Delta L_{sine}(\omega_{worst})$. If $\Delta L_{sine}(\omega_{worst}) \leq \Delta L_{step}$ for step disturbance, the designed controller settings are accepted.

4. If for the worst frequency $\Delta L_{\text{sine}}\left(\omega_{\text{worst}}\right) > \Delta L_{\text{step}}$ then controller parameter has to be adjusted by tuning chart based sinusoidal disturbance and (Figure 3.8) is used to find a new pair of tuning parameters. For this pair of tuning parameter repeats the steps from 2 to 4.

3.5.3 Flow attenuation factor

For sinusoidal disturbances flow attenuation factor r is defined as ratio of the amplitude of output flow rate to the amplitude of input flow rate at steady state. In context to process under consideration of tanks in series r is defined by

$$r(\omega) = \frac{a_{F_3}(\omega)}{a_{F_{\text{in}}}(\omega)}. \tag{3.35}$$

where a_{F_3} and $a_{F_{\text{in}}}$ are amplitude of F_3 and $F\text{in}$ respectively.

For the PI controller r is expressed by

$$r\left(\omega\right) = \left(\frac{\dfrac{1}{\tau_{\text{H}}^2} + \left(\dfrac{1}{\omega\tau_{\text{H}}\tau_{\text{I,3}}}\right)^2}{\left(\dfrac{1}{\tau_{\text{H}}^2} + \left(\omega - \dfrac{1}{\omega\tau_{\text{H}}\tau_{\text{I,3}}}\right)^2\right)} \right)^{\frac{1}{2}}. \tag{3.36}$$

It should be noted that for given frequency ω , r is a function of controller tuning parameters τ_{H} and $\tau_{\text{I,3}}$. Based on eqn. (3.36) a chart (Figure 3.9) can be prepared for flow rate attenuation factor. This chart can be used in combination of eqn. (3.24) (Figure 3.7) or eqn. (3.32) (Figure 3.8) to choose appropriate control tuning settings. For the ease of convenience these charts can be merged into one single chart in Figure 3.10 which is used for controller design based on step disturbances. Similar combined chart can be prepared for sinusoidal disturbance.

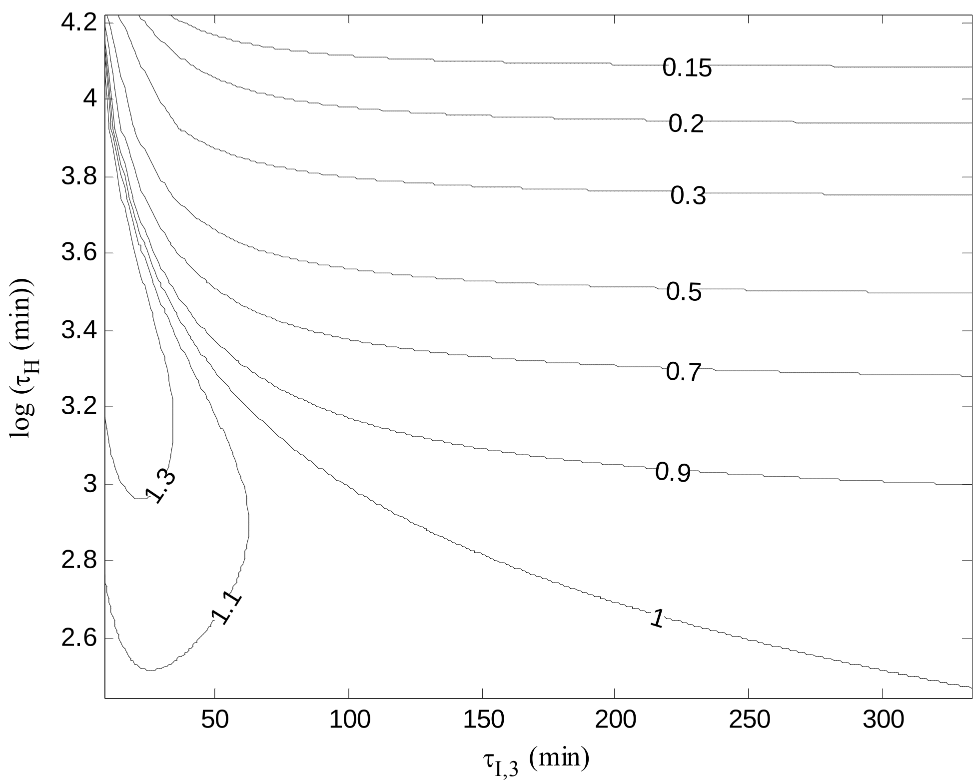

Figure 3.9. Flow rate attenuation factor r for $\omega = 5.8 * 10^{-4}$ rad/s (time period 3 hr).

3.6 Relative level controller design

The dynamics of relative level controllers (RLCs) is given by first two equations in eqn. (3.8). In the present work setpoint changes are considered to be zero. In the derivation of average level controller it has been assumed that first two equations in eqn. (3.8) are always in equilibrium with respect to average level control i.e.,very tight control of relative levels at their setpoint is required. This would result in following conditions for tuning of RLCs (see Appendix D).

First RLC:

$$K_{c,3} \ll \frac{K_{c,1}}{Y_2}, \tag{3.37}$$

$$A\omega \ll \frac{Y_1 K_{c,1}}{\tau_{I,1}\omega}, \tag{3.38}$$

$$\eta A\omega \ll \frac{K_{c,1}}{Y_2 \tau_{I,1}\omega}. \tag{3.39}$$

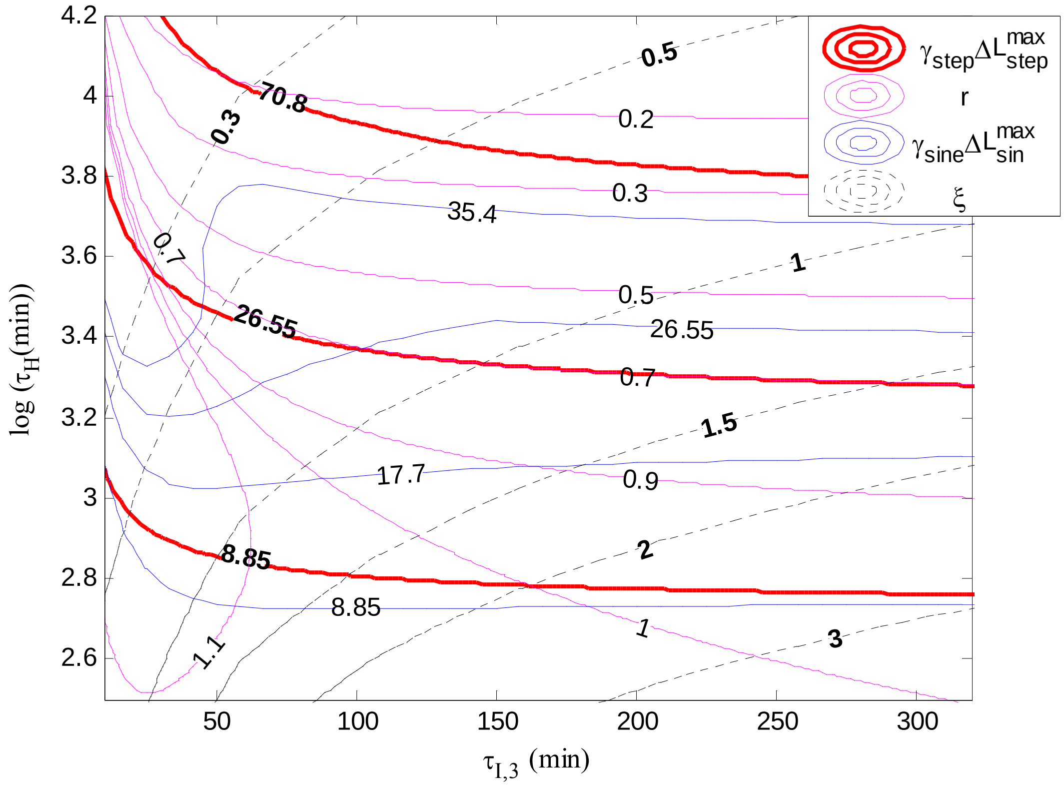

Figure 3.10. Tuning chart for step disturbance and sinusoidal disturbance of time period 3 hr.

Second RLC:

$$K_{c,3} \ll K_{c,2}, \tag{3.40}$$

$$\eta A\omega \ll \frac{K_{c,2}}{\tau_{I,2}\omega}, \tag{3.41}$$

$$A\omega - \frac{K_{c,1}}{\tau_{I,2}\omega} \ll \frac{Y_2 K_{c,2}}{\tau_{I,2}\omega}. \tag{3.42}$$

The closed-loop dynamics is governed by frequency content of the disturbance and the tuning of average level controller (the slowest control). Hence, with the knowledge of frequency content of disturbance and design of average controller the eqn. (3.37)-(3.39) and eqn. (3.40)-(3.42) provides design recommendations for PI controllers for first and second RLCs respectively. It is clear from eqn. (3.37) that $K_{c,1}$ should be large in compare to average controller gain and integral time for the same controller should satisfy eqn. (3.38) and (3.39) for all input frequencies. Similar recommendations are made for second RLC.

Based on eqns. (3.37)-(3.42) tuning parameters can be chosen for relative level controllers. One can choose integral time $\tau_{I,1}$ and $\tau_{I,2}$ to be small (5 -10 time smaller) in compare to time period of disturbances and integral time of average controller $\tau_{I,3}$. Once $\tau_{I,1}$ and $\tau_{I,2}$ are decided one can choose $K_{c,1}$ and $K_{c,2}$ which satisfy eqn. (3.37)-(3.42).

3.7 Optimal control structure

In previous sections we have proposed a new control structure and claimed that process has better control performance subject to control structure. The formulation of proposed control structure comes from physical understanding of the process explained earlier. In this section the focus is on deriving optimal control structure and corresponding controller tuning parameters as a solution of optimization problem. Two different objective functions are considered based on controller design criteria.

Case I

Objective function is formulated to remove unwanted variations in F_3 by minimization of term $\dfrac{\Delta F_3(p_j)-u_{\text{step}}}{u_{\text{step}}}$ for step disturbance of magnitude u_{step} in F_{in}. For sinusoidal disturbances the amplitude ratio of F_3 to F_{in} is minimized at steady state. Hence objective function is given as,

$$\min_{\mathbf{M},\mathbf{K},\mathbf{T}}\left(\underbrace{w\sum_{j=1}^{N}\left(\frac{\Delta F_3(p_j)-u_{\text{step}}}{u_{\text{step}}}\right)^2}_{\text{step response}}+\underbrace{\sum_{j=1}^{M}\left(\frac{a_{F_3}(\omega_j)}{a_{F_{\text{in}}}(\omega_j)}\right)}_{\text{sine response}}\right). \tag{3.43}$$

Subject to

$$\Delta L_i^{\min}\le \Delta L_i(t)\le \Delta L_i^{\max} \quad i=1,2,3\,,\; 0\le t\le t_{\max} \tag{3.44}$$

where Δ stands for deviation from equilibrium corresponding to the desired setpoint; $\Delta F_3(p_j)$ represents a peak value of F_3 at time p_j in the interval $0\le t\le t_{\max}$; N is the total number of peaks in the step response over the time interval $0\le t\le t_{\max}$; M is number of frequencies considered in the sinusoidal disturbance F_{in}; w is positive weight; $\mathbf{M}\in\Re^{3\times 3}$ is the transformation matrix in eqn. (3.6), which now has to be determined through optimization to provide the counterpart of the heuristic solution is eqn. (3.7); and the matrices $\mathbf{K},\mathbf{T}$ correspond to the three PI controllers to be designed, namely

$$\mathbf{K} = \begin{bmatrix} K_{c,1} & 0 & 0 \\ 0 & K_{c,2} & 0 \\ 0 & 0 & K_{c,3} \end{bmatrix}, \ \mathbf{T} = \begin{bmatrix} \dfrac{K_{c,1}}{\tau_{\mathrm{I},1}} & 0 & 0 \\ 0 & \dfrac{K_{c,2}}{\tau_{\mathrm{I},2}} & 0 \\ 0 & 0 & \dfrac{K_{c,3}}{\tau_{\mathrm{I},3}} \end{bmatrix}. \tag{3.45}$$

Case II

In this case objective function is formulated to remove unwanted variations in F_3 by minimization of rate of change of F_3 for step disturbance of magnitude u_{step} in F_{in}. For sinusoidal disturbances, the amplitude ratio of F_3 to F_{in} is minimized at steady state. This yields following objective function,

$$\min_{\mathbf{M},\mathbf{K},\mathbf{T}} \left(\underbrace{w \int_0^{t_{\max}} \left(\frac{dF_3}{dt} \right)^2 dt}_{\text{step response}} + \underbrace{\sum_{j=1}^{M} \left(\frac{a_{F_3}(\omega_j)}{a_{F_{\mathrm{in}}}(\omega_j)} \right)}_{\text{sine response}} \right). \tag{3.46}$$

Eqn. (3.46) is subject to inequality constraints in eqn. (3.44). The optimization variables are controller structure matrix $\mathbf{M}$ and controller tuning parameters $\mathbf{K}, \mathbf{T}$ as defined in eqn. (3.45).

Even though process under consideration is linear, the above formulated minimization problem is difficult to solve due to inequality constraints eqn. (3.44), large number of optimization variables and non-convexity of objective function (different combination of $\mathbf{M}, \mathbf{K}, \mathbf{T}$ can yield same objective function). Multiple initial points are considered to achieve global minima. Upper and lower bounds on initial guess for optimization variables $\mathbf{M}, \mathbf{K}, \mathbf{T}$ are considered and initial guesses are randomly selected.

In the case of 3 tanks in series there are 15 optimization variables. Due to non-convexity of the problem solution to optimization problem is function of initial point and not all initial guesses converged to get solution to eqn (3.43) or (3.46). Many of the initial points exploed the objective function indicating that solution to this problem is not trivial and it requires significant amount of efforts to reach global minima. The result reported in this work is based on 50 random initial guesses.

In Table 3.2 optimal control structures are compared with the control structuare developed based on hurestic approach in section 3.3. It is interesting to note that even though numbers are changed in each control structure closed-loop performance reamines nearly the same for all three control structures (Figure 3.11, Figure 3.12 Figure 3.13). Slight difference is observed in step response where the optimal solution tries to exploit dynamics more to achieve more attenuation for sinusoidal disturbance of period 3 hours. Another interesting observation is that sum of elements in first two rows of $\mathbf{M}$ (for first two controllers) is zero for all structures and it is non zero for third row. This indicates that optimal structure has particular structure which resembles what has been derived as huresric approach. Further, it is revealed that all structaures result nearly same values for the sum of attenuation factors for all three sinusoidal disturbances (periods 3, 2 and 1 hour).

Table 3.2. Control structure comparison

Approach	$\mathbf{M}$	$K_{c,i}$	$\tau_{I,i}$ (min)	Objective function	Attenuation, $\dfrac{a_{F_3}(\omega_j)}{a_{F_{in}}(\omega_j)}$
Heuristic	$\begin{bmatrix} 1 & -1 & 0 \\ 0 & 1 & -1 \\ 0.33 & 0.33 & 0.33 \end{bmatrix}$	$\begin{bmatrix} -0.2 \\ -0.2 \\ -0.023 \end{bmatrix}$	$\begin{bmatrix} 10 \\ 10 \\ 145 \end{bmatrix}$	Case I: 2.2 Case II: 2.09	0.69 0.49 0.25
Numerical optimization, Case I $w = 1$	$\begin{bmatrix} 0.84 & -.0.6 & -0.23 \\ 0 & 0.46 & -0.46 \\ 2.76 & -1.1 & 0.01 \end{bmatrix}$	$\begin{bmatrix} -0.05 \\ -0.08 \\ -0.014 \end{bmatrix}$	$\begin{bmatrix} 10 \\ 10 \\ 300 \end{bmatrix}$	2.15	0.55 0.33 0.50
Numerical optimization, Case II $w = 10^{10}$	$\begin{bmatrix} 0.83 & -0.83 & 0 \\ 0.70 & 0.40 & -1.1 \\ 4.37 & -4.80 & 0.85 \end{bmatrix}$	$\begin{bmatrix} -0.33 \\ -0.06 \\ -0.059 \end{bmatrix}$	$\begin{bmatrix} 10 \\ 10 \\ 300 \end{bmatrix}$	1.68	0.55 0.33 0.50

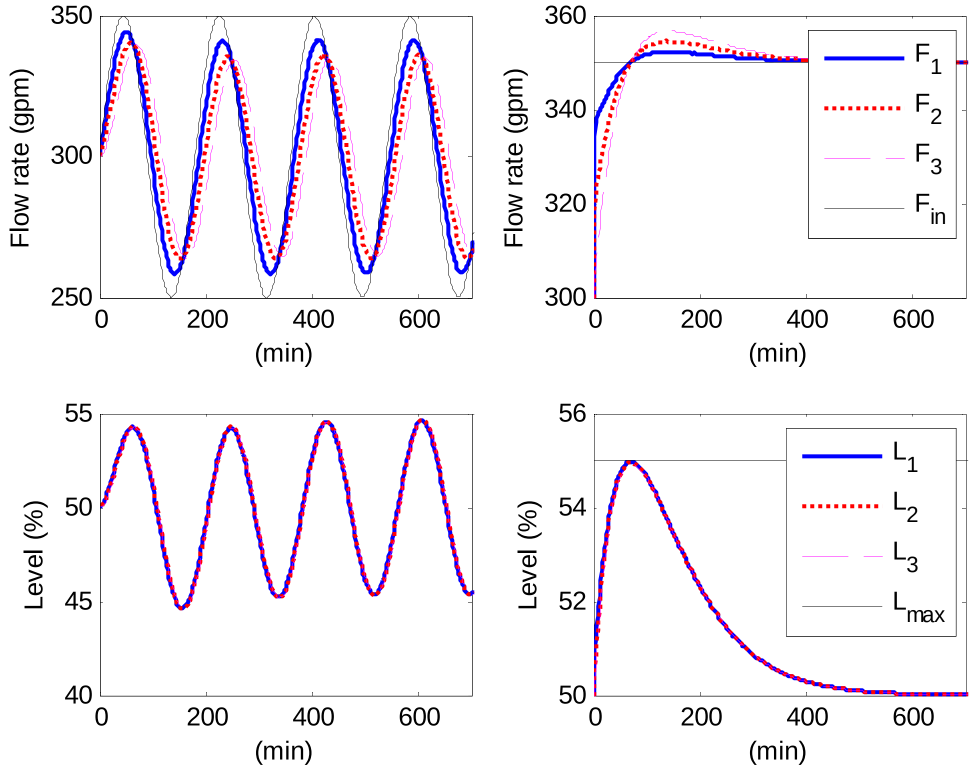

Figure 3.11. Closed-loop simulation for optimal structure derived from proposed scheme (Heuristic approach) for level constraint $\Delta L_{\max}(-\Delta L_{\min}) = 5\%$ in all tanks for sinusoidal and step disturbance of period 3 hr.

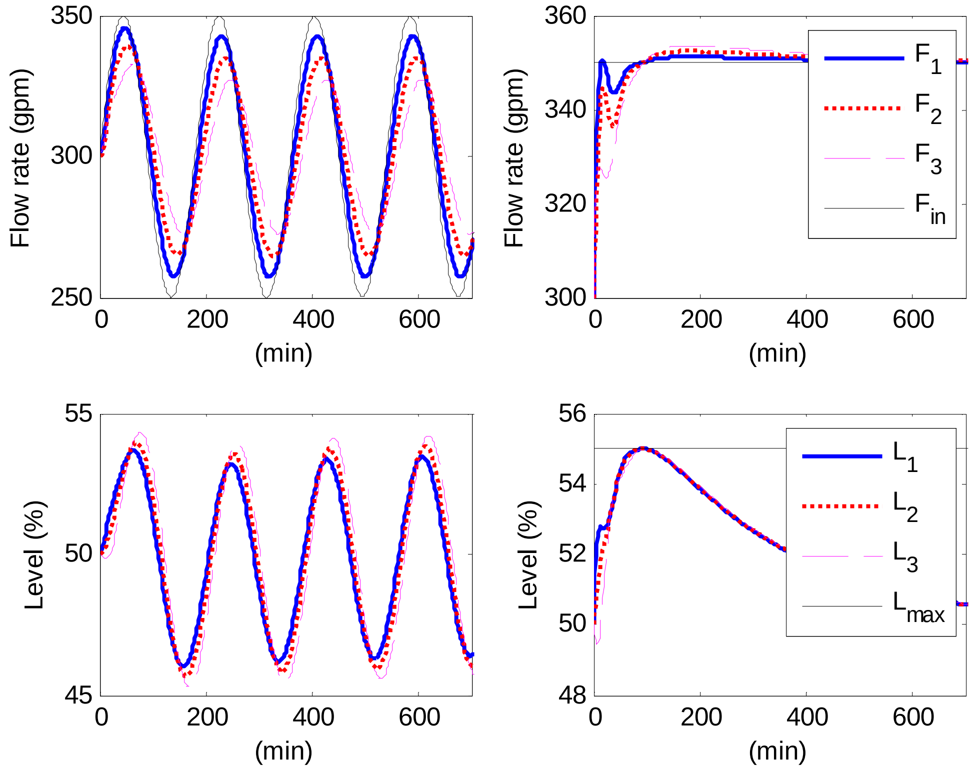

Figure 3.12. Closed-loop simulation for optimal structure derived from Case- I scheme for level constraint $\Delta L_{\max}(-\Delta L_{\min}) = 5\%$ in all tanks for sinusoidal and step disturbance of period 3 hr.

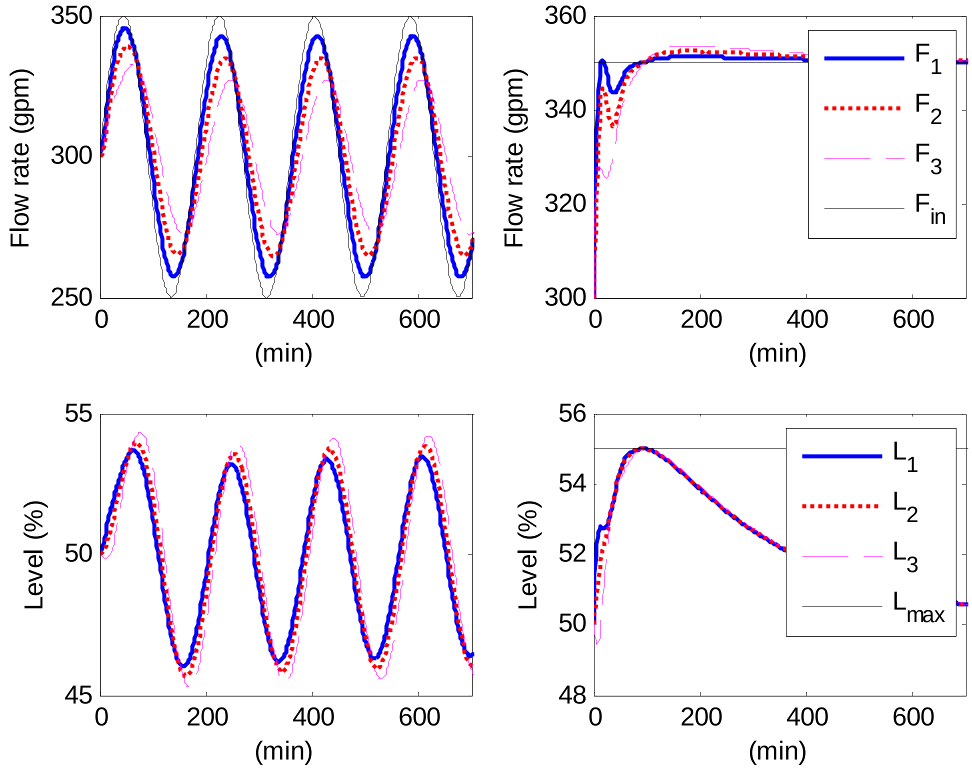

Figure 3.13. Closed-loop simulation for optimal structure derived from Case-II scheme for level constraint $\Delta L_{\max}(-\Delta L_{\min}) = 5\%$ in all tanks for sinusoidal and step disturbance of period 3 hr.

3.8 Application of proposed scheme

Control scheme which was discussed in previous sections is applied to 3 identical tanks in series for two different cases. Tuning charts Figure 3.7 and Figure 3.9 and Figure 3.8 are merged into single chart Figure 3.10 which is used to tune average level controller for step and sinusoidal disturbances using procedure described in previous section. Eqn. (3.37)-(3.42) are used for tuning of relative level controllers.

3.8.1 Case 1- Three tanks in series with same level constraints

Consider the case of 3 tanks in series with all tanks having the same inventory capacity. Process variables and constraints values are shown in Table 3.1. In this case $\gamma_{\text{step}} = \gamma_{\text{sine}} = 8.85$ and $Y_1 = Y_2 = 1$, yields $\eta = 3$ from eqn. (3.12). Thus $\gamma_{\text{step}} \Delta L_{\text{step}}^{\max} = \gamma_{\text{sine}} \Delta L_{\text{sine}}^{\max} = 26.55$ is desirable trajectory for tuning parameter in Figure 3.10. From the same figure it is clear that minimum possible flow attenuation is $r = 0.7$ and intersection of these two curves can be considered as tuning parameter. There is nearly no effect of increase in integral time $\tau_{\text{I},3} = 145$ on flow attenuation. Hence, the controller setting is chosen so that $\xi = 1$, $\gamma_{\text{step}} \Delta L_{\text{step}}^{\max} = 26.55$ and $r = 0.7$. From the Figure 3.10 this point is read as $\log(\tau_{\text{H}}) = 3.35$ ($K_{c,3} = -0.0224 \dfrac{\Delta F_3 m^3 / s}{\Delta L_3}$) and $\tau_{\text{I},3} = 145$ min. Next step is to check whether these settings for PI controller are in agreement to sinusoidal type disturbances. From eqn. (3.33) $\omega_0 = 2.23 * 10^{-4}$ rad/s at which maximum level deviation occurs. This frequency is less than the frequency content of disturbance ($1.7*10^{-3}$ – $5.28*10^{-4}$ coreesponds to time period 1 hr -3 hr). Hence in this case $\omega_{worst} = 5.28 * 10^{-4}$ rad/s (corresponds to time period of 3 hours) and Figure 3.10 indicates for $\omega_{worst} = 5.28 * 10^{-4}$ rad/s, $\Delta L_{\text{sine}}^{\max} \le \Delta L_{\text{step}}^{\max}$ for the chosen tuning settings. This suggests that design just based on step disturbance is also applicable to sinusoidal disturbances.

Tuning of relative level control is determined by eqn. (3.37)-(3.42). (Table 3.3) represents tuning recommendations for relative level controllers. Integral time of these controllers is chosen $\tau_{\text{I},1} = \tau_{\text{I},2} = 10$ min.Controllers gain are chosen $K_{\text{c},1} = -0.45 \dfrac{\Delta F_1 m^3 / s}{\Delta L_1}$

and $K_{c,2} = -0.45 \frac{\Delta F_2 m^3 / s}{\Delta L_2}$. Based on these tuning rules closed-loop response are shown in Figure 3.11 for the step disturbance and sinusoidal disturbance. The levels remain nearly same for all tanks and attenuation factor $r = 0.7$ is achieved which is in agreement to design criteria.

Table 3.3. Design of RLCs for case study 1

First RLC	Second RLC	Resulting tuning rules
$K_{c,3} \ll K_{c,1}$	$K_{c,3} \ll K_{c,2}$	$K_{c,3} \ll K_{c,2} = K_{c,1}$
$3A\omega \ll \frac{K_{c,1}}{\tau_{I,1}\omega}$	$3A\omega \ll \frac{K_{c,2}}{\tau_{I,2}\omega}$	$\tau_1 = \tau_2 \ll \frac{K_{c,1}}{3A\omega^2} = \frac{K_{c,1}}{3A\omega^2\phi}$ where $\phi \gg 1$ so that $K_{c,3} \ll K_{c,2} = K_{c,1}$
$A\omega \ll \frac{K_{c,1}}{\tau_{I,1}\omega}$	$A\omega \ll \frac{K_{c,2}}{\tau_{I,2}\omega} + \frac{K_{c,1}}{\tau_{I,1}\omega}$	

In the case of traditional feedback control scheme $\eta = 1$ and by eqn. (3.27) $\gamma = 1.77$ and $\gamma_{\text{step}} \Delta L_{\text{step}}^{\max} = \gamma_{\text{sine}} \Delta L_{\text{sine}}^{\max} = 8.85$. Figure 3.10 can be used to understand how this scheme is ineffective to achieve desired control objectives. Intersection of lines corresponding to $\xi = 2$ and $\gamma_{\text{sine}} = 8.85$ (it is noticeable that sinusoidal disturbance has more level variation than step disturbance for $\gamma_{\text{step}} \Delta L_{\text{step}}^{\max} = \gamma_{\text{sine}} \Delta L_{\text{sine}}^{\max} = 8.85$) results in $\log(\tau_{\text{H}}) = 2.73$ and $\tau_{\text{I},3} = 143$ min and this combination results in minimum value $r = 1.05 > 1$. It is clear that the proposed scheme perfoms much better as compared to traditional feedback scheme.

3.8.2 Case 2- Three tanks in series with different level constraints

System under consideration in this example is the same as the previous expect the level constraint is different in the second tank (Table 3.4). This example is corresponding to one of the plant implementation of proposed scheme. It has been realized that level variation in tank 1 and tank 3 should be kept at 5% while and most of level variation (30%) should happening in tank 2 (Bayer 2008). This yields $Y_1 = 6, Y_2 = 1/6$ and $\gamma_{\mathrm{step}} \Delta L_{\mathrm{step}}^{\max} = 70.8$ (it is evident from Figure 3.7 and Figure 3.9 that if combination of tuning parameter satisfies level constraint for step disturbance it will always satisfy level constraint for sinusoidal disturbance). For values of ξ in between 0.5 and 1, the minimum value of attenuation factor is $r = 0.24$ at $\xi = 0.5$ for $\gamma_{\mathrm{step}} \Delta L_{\mathrm{step}}^{\max} = 70.8$ and this yields tuning parameters as $\log(\tau_{\mathrm{H}}) = 3.89$ ($K_{\mathrm{c},3} = -0.0174 \dfrac{\Delta F_3 m^3/s}{\Delta L_3}$) and $\tau_{\mathrm{I},3} = 139$ min. From eqn. (3.33) $\omega_0 = 1.095*10^{-4}$ for at which maximum occurs for level deviation. This frequency is less than the frequency content of disturbance ($1.7*10^{-3}$ – $5.28*10^{-4}$) and hence $\omega_{\mathrm{worst}} = 5.28*10^{-4}$ rad/s. Tuning of relative controllers has been performed based on Table 3.5 which yields $\tau_{\mathrm{I},1} = \tau_{\mathrm{I},2} = 10$ min, $K_{\mathrm{c},1} = -0.6 \dfrac{\Delta F_1 m^3/s}{\Delta L_1}$ and $K_{\mathrm{c},2} = -3.6 \dfrac{\Delta F_2 m^3/s}{\Delta L_2}$. Closed -loop response for step change and sinusoidal disturbance are shown in Figure 3.14.

Table 3.4. Tank model parameters and constraints for case-2

$A\,[\text{m}^2]$	F_0 [gpm]	u_{step} [gpm]	$a_{F_{\text{in}}}$ [gpm]	$L_{\max}\,(=L_{\min})$ [%]	H [m]	Time period of disturbances [hr]
16.72	300	50	50	5,30,5	2	1-3

This particular scheme is implemented in the real plant. Figure 1.2 and Figure 1.3 show actual plant data for level and flow variations with tradition feedback scheme. Figure 3.15 and Figure 3.16 compare the response of closed loop before and after the installation of proposed control scheme. Level variations in tank # 3 has reduced and most of level variation is happening in tank 2. These results show that the proposed scheme has improved the performance of closed loop and it is in agreement to the simulated results.

Table 3.5. Design of RLCs for case study 2

First RLC	Second RLC	Resulting tuning rules
$K_{c,3} \ll 6K_{c,1}$	$K_{c,3} \ll K_{c,2}$	$K_{c,3} \ll K_{c,2} = 6K_{c,1}$
$3A\omega \ll \dfrac{6K_{c,1}}{\tau_{\text{I},1}\omega}$	$8A\omega \ll \dfrac{K_{c,2}}{\tau_{\text{I},2}\omega}$	$\tau_1 = \tau_2 \ll \dfrac{6K_{c,1}}{8A\omega^2} = \dfrac{6K_{c,1}}{8A\omega^2\phi}$ where $\phi \gg 1$ so that $K_{c,3} \ll K_{c,2} = 6K_{c,1}$
$A\omega \ll \dfrac{6K_{c,1}}{\tau_{\text{I},1}\omega}$	$A\omega \ll \dfrac{K_{c,2}}{\tau_{\text{I},2}\omega} + \dfrac{K_{c,1}}{\tau_{\text{I},1}\omega}$	

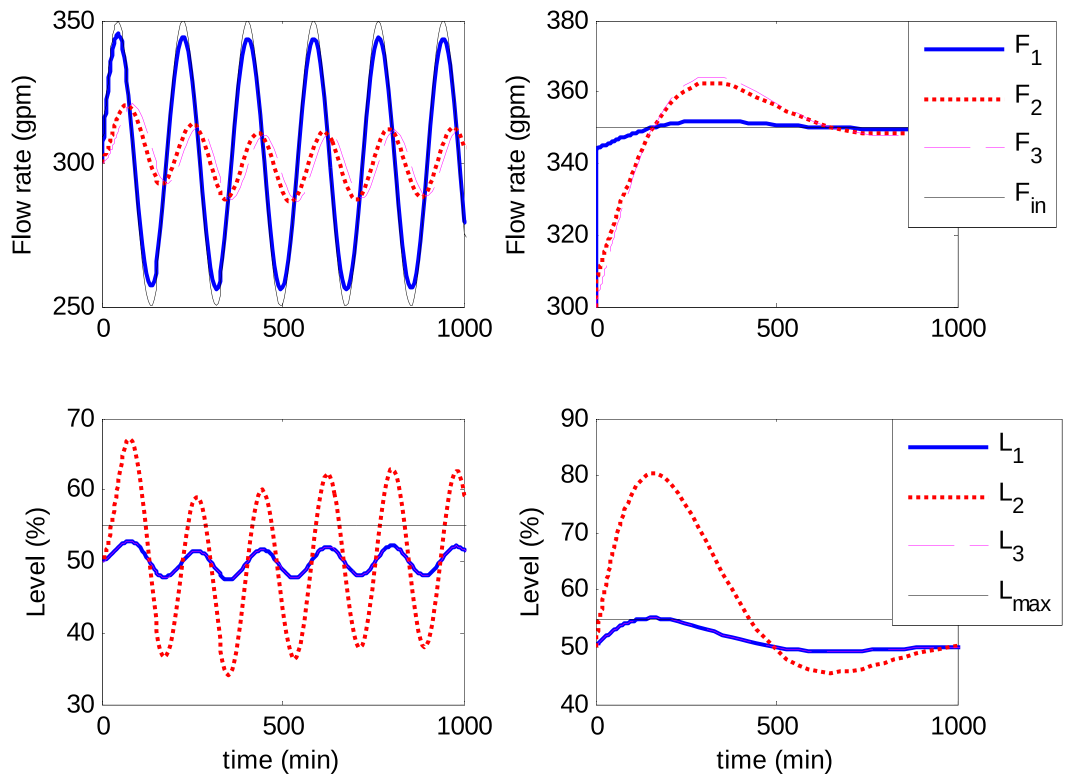

Figure 3.14. Closed-loop response for sinusoidal and step disturbance of time period 3 hr with $\Delta L_{\max} = 5, 30, 5\%$ for 1st, 2nd and 3rd tank respectively.

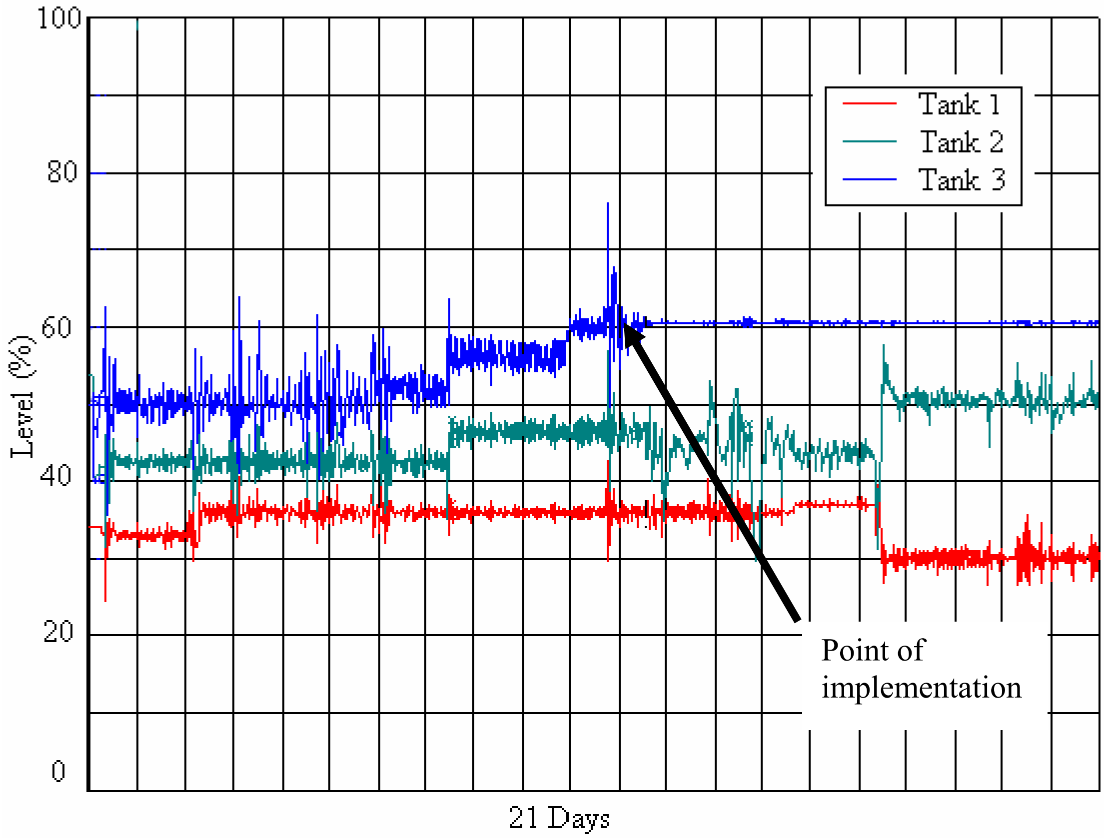

Figure 3.15. Level variations in real plat for traditional and proposed schemes.

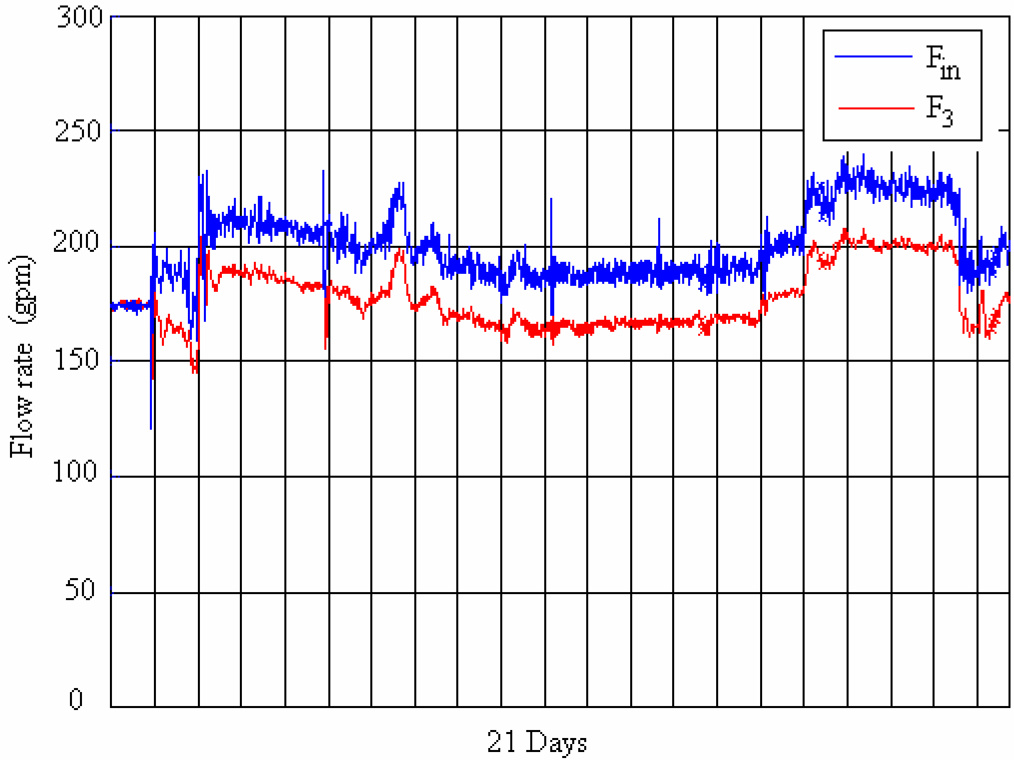

Figure 3.16. Inlet and outlet flow variations in real plat for proposed schemes.

3.9 Feedforward scheme

Feedforward scheme is simple to implement for proposed feedback control structure. Since, the closed-loop behavior of tanks in series is represented by a single tank (eqns. (3.11)-(3.12)), effectively one has to design feedforward scheme for a single tank where flow rate F_{in} is feedforwarded to the last tank's level controller. It is important to determine how much information should be forwarded to feedback controller. In Figure 3.17 if $C_{ff} = 0$ closed loop is feedback only and if $C_{ff} = 1$ then closed loop is feedforward only and controller response will be very fast to any disturbance. In this case level will remain unchanged but there will be no flow attenuation. Hence, the optimal value of C_{ff} will be in between 0 and 1 and will depend on frequency content of inlet feed disturbance and choice of tuning parameters. To determine C_{ff} for proposed heurestic scheme, an optimization problem is formulated which minimizes the amplitude ratio of F_3 to F_{in} and given by

$$\min_{C_{\mathrm{ff}}} \sum_{j=1}^{M} r_j(\omega) = \min_{C_{\mathrm{ff}}} \sum_{j=1}^{M} \left(\frac{\dfrac{1}{\tau_{\mathrm{H}}^2} + \left(\dfrac{1}{\omega_j \tau_{\mathrm{H}} \tau_{\mathrm{I},3}} \right)^2}{\left(\dfrac{1}{\tau_{\mathrm{H}}^2} + \left(\omega_j - \dfrac{1}{\omega_j \tau_{\mathrm{H}} \tau_{\mathrm{I},3}} \right)^2 \right)} \right)^{\frac{1}{2}}, \tag{3.47}$$

subject to level constraints in eqn. (3.2) and

$$0.5 \le \xi \le 2\,. \tag{3.48}$$

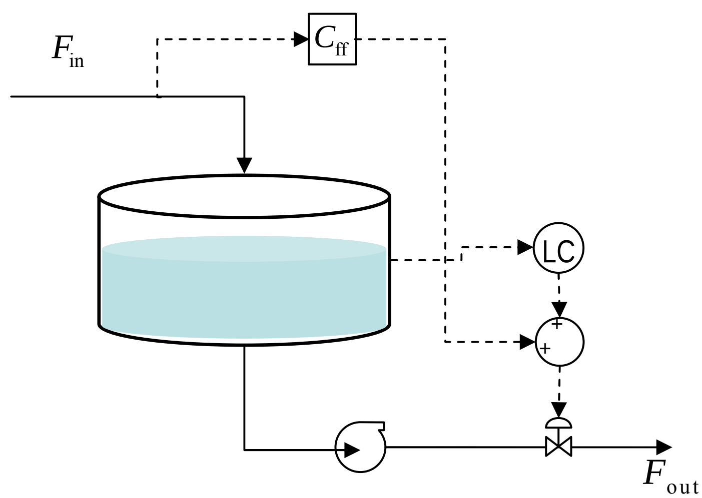

Figure 3.17. Feedback-Feedforward configuration for level control

(Cheung and Luyben 1979) have proposed feedback feedforward (FB-FF) control structure for several tanks in series. This controller scheme is designed for step disturbance and the objective is only disturbance rejection, hence $C_{\mathrm{ff},i} = 1$ is considered for tight level control. However, in the present work sinusoidal disturbance is also present and flow attenuation is important. This requires that optimal values of $C_{\text{ff},i}$ for $i=1,2,3$ (feedfordward for each tank) are used which can be determined by minimizing the amplitude ratio of F_3 to F_{in}, given by

$$\min_{C_{\text{ff},i}} \sum_{j=1}^{M} r_j(\omega) = \min_{C_{\text{ff},i}} \sum_{j=1}^{M} \left(\prod_{i=1}^{3} \left(\frac{\frac{1}{\tau_{\text{H},i}^2} + \left(\frac{1}{\omega_j \tau_{\text{H,i}} \tau_{\text{I},3}} \right)^2}{\left(\frac{1}{\tau_{\text{H},i}^2} + \left(\omega_j - \frac{1}{\omega_j \tau_{\text{H},i} \tau_{\text{I},3}} \right)^2 \right)} \right) \right)^{\frac{1}{2}}, \tag{3.49}$$

subject to level constraints in eqn. (3.2) and constraints

$$0.5 \le \xi_i \le 2 \text{ for } i = 1,2,3\,. \tag{3.50}$$

Based on the above optimized feedforward structure, comparison of FB-FF scheme with the proposed heuristic scheme which is based on average level feedback feedforward (Avg-FB-FF) scheme is performed for the three tanks in series with specification given in Table 3.1. For simple comparison it is assumed process is subject to only disturbance of frequency 5.8*10^{-4} rad/s and tuning is done for critically damped closed-loop (i.e., $\xi = 1$). For Avg-FB-FF $C_{\text{ff}} = 0.24$ and for FB-FF scheme $C_{\text{ff},1} = 0.69, .C_{\text{ff},2} = 0.71,\ C_{\text{ff},3} = 0.72$ Controllers are tuned based on optimized values of C_{ff} and $C_{\text{ff},i}$ for $i=1,2,3$ for Avg-FB-FF and FB-FF schemes repectively. Figure 3.18 shows closed-loop response of both schemes. It is clear that both schemes are able to achieve flow rate attenuation of 70%. In FB-FF scheme $C_{\text{ff},\,i}$ are nearly three times higher than Avg-FB-FF scheme and this compensates for 3 times inventory available in Avg-FB-FF scheme. Therefore it is concluded that both schemes when properly optimized performs similarly for the disturbance they have been optimized. However, it is important to analyze the performance of both schemes at other frequencies. Figure 3.19 shows bode plot for attenuation factor defined by optimization problem in eqns.(3.47) and (3.49) for Avg-FB-FF scheme and FB-FF scheme respectively. It is clear that Avg-FB-FF scheme has better performance for all the frequencies higher than designed frequency ($5.8*10^{-4}$ rad/s). This suggests that the performance of FB-FF scheme is more sensitive towards the disturbances for which is it not optimized in compare to Avg-FB-FF scheme. This is actually true as effective inventory capacity is more in the Avg-FB-FF scheme and hence its dependence on feedforward information to achieve attenuation is less in compare to FB-FF scheme (as suggested by C_{ff} values). Any discrepancy in inlet flow will affect the performance of FB-FF shceme more significantly than Avg-FB-FF scheme.

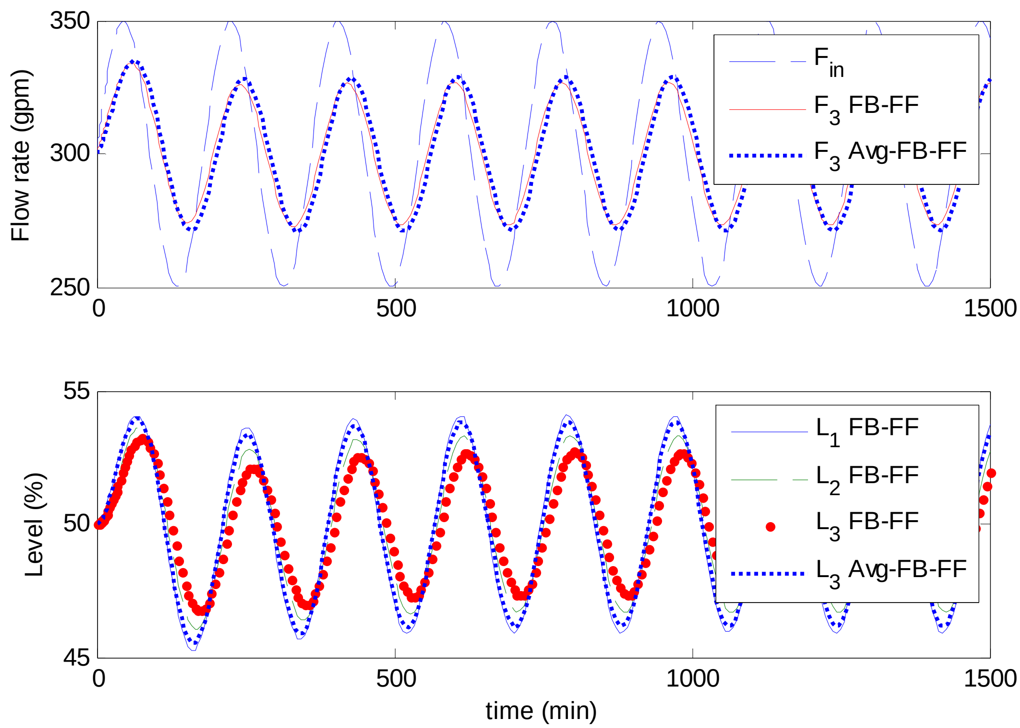

Figure 3.18. Comparison of proposed scheme to Luyben's scheme with feedforwardstructure for sinusoidal disturbance of period 3 hr.

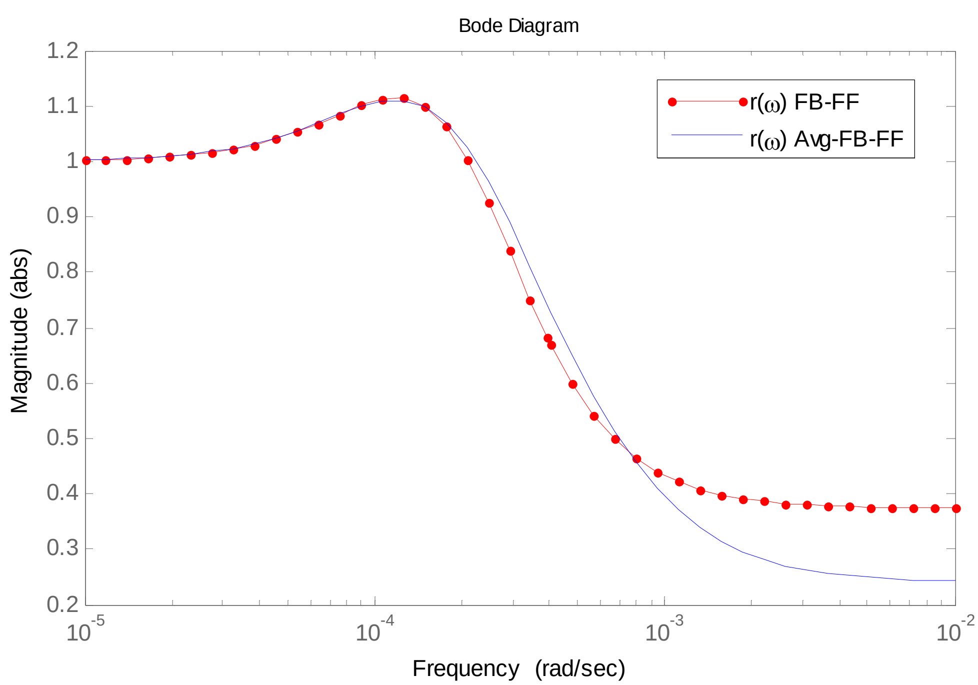

Figure 3.19. Attenuation factor r for proposed and Luyben's feedforward scheme for various frequencies.

3.10 Conclusions and future work

Plant bottlenecking is one of practical issues with process industries. The proposed scheme suggests that it is possible to remove bottlenecking of level control without increasing equipment capacity, by exploiting the dynamics of closed loop in better way. It has been demonstrated that multivariate control structure design has improved the performace of the level control in an industrial liquid-liquid extraction process performed in three tanks in series. Eventually whole system works as a single tank and one need to design average control based on tuning chart presented in Figure 3.10. The designing criteria for relative level control suggests that these controllers have to be fast enough in compared to time period of disturbance and integral time of average controller.

The augumentation of feedforward control structure for proposed scheme is simple and is less dependent on feedforward strcuture in comparison to other schemes. An important finding is that the solutions to numerical optimization to minimize the desired control objective for optimal control structure along with tuning parameters of PI controller; result in control structure which resemble to proposed control structure in section 3.3. However such an optimization is not at all trivial, even though level control process considered here is relatively simple with 3 tanks in series. This suggests that such heuristic approach has practical significance.

The proposed control scheme is not limited to debottleneck level control problem in tanks in series. It can be easily used to couple two or more distillations column for control of bottom level or reactors for their liquid level. However, additional attention is required in those situations so that coupling does not effect columns/reactors performances.

CHAPTER 4

OPTIMAL RULES FOR CENTRAL BANK INTEREST RATE SUBJECT TO ZERO LOWER BOUND

4.1 Introduction and Motivation

As mention in section 1.3 that central bank interest rate can be expressed by Taylor rule Figure 1.6. The general form of the standard Taylor rule suggests that the short-term interest rate i_t applied by the central bank at time t can be set according to the formula

$$i_t = \phi_y(y_t - y^*) + \phi_\pi(\pi_t - \pi^*) + r^* + \pi^* \tag{4.1}$$

where y, π, and i are defined section 1.3.2; subscript t refers to the time the rule is applied, using information up to that time; superscript * represents the desired equilibrium value; $r \mathrel{\hat{=}} i - \pi$ is the real interest rate; and ϕ_y, ϕ_π are coefficients associated with the output gap and inflation rate respectively. In the original publication (Taylor 1993) Taylor assumed $y^* = 0$, $\pi^* = 2\%$, $r^* = 2\%$, $\phi_\pi = 1.5$, $\phi_y = 0.5$, quarterly data for output gap, and annual data for inflation rate. Variants of the above basic Taylor rule have studied in literature, such as rules with an inertia term containing i_{t-1} and/or with projected future values of π and y in the right-hand side of eqn. (4.1) (Taylor and Williams 2010, and references therein).

Taylor has been systemically derived as a solution to minimization of quadratic objective function using small economy model when optimization does not involves ZLB constraint (Ball 1999; Orphanides and Wieland 2000; Giannoni and Woodford 2002; Orphanides 2003). However, in the presence of ZLB, no such rules have been derived because researchers have focused to solve the constrained optimization problem by formulation of dynamic programming whose explicit solution is hard to get. While solution to the optimization problem in the framework of dynamic programming can produce optimal numbers for interest rate but it does not provide a rule. At the same time some of the researchers have proposed simple ad-hoc rules that rely on truncation to zero of an interest rate i_t^{TR} calculated by a Taylor rule (i.e., $i_t = \max[0, i_t^{\mathrm{TR}}]$)(Reifschneider and Williams 2000; Williams 2006; Nakov 2008). However, such rules may not be optimal.

Interesting observations were made in simulation studies. For example, it was observed (Orphanides and Wieland 2000; Kato and Nishiyama 2005) that resulting policies may be nonlinear, (rather than piecewise linear, according to truncated Taylor rules) and more aggressive for interest rates close to ZLB (a behavior characterized as pre-emptiveness). However, a rigorous derivation of simple explicit Taylor rule subject to ZLB is, to our knowledge, not currently available.

In this research work, we rigorously derive explicit rules for interest rate subject to ZLB. Our approach relies on a formalism known as multi-parametric programming (mp), a technique applied by the engineering community to constrained model predictive control (MPC) (Pistikopoulos, Dua et al. 2000) or constrained state estimation problems (Darby and Nikolaou 2007). The following are the key elements of the proposed approach.

- When a ZLB is present, explicit rules can be developed that produce a value for the interest rate through application of one from a finite number of explicit formulas. These formulas entail a finite number of Taylor-like rules as well as the value of the lower bound (assumed here to be zero). To know which of these formulas will be applied at any time, one has to simply check which inequality is satisfied out of a finite number of a priori developed mutually exclusive linear inequalities on the inflation and output gap.

- Various forms of Taylor-like rules result rigorously from the particular form of the quadratic objective used in MPC. For example, Taylor rules with inertia terms arise from inclusion of a quadratic penalty on the rate of change of the interest rate (rather than on the interest rate itself).
- Application of any interest rate policy, Taylor-like or not, on an economy essentially creates a closed-loop feedback controlled system. As such, any policy should, at the very least, result in a stable closed loop. Additionally, it should be fairly robust, namely produce sensible results in the presence of discrepancies between assumed economy models and the actual economy.

In the rest of the research work we first provide some background on MPC and mpMPC, and elaborate on the small-scale economy model used. Within this setting, we derive a number of Taylor-like rules, based on a number of MPC quadratic objectives, and examine their dependence on relative weights of various terms in the MPC objective. The effect of these rules on the resulting closed-loop behavior is examined. Comparison with the standard Taylor rule and actual interest rates implemented by the Central bank is provided. Finally, future extensions are proposed.

4.2 Preliminaries: Model Predictive Control (MPC) and Taylor rules

MPC is a class of model-based feedback control algorithms for systems with constraints (Maciejowski 2000; Rawlings and Mayne 2009). MPC finds the value of the manipulated input (interest rate in our case) of a controlled process at each point in time by setting up and solving a constrained optimization problem at that time. The optimization involves an objective function (usually quadratic) over a finite future horizon. The objective contains terms involving future predictions of the controlled variables (output gap and inflation in our case) as well as penalty terms on manipulated inputs within the finite horizon. Future output predictions are established in terms of a model.

As will be made clear below, MPC (also known as "open-loop optimal feedback") differs from stochastic dynamic programming (also known as "closed-loop optimal feedback") in that MPC does not explicitly account for information that is now expected to be available in the future, thus avoiding the computational complexity of the nested optimization (curse of dimensionality from Bellman's principle of optimality) which burdens stochastic dynamic programming.

Next, we first provide a description of the model we use, and subsequently explain its use in formulating the MPC optimization.

4.2.1 Economy model structure

A semi-empirical linear model around a baseline can describe the evolution of the economy as

$$y_{t+1} = \rho y_t - \xi \left(i_t - \pi_t \right) + e_{t+1}^{y}, \tag{4.2}$$

$$\pi_{t+1} = \pi_t + \alpha y_t + e_{t+1}^{\pi}. \tag{4.3}$$

(Ball 1999) where y, π, and i are as above; α and ξ are positive constants; $\rho \in [0,1)$; e_{t+1}^{y} and e_{t+1}^{π} are zero-mean white noise signals; and the sampling period (time interval from t to $t+1$) is one year. The above model is similar in spirit to more complicated models used by many central banks. The model's main purpose is to capture the dynamic causal relationship between the manipulated input i and the two controlled outputs, y, π.

At steady state (equilibrium point), $i_t = i^*$, $y_t = 0$ and $\pi_t = \pi^*$, with $r^* = i^* - \pi^*$. Hence in the terms of deviation variables from the equilibrium point, eqns. (4.2) and (4.3), can be written as

$$\mathbf{x}_{t+1} = \mathbf{A}\mathbf{x}_t + \mathbf{B}u_t + \boldsymbol{\varepsilon}_{t+1}, \tag{4.4}$$

where

$$\mathbf{x} \triangleq \begin{bmatrix} \Delta y \\ \Delta \pi \end{bmatrix} \triangleq \begin{bmatrix} y - y^* \\ \pi - \pi^* \end{bmatrix},\ u \triangleq \Delta i \triangleq i - i^*,\ \boldsymbol{\varepsilon} \triangleq \begin{bmatrix} e^{y} \\ e^{\pi} \end{bmatrix}, \tag{4.5}$$

$$\mathbf{A} \triangleq \begin{bmatrix} \rho & \xi \\ \alpha & 1 \end{bmatrix}, \tag{4.6}$$

$$\mathbf{B} \triangleq \begin{bmatrix} -\xi \\ 0 \end{bmatrix}. \tag{4.7}$$

Using the above model, the optimal k-step-ahead prediction for the state $\mathbf{x}$ with initial condition $\mathbf{x}_t$ is

$$\hat{\mathbf{x}}_{t+k|t} = \sum_{\ell=0}^{k-1} \mathbf{A}^{\ell}\mathbf{B}u_{t+k-\ell-1|t} + \mathbf{A}^{k}\mathbf{x}_t, \tag{4.8}$$

(Ljung 1999) where $\hat{\mathbf{x}}_{t+k|t}$ stands for the expected value of $\mathbf{x}$ at time $t+k$ using all information available at time t. The above prediction will be used in the formulation of the MPC objective below.

It should be noted that the idea here is not to fully explain the complex dynamics of the economy with such a simple linear model. Rather, the intended use of the above model is to help understand how optimal monetary policies are affected by various objective functions and by a ZLB on the interest rate when constrained MPC is used to derive such policies. The dimension of the state vector $\mathbf{x}$ is also limited to two, so that the solution of the constrained MPC optimization problem can be easily understood graphically in 2-D and 3-D plots using the mpMPC approach.

4.2.2 Economy model calibration

The economy model expressed by eqns. (4.2) and (4.3) is calibrated based on US revised economy data over the time period 1976-2007. The annual revised output gap data is taken from the Congressional Budget Office (CBO 2011). Inflation is calculated as annual percentage change in the GDP deflator Q4/Q4 basis (Bureau of economic Analysis). The real interest rate, r, is calculated as the annual average of the interest rate (federal fund rate) deflated by the annual inflation rate. Interest rates are taken from the database of the Federal Reserve System. Figure 1.4 plots these data for the time period 1976-2010. Based on these data, Table 4.1 presents estimated values of parameters for the economy model, obtained using the prediction error method. Based on the parameter estimates in Table 4.1, the matrix $\mathbf{A}$, eqn. (4.6) turns out to be

$$\mathbf{A} = \begin{bmatrix} 0.63 & 0.19 \\ 0.12 & 1 \end{bmatrix}. \tag{4.9}$$

Table 4.1. Parameter estimates of US economy model

Parameter	Estimate	Standard Error
ρ	0.63	0.06
ξ	0.19	0.05
$r*$	1.9	0.74
α	0.12	0.06
σ_{e^y}	1.4	
σ_{e^π}	0.93	

The eigenvalues of $\mathbf{A}$ are 0.58 and 1.05, suggesting that the economy model for the US economy is unstable. Consequently, whatever control policy ones chooses to control the US economy, such a policy must be, at the very least, a stabilizing policy. We develop such a policy below via MPC.

4.2.3 Formulation of MPC optimization

The central bank's generalized loss function projected to infinity at time t is generally of the form

$$\sum_{k=0}^{\infty} \beta^k L(\hat{\mathbf{x}}_{t+k|t}, u_{t+k|t}) . \tag{4.10}$$

After minimizing the above objective at time t, the first element $u_{t|t}^{\text{opt}}$ of the optimal sequence $\{u_{t|t}^{\text{opt}}, u_{t+1|t}^{\text{opt}}, ...\}$ is implemented, and the system (i.e.,the economy) runs until the next decision making point, t_{next}. At time t_{next} the optimization problem in eqn. (4.10) is reformulated, solved, the first element $u_{t_{\text{next}}|t_{\text{next}}}^{\text{opt}}$ of the optimal sequence $\{u_{t_{\text{next}}|t_{\text{next}}}^{\text{opt}}, u_{t_{\text{next}}+1|t_{\text{next}}}^{\text{opt}}, ...\}$ is implemented, the system runs until the next time, and the process continues to infinity. The difference $t_{\text{next}} - t$ is selected here to be one quarter. It should be stressed that, in general, $u^{\text{opt}}_{t_{\text{next}}|t_{\text{next}}} \neq u^{\text{opt}}_{t+1|t}$ because of modeling uncertainty and external disturbances.

It has been shown (Muske and Rawlings 1993) that for quadratic $L(\hat{\mathbf{x}}_{t+k|t}, u_{t+k|t})$ stability of constrained MPC can be ensured if the objective in eqn. (4.10), which involves an infinite number of terms, is replaced by an equivalent objective that involves summation of a finite number of terms plus a terminal cost and/or terminal constraints. A particular realization of this idea can take the form

$$\min_{\mathbf{u}} \left\{ \sum_{k=0}^{N-1} \beta^k \left(\hat{\mathbf{x}}^T_{t+k|t} \mathbf{Q} \hat{\mathbf{x}}_{t+k|t} + R^2 u^2_{t+k|t} + S^2 \delta u^2_{t+k|t} \right) + \hat{\mathbf{x}}^T_{t+N|t} \beta^N \overline{\mathbf{Q}} \hat{\mathbf{x}}_{t+N|t} + \beta^N S^2 \delta u^2_{t+N|t} \right\}, \tag{4.11}$$

subject to the model constraints

$$\hat{\mathbf{x}}_{t+k|t} = \sum_{\ell=0}^{k-1} \mathbf{A}^{\ell} \mathbf{B} u_{t+k-\ell-1|t} + \mathbf{A}^k \mathbf{x}_t,\ k = 1, \ldots, N, \tag{4.12}$$

$$\hat{\mathbf{x}}_{t|t} = \mathbf{x}_t, \tag{4.13}$$

the unstable mode stabilization constraints

$$\tilde{\mathbf{v}}^T_{\mathrm{u}} \left[\mathbf{A}^{N-1}\mathbf{B}, \mathbf{A}^{N-2}\mathbf{B}, \ldots, \mathbf{B} \right] \mathbf{u} = -\tilde{\mathbf{v}}^T_{\mathrm{u}} \mathbf{A}^N \mathbf{x}_t, \tag{4.14}$$

the input move restriction constraints

$$u_{t+k|t} = u_{t+m-1|t},\ k = m, \ldots, N-1, \tag{4.15}$$

and the inequality constraints

$$u_{t+k|t} \geq -i^*,\ k = 0, \ldots, N-1, \tag{4.16}$$

where

$$\mathbf{u} \triangleq \begin{bmatrix} \Delta i_t \\ \Delta i_{t+1|t} \\ . \\ . \\ \Delta i_{t+N-1|t} \end{bmatrix}, \tag{4.17}$$

$$\delta u_{t+k|t} \triangleq u_{t+k|t} - u_{t+k-1|t}, \; k = 0, \ldots, N, \tag{4.18}$$

$$\mathbf{Q} \triangleq \begin{bmatrix} 1-\lambda & 0 \\ 0 & \lambda \end{bmatrix} \succ 0, \;\; 0 < \lambda < 1 \tag{4.19}$$

$$\bar{\mathbf{Q}} \triangleq \frac{\mathbf{v}_\mathrm{s}^T \mathbf{Q} \mathbf{v}_\mathrm{s}}{1-\beta J_\mathrm{s}^2} \tilde{\mathbf{v}}_s \tilde{\mathbf{v}}_\mathrm{s}^T \succ 0, \tag{4.20}$$

(see Appendix E) with the vectors $\mathbf{v}_\mathrm{s}$ and $\tilde{\mathbf{v}}_\mathrm{s}$ coming from the diagonalization of the matrix $\mathbf{A}$ as

$$\mathbf{A} = \mathbf{V}\mathbf{J}\mathbf{V}^{-1} = \left[\begin{array}{c|c} \mathbf{v}_\mathrm{u} & \mathbf{v}_\mathrm{s} \end{array} \right] \begin{bmatrix} J_\mathrm{u} & 0 \\ 0 & J_\mathrm{s} \end{bmatrix} \begin{bmatrix} \tilde{\mathbf{v}}_\mathrm{u}^T \\ \hline \tilde{\mathbf{v}}_\mathrm{s}^T \end{bmatrix}, \tag{4.21}$$

where J_u and J_s refer to the unstable and stable eigenvalues of the matrix $\mathbf{A}$ with corresponding eigenvectors, $\mathbf{v}_\mathrm{u}$ and $\mathbf{v}_\mathrm{s}$, respectively.

The main rationale behind the above formulation is that closed-loop stability can be guaranteed by including the terminal penalty term $\hat{\mathbf{x}}_{t+N|t}^T \bar{\mathbf{Q}} \hat{\mathbf{x}}_{t+N|t}$ in the objective, eqn. (4.11), and by explicitly forcing a terminal constraint, eqn. (4.14), to stabilize the unstable mode corresponding to the eigenvalue J_u. The values of the weights R and S determine the aggressiveness of the resulting control action, with small values of R and S encouraging more aggressive action and faster closed-loop response, at the cost of decreased closed-loop robustness (Orphanides 2003; Orphanides and Williams 2007). In particular, higher values of S are preferred when persistent external disturbances force the input i away from its nominal equilibrium value i^*. Finally, the values of $1-\lambda$ and λ in eqn. (4.19) determine the relative attention paid by the policy to output gap and inflation, respectively.

4.3 Taylor rules from MPC

In this section we show how Taylor rules can be derived from unconstrained MPC. Specifically, in section 4.3.1 we derive rules that follow the Taylor structure (eqn. (4.1)) while in section 4.5 we show how Taylor rules with inertia can be naturally derived from MPC with an additional quadratic penalty on the rate of change of interest rate. For both cases we examine the effects of MPC weights (λ, R, or S in eqn. (4.11)).

4.3.1 Taylor rules from MPC without zero lower bound

In the absence of ZLB, eqn. (4.16), and without penalty on the change of interest rate ($S=0$), the MPC optimization with objective function in eqn. (4.11) subject to equality constraints in eqns. (4.12)-(4.15) results in the unconstrained quadratic minimization

$$\min_{\mathbf{u}_m}\left[\frac{1}{2}\mathbf{u}_m^T\mathbf{H}\mathbf{u}_m+\mathbf{x}_t^T\mathbf{F}\mathbf{u}_m+\frac{1}{2}\mathbf{x}_t^T\mathbf{Y}\mathbf{x}_t\right], \tag{4.22}$$

where $\mathbf{H}\in\Re^{(m-1)\times(m-1)}$, $\mathbf{F}\in\Re^{2\times(m-1)}$, $\mathbf{Y}\in\Re^{2\times2}$ are function of $\mathbf{A}$, $\mathbf{B}$, β, N, m, and the weights R and λ; and the decision variable is

$$\mathbf{u}_m \triangleq \begin{bmatrix} \Delta i_t \\ \Delta i_{t+1|t} \\ . \\ . \\ \Delta i_{t+m-2|t} \end{bmatrix}. \tag{4.23}$$

(see Appendix E). The minimum in eqn. (4.22) is attained at $\mathbf{u}_m^{\text{opt}} = -\mathbf{H}^{-1}\mathbf{F}^T\mathbf{x}_t$, resulting in the optimal interest rate,

$$i_t = -\underbrace{\begin{bmatrix} 1 & 0 & \cdots & 0 \end{bmatrix}}_{m-1}\mathbf{H}^{-1}\mathbf{F}^T\mathbf{x}_t + r^* + \pi^* = \phi_y(y_t - y^*) + \phi_\pi(\pi - \pi^*) + r^* + \pi^*. \tag{4.24}$$

at time t, which is clearly a Taylor-like rule, as in eqn. (4.1). It is also clear that ϕ_y, ϕ_π are functions of the economic model matrices $\mathbf{A}$, $\mathbf{B}$, and of the weights R, λ, given N, m and β.

4.3.1.1 Choice of prediction horizon length, N

For an unstable system such as the one described by eqns. (4.2) and (4.3), the horizon length, N, should be made long enough to ensure that the MPC optimization problem is feasible and ensure closed-loop stability. Systematic methods can be used for selecting N (Chmielewski and Manousiouthakis 1996; Scokaert and Rawlings 1998; Grieder, Borrelli et al. 2004).

In all subsequent developments we will consider $N = 80$.

4.3.1.2 Choice of control horizon length, m

As eqn. (4.15) indicates, only a small number of inputs are included as decision variables in the MPC optimization. In addition to convenience (i.e., a small number of decision variables) there are deeper reasons for this choice.

First, increasing the value of m (with $1 \le m \le N$) quickly reaches a point of diminishing returns, namely no appreciable change in the closed-loop dynamics. Table 4.2 substantiates this claim by example, showing that the closed-loop poles remain almost unchanged after increasing the value of m beyond 4. The associated Table 4.3 shows the resulting coefficient for the Taylor-like solution provided by MPC.

Table 4.2. Closed-loop eigenvalues for Taylor-like rules derived from unconstrained MPC for $\lambda = 0.05$ and $R = 0.07$

m	N							
	20		40		60		80	
	μ_1	μ_2	μ_1	μ_2	μ_1	μ_2	μ_1	μ_2
2	0.05	0.95	0.05	0.95	0.05	0.95	0.05	0.94
3	0.07	0.95	0.07	0.97	0.07	0.96	0.07	0.96
4	0.07	0.95	0.07	0.97	0.07	0.97	0.07	0.96
8	0.07	0.95	0.07	0.97	0.07	0.97	0.07	0.97
12	0.07	0.95	0.07	0.97	0.07	0.97	0.07	0.97
16	0.07	0.95	0.07	0.97	0.07	0.97	0.07	0.97

Table 4.3. Output gap and inflation coefficients in Taylor-like rules (eqn. (4.1)) derived from unconstrained MPC for $\lambda = 0.05$ and $R = 0.07$

m	N							
	20		40		60		80	
	ϕ_y	ϕ_π	ϕ_y	ϕ_π	ϕ_y	ϕ_π	ϕ_y	ϕ_π
2	3.2	2.9	3.1	2.4	3.1	2.4	3.1	2.5
3	3.2	2.9	3.1	2.4	3.1	2.4	3.1	2.5
4	3.2	2.9	3.1	2.4	3.1	2.4	3.1	2.5
8	3.2	2.9	3.1	2.3	3.1	2.3	3.1	2.3
12	3.2	2.9	3.1	2.2	3.1	2.2	3.1	2.2
16	3.2	2.9	3.1	2.2	3.1	2.1	3.1	2.2

Second, it has been rigorously shown that keeping m small improves the robustness of the closed loop, namely it helps maintain closed-loop stability in the presence of discrepancies between the model used by MPC and the actual system under control (Garcia and Morari 1982; Genceli and Nikolaou 1993; Vuthandam, Genceli et al. 1995).

In all subsequent developments we will consider $m = 4$.

4.3.1.3 Choice of discount factor, β

Following the literature (Jung, Teranishi et al. 2005; Adam and Billi 2007) we use a value of the discount factor $\beta = 0.99$, except in situations where we explicitly specify a different value. We will comment below on how different values of β affect the resulting Taylor rules and closed-loop stability and performance.

4.3.1.4 Effects of MPC objective function weights on resulting Taylor rules

For the choice of $N = 80$, $m = 4$, and $\beta = 0.99$, discussed in the preceding sections, we now proceed to examine the effect of R and λ on the resulting Taylor rules, via eqn. (4.24). Following the calculations in Appendix E, the matrices $\mathbf{H}$ and $\mathbf{F}$ in eqn. (4.22) are calculated as functions of R and λ, and coefficients of the output gap and inflation in the Taylor rule or eqn. (4.1) are expressed analytically in terms of R and λ, as

$$\phi_y = \frac{q_{y,3}R^6 + q_{y,2}(\lambda)R^4 + q_{y,1}(\lambda)R^2 + q_{y,0}(\lambda)}{p_3R^6 + p_2(\lambda)R^4 + p_1(\lambda)R^2 + p_0(\lambda)}, \tag{4.25}$$

$$\phi_\pi = \frac{q_{\pi,3}R^6 + q_{\pi,2}(\lambda)R^4 + q_{\pi,1}(\lambda)R^2 + q_{\pi,0}(\lambda)}{p_3R^6 + p_2(\lambda)R^4 + p_1(\lambda)R^2 + p_0(\lambda)}, \tag{4.26}$$

respectively, where the values of the corresponding parameters are shown in Table 4.4. In general, the numerator and denominator for ϕ_y and ϕ_π are polynomial functions of degree $m-1$ in both R^2 and λ.

Table 4.4. Polynomial coefficients in eqns. (4.25) and (4.26) as functions of λ

$$
\begin{aligned}
q_{y,3} &= 1.04 \\
q_{y,2} &= 0.297 + 0.444\lambda \\
q_{y,1} &= -0.04(-1.04+\lambda)(0.420+\lambda) \\
q_{y,0} &= 6.11\times10^{-4}(-1.06+\lambda)(-1.01+\lambda)(0.365+\lambda) \\
q_{\pi,3} &= 3.67 \\
q_{\pi,3} &= 0.37 + 2.28\lambda \\
q_{\pi,1} &= -0.124(-1.09+\lambda)(0.084+\lambda) \\
q_{\pi,0} &= 1.59\times10^{-3}(-1.12+\lambda)(-1.01+\lambda)(0.059+\lambda) \\
p_3 &= 1.48 \\
p_2 &= 0.197 + 0.157\lambda \\
p_1 &= -0.0108(-1.02+\lambda)(0.641+\lambda) \\
p_0 &= 1.32\times10^{-4}(-1.03+\lambda)(-1.01+\lambda)(0.512+\lambda)
\end{aligned}
$$

Figure 4.1 employs the preceding eqns. (4.25) and (4.26) to calculate the policy coefficients ϕ_y, ϕ_π for a range of values of R and λ. The point corresponding to original Taylor rule ($\phi_y = 0.5$, $\phi_\pi = 1.5$) is not present in Figure 4.1. However, various values of R and λ result in ϕ_y in the range of 1 to 3 (Figure 4.2) and ϕ_π in the range of 2 to 6 (Figure 4.3).

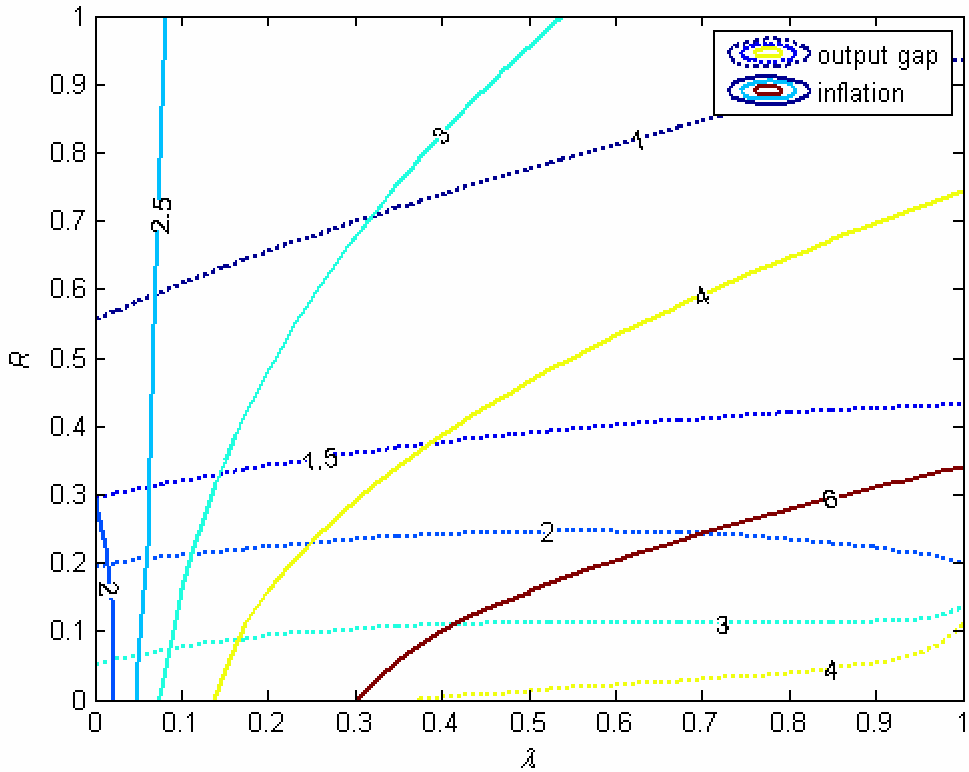

Figure 4.1. Taylor-like interest rate rule for when there is no constraint on interest rate for various values of tuning parameters R and λ. Solid and dotted lines represent inflation and output gap coefficient respectively based on eqn. (4.25)-(4.26). This solution is also valid when no constraint is active in case of constrained MPC.

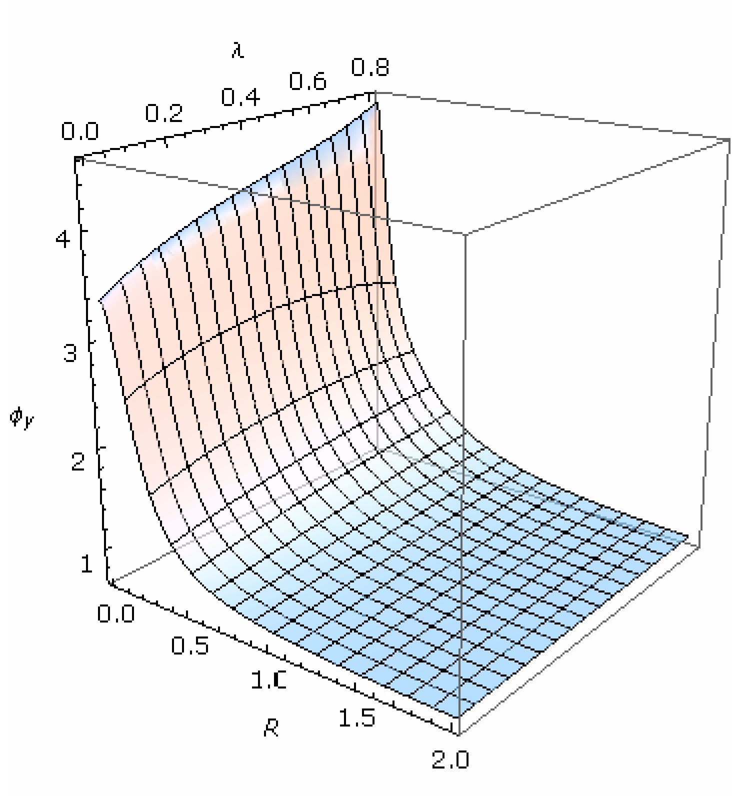

Figure 4.2. Output gap coefficient ϕ_y for Taylor rule when $\beta = 0.99$.

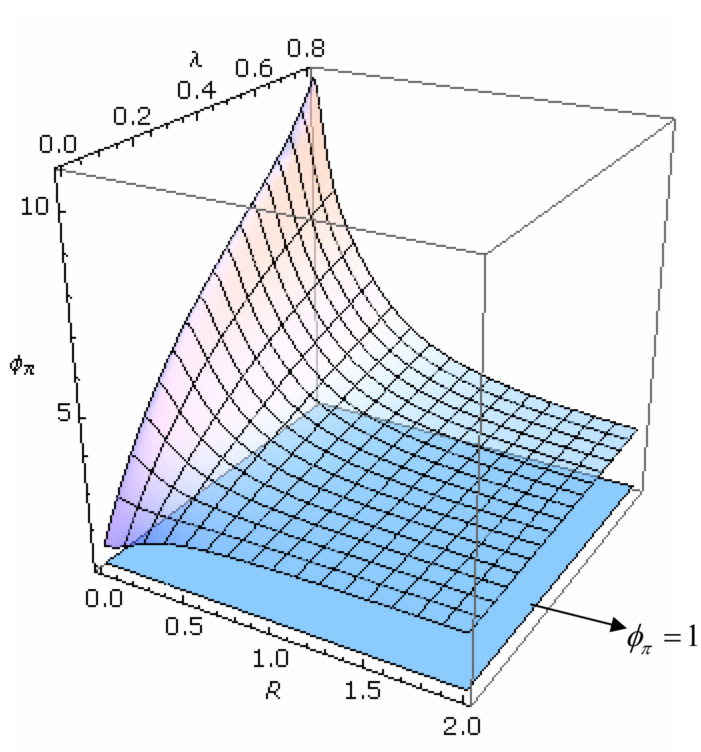

Figure 4.3. Inflation coefficient ϕ_π for Taylor rule when $\beta = 0.99$.

The following general observations can be made on Figure 4.2 and Figure 4.3:

- When R is small (i.e.,control is aggressive) it has a strong effect on ϕ_y and ϕ_π.
- The value $R = 0$ results in large values of ϕ_y and ϕ_π, i.e.,aggressive policy.
- When R is small, the inflation coefficient ϕ_π is more sensitive to the choice of λ than ϕ_y is.
- After approximately $R > 1$, further increase in R has very small effect on ϕ_y and ϕ_π.

For the economic model under consideration, the nearest point to the original Taylor rule is found at $\phi_y = 1$, $\phi_\pi = 2.4$ for $R = 0.55$ and $\lambda = 0.05$. These values are close to the original Taylor rule and other Taylor-like rules (Rotemberg and Woodford 1997; Orphanides and Wieland 2000).

4.3.1.5 Original Taylor rule in MPC framework

Even though the specific ϕ_y and ϕ_π values of the original Taylor rule were not recovered in the preceding section for the value of β used mostly in literature, such values can be obtained if a different value of β is considered. It turns out that the original Taylor rule can be recovered for $\beta \le 0.96$, for which expressions for ϕ_y and ϕ_π similar to eqns. (4.25) and (4.26) can be derived in the same way. As shown in Figure 4.4 and Figure 4.5, the original Taylor rule values for ϕ_y and ϕ_π can be derived when $\beta = 0.96$ for $R = 1.06$ and $\lambda = 0.36$ in eqn. (4.11).

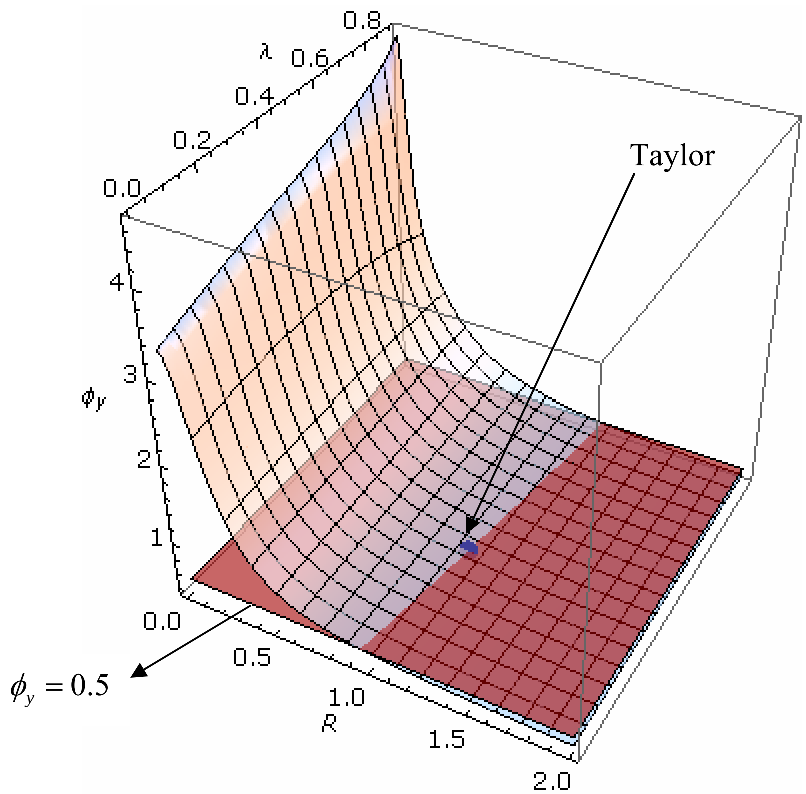

Figure 4.4. Output gap coefficient ϕ_y for Taylor rule when $\beta = 0.96$. The location of Taylor coefficient $\phi_y = 0.5$ is shown by the circle.

In general, determining values of MPC weights that would correspond to specific values of ϕ_y and ϕ_π is an instance of the inverse linear quadratic regulator problem. An infinite number of solutions generally exist for that problem. Feasibility and characterization of these solutions can be obtained in terms of linear matrix inequality algorithms (Boyd, El Ghaoui et al. 1994, section 10. 6, p. 147). This issue will be explored elsewhere.

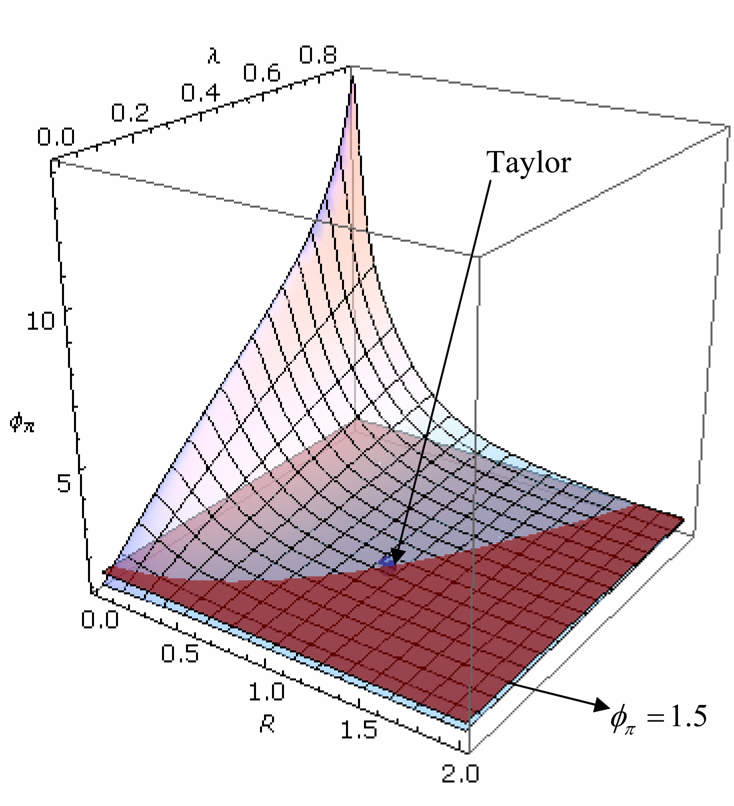

Figure 4.5. Inflation rate coefficient ϕ_π for Taylor rule when $\beta = 0.96$. The location of Taylor coefficient $\phi_\pi = 1.5$ is shown by the circle.

4.3.1.6 Taylor rules and resulting closed-loop stability

For any rule proposed, it is important to determine, at the very least, whether such a rule results in a stable closed loop. Combination of the Taylor rule in eqn. (4.1) with the simple economy model, eqn. (4.4), yields (Appendix F) the closed loop structure

$$\mathbf{x}_{t+1} = \mathbf{A}_{\mathrm{CL}} \mathbf{x}_t + \boldsymbol{\varepsilon}_{t+1}, \tag{4.27}$$

where

$$\mathbf{A}_{\mathrm{CL}} \triangleq \mathbf{A} + \mathbf{B}\mathbf{c}^T = \begin{bmatrix} \rho - \xi\phi_y & \xi - \xi\phi_\pi \\ \alpha & 1 \end{bmatrix}. \tag{4.28}$$

It can be shown (Appendix F) that both eigenvalues of $\mathbf{A}_{\mathrm{CL}}$ are inside the unit disk, i.e.,the closed-loop system is stable, if and only if

$$\phi_\pi > 1, \tag{4.29}$$

$$-2.1 + 0.12\phi_\pi < \phi_y < 8.5 + 0.06\phi_\pi. \tag{4.30}$$

as illustrated in Figure 4.6. This is in agreement with the well established *Taylor principle* that the central bank should raise its interest rate *more than one-for-one* with increase in inflation (Woodford 2001; Davig and Leeper 2007). Figure 4.3 shows that this requirement is satisfied for all combinations of the MPC weighting parameters R and λ. In fact, Figure 4.7 illustrates that the stability conditions, eqns. (4.29) and (4.30), are satisfied for all choices of R and λ when $\beta = 0.99$. However, this is not the case for $\beta \le 0.95$, as illustrated in Figure 4.8, which shows that as the value of β is reduced, the value of R should not be too small, to avoid closed-loop instability.

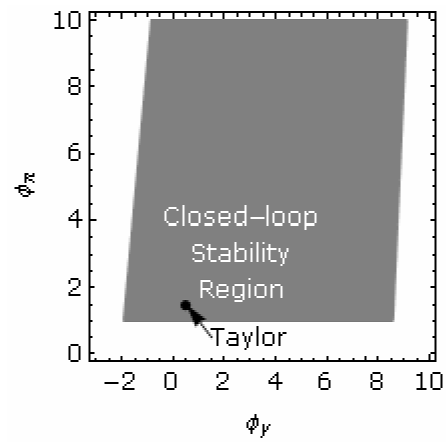

Figure 4.6. Closed-loop stability region for the US economy model in terms of Taylor rule coefficients ϕ_y and ϕ_π when $\beta = 0.99$.

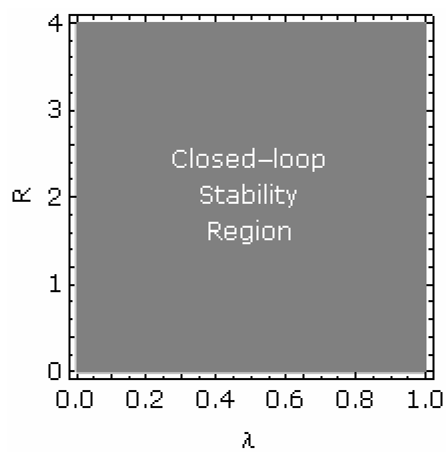

Figure 4.7. Closed-loop stability region in terms of MPC tuning parameters R and λ for $\beta = 0.99$.

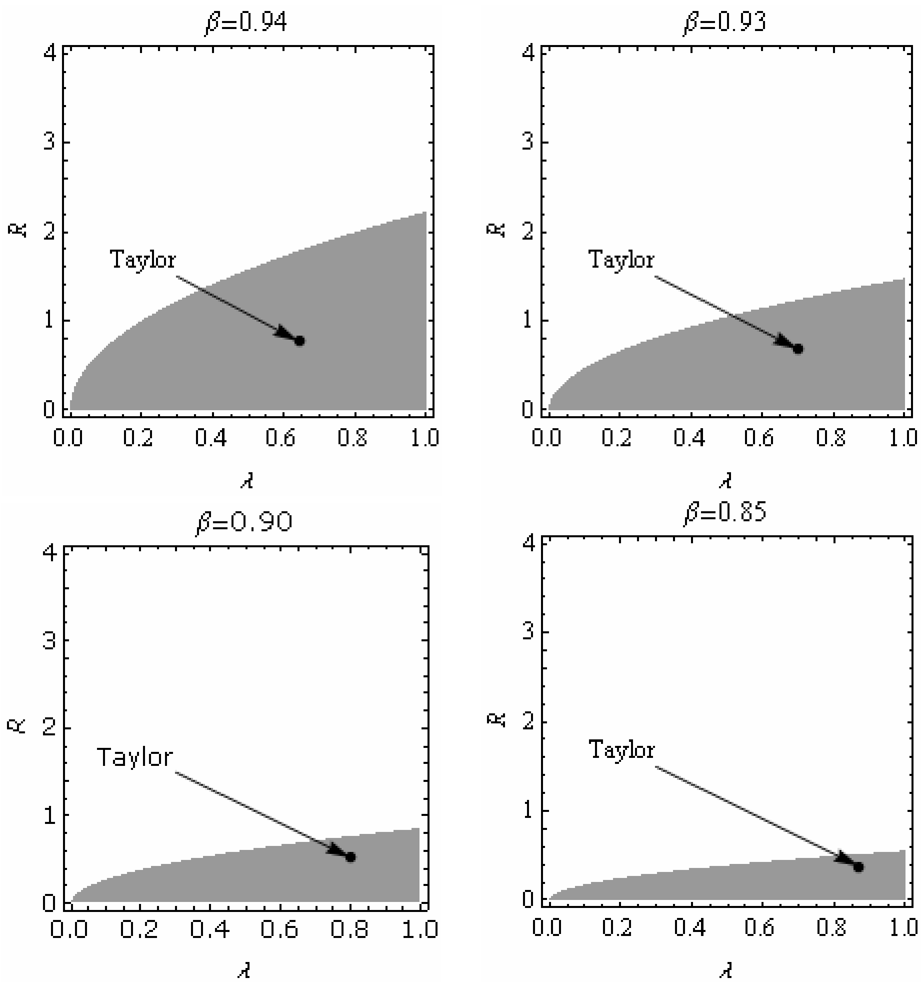

Figure 4.8. Closed-loop stability region (shaded) in terms of MPC weight parameters R and λ for various values of $\beta < 0.95$. The location of original Taylor rule is shown by circle.

It is interesting to note that as $R \to \infty$, namely high values of interest rate are heavily penalized, the closed loop remains stable, due to the stabilizing equality constraint, eqn. (4.14). For $R \to \infty$, eqns. (4.25) and (4.26) suggest that $\phi_y = \dfrac{q_{y,3}}{p_3} = 0.70$ and $\phi_\pi = \dfrac{q_{\pi,3}}{p_3} = 2.5$.

Following the preceding observations, it should be noted that the widespread practice of using a discount factor β may be more problematic than realized, in the sense that it may not result in robustly stabilizing strategies. This situation, namely the need to shape weights of the terms in the MPC objective in an *increasing* rather than decreasing fashion in order to ensure robustness, has been rigorously analyzed in the past (Genceli and Nikolaou 1993; Vuthandam, Genceli et al. 1995) and should be explored further.

4.4 Taylor rules from MPC with zero lower bound

When the interest rate must satisfy a ZLB constraint, the optimization problem to be solved by MPC entails the objective in eqn. (4.11), the equality constraints in eqns. (4.12)-(4.15), and the inequality constraint in eqn. (4.16). It can be shown (see Appendix G) that for $S = 0$, the entire optimization problem can be cast in the form

$$\min_{\mathbf{z}} \frac{1}{2}\mathbf{z}^T\mathbf{H}\mathbf{z}, \tag{4.31}$$

subject to

$$\mathbf{G}\mathbf{z} \le \mathbf{w} + \mathbf{D}\mathbf{x}_t, \tag{4.32}$$

where $\mathbf{z} \triangleq \mathbf{u}_m + \mathbf{H}^{-1}\mathbf{F}^T\mathbf{x}_t$, $\mathbf{D} \triangleq \mathbf{E} + \mathbf{G}\mathbf{H}^{-1}\mathbf{F}^T$, and $\mathbf{G}$, $\mathbf{w}$, $\mathbf{E}$ are defined in Appendix G.

Eqns. (4.31) and (4.32) suggest that the optimization problems solved by MPC at successive points in time differ only by the right-hand side of eqn. (4.32), which is affine in the state $\mathbf{x}_t$. No single formula exists for the explicit solution of all of these problems. However, the optimal solution can be expressed explicitly at each point as

$$\mathbf{z}_{t|t}^{\text{opt}} = \mathbf{H}^{-1}\mathbf{G}_A^T\left(\mathbf{G}_A\mathbf{H}^{-1}\mathbf{G}_A^T\right)^{-1}\left(\mathbf{w}_A + \mathbf{D}_A\mathbf{x}_t\right), \tag{4.33}$$

where $\mathbf{G}_A$, $\mathbf{w}_A$, $\mathbf{D}_A$ correspond to the set of active inequality constraints in eqn. (4.32), and are finite in number. Which inequality constraints in eqn. (4.32) will be active (i.e equalities) at any time point t depends only on $\mathbf{x}_t$ and this can be shown (Pistikopoulos, Dua et al. 2000) to be easily determined by checking the conditions

$$\mathbf{G}\mathbf{H}^{-1}\mathbf{G}_A^T\left(\mathbf{G}_A\mathbf{H}^{-1}\mathbf{G}_A^T\right)^{-1}\left(\mathbf{w}_A + \mathbf{D}_A\mathbf{x}_t\right) < \mathbf{w} + \mathbf{D}\mathbf{x}_t \tag{4.34}$$

and

$$-\left(\mathbf{G}_A\mathbf{H}^{-1}\mathbf{G}_A^T\right)^{-1}\left(\mathbf{w}_A + \mathbf{D}_A\mathbf{x}_t\right) \geq 0, \tag{4.35}$$

for each of the possible choices of $\{\mathbf{G}_A,\ \mathbf{w}_A,\ \mathbf{D}_A\}$. While the number of combinations of active/inactive inequality constraints may be generaly large, we show in the sequel that this number is fairly small for the problem at hand, resulting in a small set of explicit rules in the form of eqn. (4.33), which are shown to be Taylor-like.

More specifically, for a certain $\{\mathbf{G}_A,\ \mathbf{w}_A,\ \mathbf{D}_A\}$, the inequalities in eqn. (4.34) and (4.35) define a linear polytope, for which the same sets of constraints remain active or inactive, and the same formula, eqn. (4.33), can be used to express the optimal solution for any $\mathbf{x}_t$ in that polytope. The collection of all polytopes, which are finite in number, spans the entire set in which $\mathbf{x}_t$ lies and which is bounded for a stable closed loop. Therefore, determining the active and inactive constraints in eqn. (4.32), and consequently the corresponding $\mathbf{G}_A$, $\mathbf{w}_A$, $\mathbf{D}_A$, is a simple matter of using a look-up table, to determine in which polytope $\mathbf{x}_t$ lies, i.e.,for which of the possible $\{\mathbf{G}_A,\ \mathbf{w}_A,\ \mathbf{D}_A\}$

eqns. (4.34) and (4.35) are satisfied. Then, eqn. (4.33) can be used to determine the optimal interest rate either as

$$\begin{aligned} i_t &= -[\underbrace{1 \quad 0 \quad \cdots \quad 0}_{m-1}]\mathbf{H}^{-1}\left(\mathbf{G}_A^T\left(\mathbf{G}_A\mathbf{H}^{-1}\mathbf{G}_A^T\right)^{-1}\left(\mathbf{w}_\mathbf{A}+\mathbf{D}_\mathbf{A}\mathbf{x}_t\right)-\mathbf{F}^T\mathbf{x}_t\right)+r^*+\pi^* \\ &= \phi_y(y_t-y^*)+\phi_\pi(\pi-\pi^*)+r^*+\pi^* \end{aligned}, \quad (4.36)$$

which is a Taylor-like rule, or as

$$i_t = 0\,, \quad (4.37)$$

namely at the ZLB value.

To our knowledge, the above development is the first rigorous derivation of an explicit Taylor-like rule that satisfies the ZLB without resorting to either clipping of the interest rate value produced by a Taylor rule (Reifschneider and Williams 2000; Williams 2006; Nakov 2008) or numerical simulation (Orphanides and Wieland 2000; Hunt and Laxton 2003; Jung, Teranishi et al. 2005; Kato and Nishiyama 2005; Adam and Billi 2007).

4.5 Taylor rules with inertia from MPC

A simple form of a Taylor-like rule with an inertia term is

$$i_t = \phi_y(y_t-y^*)+\phi_\pi(\pi_t-\pi^*)+\phi_i(i_{t-1}-i^*)+r^*+\pi^*\,. \quad (4.38)$$

Rules such as the above have been proposed based on empirical arguments and simulation studies, in efforts to reduce large interest rate fluctuations (Goodfriend 1991; Taylor and Williams 2010, and references therein). We explain below that such rules result naturally from appropriate tailoring of the MPC objective function to include terms that penalize the rate of change of interest rate.

To illustrate this, consider again the MPC optimization problem formulated in eqn. (4.11) with $R = 0$ and $S > 0$, namely no penalty on the interest rate itself, but a penalty on its rate of change. As in section 4.3.1, it can be shown (Appendix H), that the resulting MPC optimization in this case becomes

$$\min_{\mathbf{u}_m} \left[\frac{1}{2} \mathbf{u}_m^T \tilde{\mathbf{H}} \mathbf{u}_m + \tilde{\mathbf{x}}_t^T \tilde{\mathbf{F}} \mathbf{u}_m + \frac{1}{2} \tilde{\mathbf{x}}_t^T \tilde{\mathbf{Y}} \tilde{\mathbf{x}}_t \right], \tag{4.39}$$

where $\tilde{\mathbf{H}} \in \Re^{(m-1)\times(m-1)}$, $\tilde{\mathbf{F}} \in \Re^{3\times(m-1)}$, $\tilde{\mathbf{Y}} \in \Re^{3\times 3}$ are functions of $\mathbf{A}$, $\mathbf{B}$, S, and λ; and the vector $\tilde{\mathbf{x}}$ is defined as

$$\tilde{\mathbf{x}}_t \mathrel{\hat{=}} \begin{bmatrix} \Delta y_t \\ \Delta \pi_t \\ \Delta u_{t-1} \end{bmatrix} \mathrel{\hat{=}} \begin{bmatrix} y_t - y^* \\ \pi_t - \pi^* \\ u_{t-1} - u^* \end{bmatrix}. \tag{4.40}$$

In the absence of a ZLB, the minimum in the optimization problem in eqn. (4.39) is attained at $\mathbf{u}_m^{\text{opt}} = -\tilde{\mathbf{H}}^{-1} \tilde{\mathbf{F}}^T \tilde{\mathbf{x}}_t$, resulting in the optimal interest rate

$$\begin{aligned} i_t &= -\underbrace{\begin{bmatrix} 1 & 0 & \cdots & 0 \end{bmatrix}}_{m-1} \tilde{\mathbf{H}}^{-1} \tilde{\mathbf{F}}^T \tilde{\mathbf{x}}_t + r^* + \pi^* \\ &= \phi_y (y_t - y^*) + \phi_\pi (\pi - \pi^*) + \phi_i (i_{t-1} - i^*) + r^* + \pi^* \end{aligned} . \tag{4.41}$$

which is exactly eqn. (4.38).

A parametric analysis similar to that in section 4.3.1.4 can be performed again to assess the effect of the MPC weights S and λ on the parameters ϕ_y, ϕ_π, and ϕ_i. Similar choices of $N = 80$, $m = 4$ and $\beta = 0.99$ as before yield

$$\phi_y = \frac{\tilde{q}_{y,3}S^6 + \tilde{q}_{y,2}(\lambda)S^4 + \tilde{q}_{y,1}(\lambda)S^2 + \tilde{q}_{y,0}(\lambda)}{\tilde{p}_3S^6 + \tilde{p}_2(\lambda)S^4 + \tilde{p}_1(\lambda)S^2 + \tilde{p}_0(\lambda)}, \tag{4.42}$$

$$\phi_\pi = \frac{\tilde{q}_{\pi,3}S^6 + \tilde{q}_{\pi,2}(\lambda)S^4 + \tilde{q}_{\pi,1}(\lambda)S^2 + \tilde{q}_{\pi,0}(\lambda)}{\tilde{p}_3S^6 + \tilde{p}_2(\lambda)S^4 + \tilde{p}_1(\lambda)S^2 + \tilde{p}_0(\lambda)}, \tag{4.43}$$

$$\phi_i = \frac{S^2\left(\tilde{q}_{i,3}\mathrm{S}^4 + \tilde{q}_{i,2}(\lambda)S^2 + \tilde{q}_{i,1}(\lambda)\right)}{\tilde{p}_3S^6 + \tilde{p}_2(\lambda)S^4 + \tilde{p}_1(\lambda)S^2 + \tilde{p}_0(\lambda)}, \tag{4.44}$$

respectively, where the values of the corresponding parameters are shown in Table 4.5.

Table 4.5. Polynomial coefficients in eqns. (4.42) -(4.44) as functions of λ

$$\begin{aligned}
\tilde{q}_{y,3} &= 0.428 \\
\tilde{q}_{y,2} &= 1.03 + 3.17\lambda \\
\tilde{q}_{y,1} &= -0.117(-1.05+\lambda)(0.372+\lambda) \\
\tilde{q}_{y,0} &= 6.11\times10^{-4}(-1.06+\lambda)(-1.01+\lambda)(0.365+\lambda) \\
\tilde{q}_{\pi,3} &= 1.51 \\
\tilde{q}_{\pi,2} &= 0.911 + 14.0\lambda \\
\tilde{q}_{\pi,1} &= -0.323(-1.11+\lambda)(0.0653+\lambda) \\
\tilde{q}_{\pi,0} &= 1.59\times10^{-3}(-1.12+\lambda)(-1.01+\lambda)(0.0588+\lambda) \\
\tilde{q}_{i,3} &= 3.19 \\
\tilde{q}_{i,2} &= 0.294 + 0.370\lambda \\
\tilde{q}_{i,1} &= -0.00278(-1.02+\lambda)(0.690+\lambda) \\
\tilde{p}_3 &= 4.50 \\
\tilde{p}_2 &= 0.920 + 1.42\lambda \\
\tilde{p}_1 &= -0.0326(-1.03+\lambda)(0.553+\lambda) \\
\tilde{p}_0 &= 1.32\times10^{-4}(-1.03+\lambda)(-1.01+\lambda)(0.512+\lambda)
\end{aligned}$$

From eqn. (4.44) it is clear that inertial term ϕ_i is zero for $S=0$. Using eqns. (4.42), (4.43), and (4.44) all three coefficients ϕ_y, ϕ_π, ϕ_i are shown in Figure 4.9, Figure 4.10, and Figure 4.11 as a function of λ and S. The following trends can be observed.

- The policy coefficients ϕ_y and ϕ_π decrease with increase in S.
- When S is small the effect of λ on ϕ_π is dominant compared to the effect on ϕ_y.
- After approximately $S>2$ further increase on S does not change the policy coefficients by much.
- The inertial term ϕ_i increases with increase in S and eventually converges to 0.7. This result can be explained on the basis of stabilizing policy criterion. If ϕ_i is large compared to ϕ_π and ϕ_y, the closed loop will behave like an open loop and due to the unstable nature of the open-loop economy model, related policies will not stabilize the economy. These results are consistent with prior literature observations (Taylor and Williams 2010, and references therein).

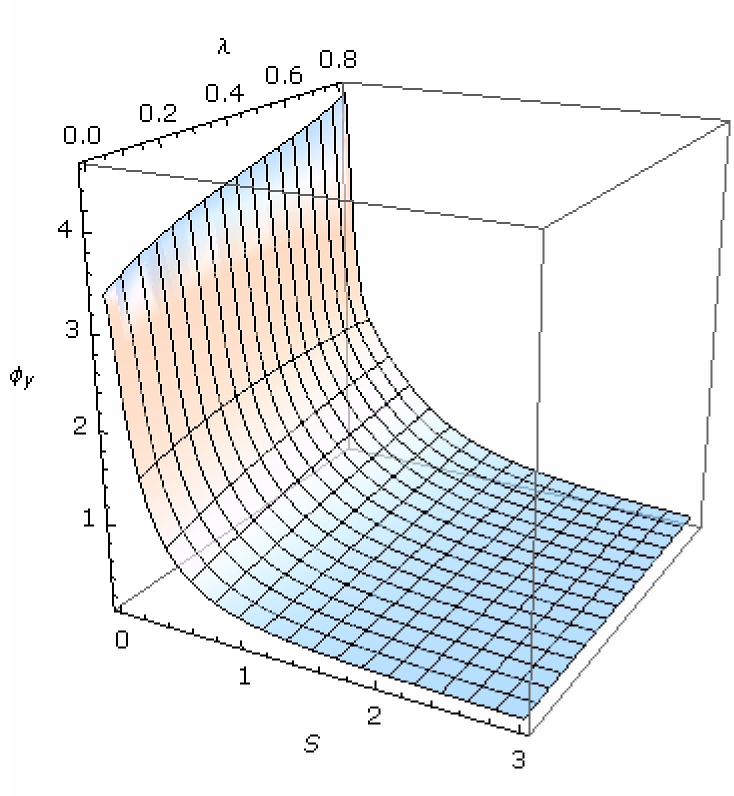

Figure 4.9. Output gap coefficient ϕ_y for Taylor rules with inertia.

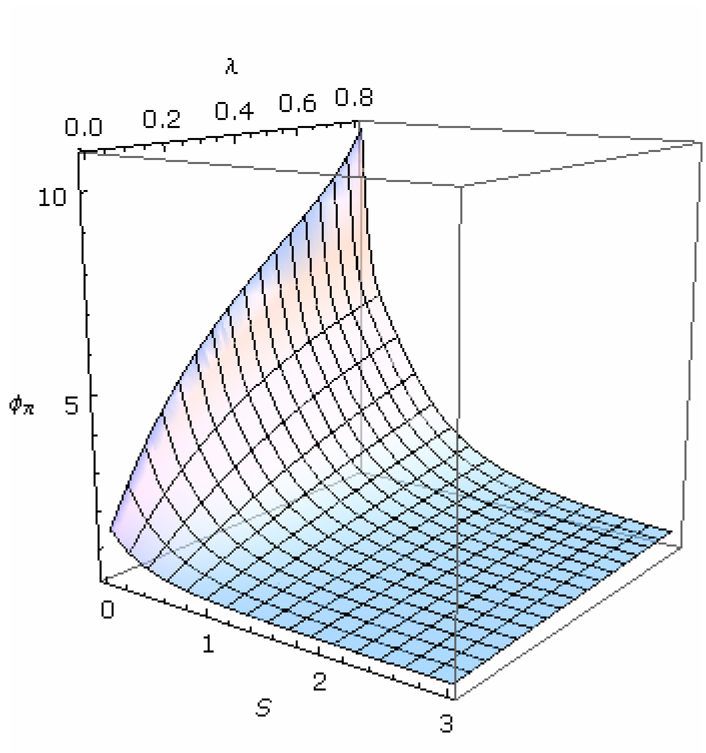

Figure 4.10. Inflation coefficient ϕ_π for Taylor rules with inertia.

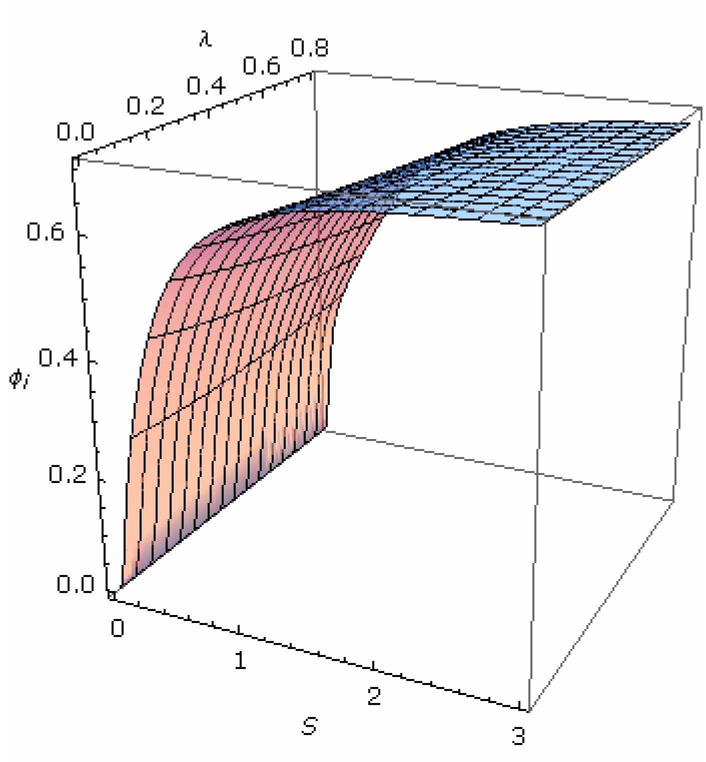

Figure 4.11. Lagged inertest rate coefficient ϕ_i for Taylor rules with inertia

4.5.1 Inertia-based rules and resulting closed-loop stability

For Taylor rules with inertia as in eqn. (4.38) the corresponding closed-loop is

$$\begin{bmatrix} \mathbf{x} \\ \psi \end{bmatrix}_{t+1} = \tilde{\mathbf{A}}_{\mathrm{CL}} \begin{bmatrix} \mathbf{x} \\ \psi \end{bmatrix}_t , \tag{4.45}$$

where

$$\tilde{\mathbf{A}}_{\mathrm{CL}} \triangleq \begin{bmatrix} \mathbf{A}+\mathbf{B}\mathbf{c}^T & \mathbf{B} \\ \phi_i \mathbf{c}^T & \phi_i \end{bmatrix} \triangleq \left[\begin{array}{cc|c} \rho-\xi\phi_y & \xi-\xi\phi_\pi & -\xi \\ \alpha & 1 & 0 \\ \hline \phi_i\phi_y & \phi_i\phi_\pi & \phi_i \end{array}\right], \tag{4.46}$$

and $\psi_t = u_t - \mathbf{c}^T \mathbf{x}_t$. It can be shown (Appendix I) that all eigenvalues of $\tilde{\mathbf{A}}_{CL}$ are inside the unit disk if and only if

$$\phi_i + \phi_\pi > 1 \tag{4.47}$$

$$\phi_\pi > -142 - 142\phi_i + 16.7\phi_y \tag{4.48}$$

$$176 - 108\phi_i > \phi_\pi \tag{4.49}$$

$$33.5 - 35.5\phi_i + 16.7\phi_y > \phi_\pi \tag{4.50}$$

$$17.2 + 10.5\phi_i^2 + 8.33\phi_y + \phi_i(-28.1 - 5.06\phi_y) > \phi_\pi \tag{4.51}$$

as shown in Figure 4.12. As in section 4.3.1.4, it is also found that all combinations of S and λ result in stabilizing monetary policies. Eqn. (4.47) is the counterpart of eqn. (4.29)and has been derived before in a different setting, using a rational expectations approach (Woodford 2003).

It is again interesting to note that as $S \to \infty$, namely aggressive changes in the value of interest rate are heavily penalized, the closed loop remains stable, due to the stabilizing equality constraint, eqn. (4.14). For $S \to \infty$, eqns. (4.42)-(4.44) suggest that $\tilde{\phi}_y = \frac{\tilde{q}_{y,3}}{\tilde{p}_3} = 0.095$, $\tilde{\phi}_\pi = \frac{\tilde{q}_{\pi,3}}{\tilde{p}_3} = 0.34$, and $\tilde{\phi}_i = \frac{\tilde{q}_{i,3}}{\tilde{p}_3} = 0.71$, which satisfy the inequalities in eqns. (4.48)-(4.51).

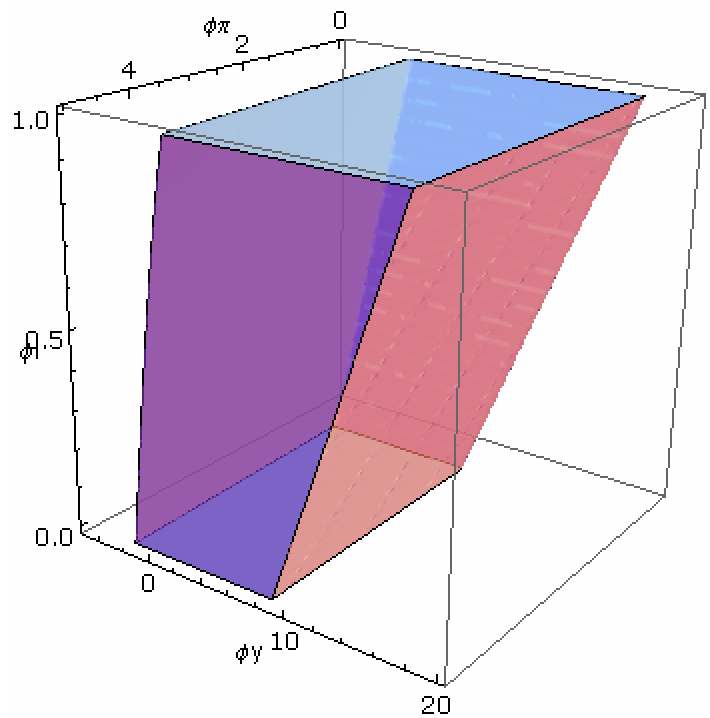

Figure 4.12. Closed-loop stability region for the US economy model in terms of coefficients ϕ_y, ϕ_π and ϕ_i for Taylor rule with inertia.

4.5.2 Taylor rules with inertia from MPC with zero lower bound

Following the same approach as in section 4.4, the optimization problem with eqn. (4.11) with $R = 0$, $S > 0$, subject to the equality constraints in eqns. (4.12)-(4.15), and the inequality constraint in eqn. (4.16) can be cast in the form

$$\min_{\tilde{\mathbf{z}}} \frac{1}{2} \tilde{\mathbf{z}}^T \tilde{\mathbf{H}} \tilde{\mathbf{z}}, \tag{4.52}$$

subject to

$$\mathbf{G}\tilde{\mathbf{z}} \leq \mathbf{w} + \tilde{\mathbf{D}} \tilde{\mathbf{x}}_t, \tag{4.53}$$

where $\tilde{\mathbf{z}} \triangleq \mathbf{u}_m + \tilde{\mathbf{H}}^{-1}\tilde{\mathbf{F}}^T\tilde{\mathbf{x}}_t$, $\tilde{\mathbf{D}} \triangleq \tilde{\mathbf{E}} + \mathbf{G}\tilde{\mathbf{H}}^{-1}\tilde{\mathbf{F}}^T$ (see Appendix H). Again, an explicit solution through Taylor-like formulas can be obtained by applying the mpMPC solution to get direct counterparts of eqns. (4.33) through (4.35).

4.6 Taylor rules and stability

As already mentioned in section 4.3.1.6, the stability of an economy under closed-loop control by central bank interest rate adjustment is of primary significance. For Taylor rules this is captured by the Taylor principle, namely that the central bank should raise its interest rate *more than one-for-one* with increase in inflation (Woodford 2001; Davig and Leeper 2007). It appears that proposed interest rate strategies may not explicity address this issue. For example, Giannoni and Woodford (Giannoni and Woodford 2003) derive inertial rules based on an economy model that includes future expectations; assuming perfect expectations, the derived rules result in a closed loop with eigenvalues $\{10.1, 1.13, 0.89, 0.10\}$, which imply closed-loop instability. As another example, Orphanides (Orphanides 2003) has developed Taylor rules that aim to deliver robust performance based on an economy model estimated under the assumption of colored noise in output gap measurements; some of the resulting rules, however, violate eqn.(4.29), and would result in closed-loop instability.

4.7 Numerical Simulations

The objective of this section is to illustrate the interest rate rules resulting from application of the methodology we outlined in the previous section. Emphasis is placed on directly including the ZLB constraint in the development of explicit rules.

4.7.1 Taylor rules form MPC with ZLB

The optimization problem defined by eqn. (4.31) with inequality constraints given by eqn. (4.32) is solved with the help of the mpMPC framework presented in section 4.4, to find the optimal interest rate rule. For the economic model discussed in section 4.2, the solution to the optimization problem depends on the weights λ and R in eqn. (4.11), for selected values of N, m and β (sections 4.3.1.1-4.3.1.3) and with $S = 0$. For each combination of λ and R, a small number of Taylor-like rules emerge, depending on the linear polytope in which the inflation and output gap lie, as presented in Table 4.6 through Table 4.11. The corresponding linear polytopes are illustrated in Figure 4.13 through Figure 4.18.

Comparison of these tables and corresponding figures shows that the following four classes of rules emerge:

- Similar in nature to the standard Taylor rule, eqn. (4.1) (polytope 1),
- Setting the interest rate at its ZLB while maintaining closed-loop stability (polytope 2),
- Setting the interest rate at its ZLB *but with loss of* closed-loop stability (polytope 3) – a case of liquidity trap (Reifschneider and Williams 2000) – and

- Piecewise linear rules that are more aggressive than the Taylor-like rules that would result from optimization without anticipation of ZLB activation in the future (remaining polytopes).

Of these tables, Table 4.7, corresponding to Figure 4.14, suggests a rule in polytope 1 closest to the standard Taylor rule, in terms of both the values of $\{\phi_y, \phi_\pi\}$ ($\{1.0, 2.4\}$ vs. $\{0.5, 1.5\}$) and the closed-loop eigenvalues ($\{0.50, 0.94\}$ vs. $\{0.56, 0.97\}$).

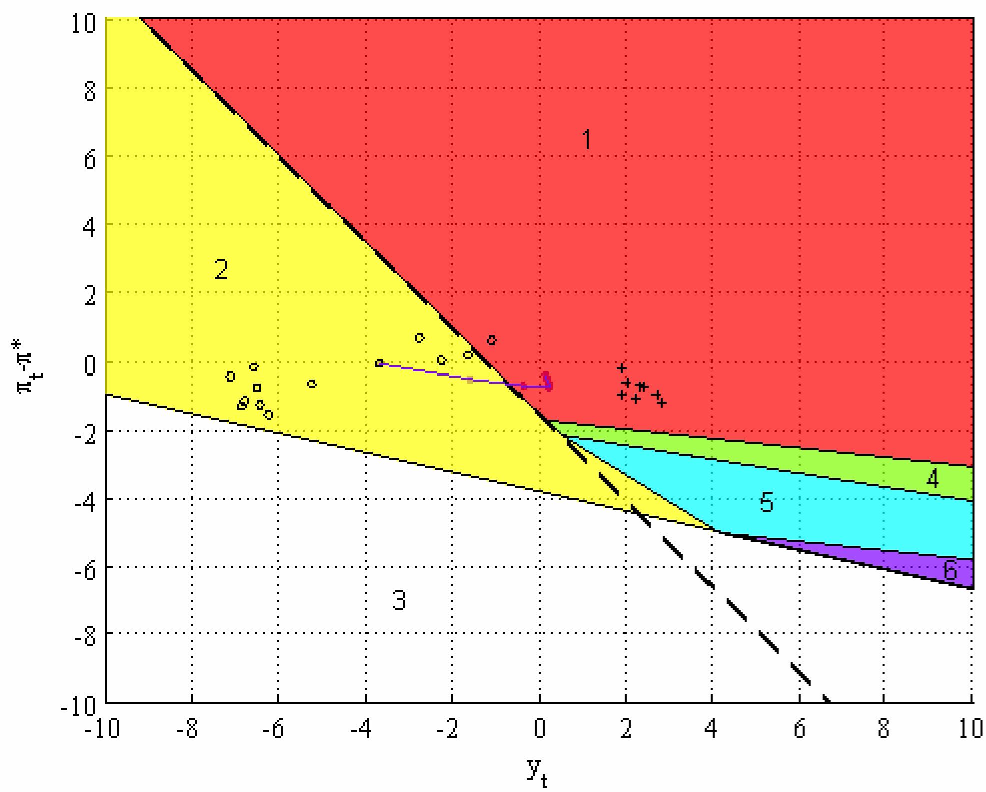

Figure 4.13. State space partition for $R = 0.07$ and $\lambda = 0.05$, corresponding rules are in Table 4.6, $\circ$ represents actual economy data points for period 08Q1-11Q1, $+$ represents actual economy data points for period 98Q1:99Q4, solid curve represent closed loop response from initial state (-3.7, 1.9), dashed line represents truncated solution of unconstrained case.

Table 4.6. mpMPC solution and state space partition for $R = 0.07$ and $\lambda = 0.05$

No.	Polytope bounds	Interest rate Δi_t	Closed-loop Eigenvalues
1	$\begin{bmatrix} -0.78 & -0.62 \\ -0.14 & -0.99 \end{bmatrix} \begin{bmatrix} \Delta y_t \\ \Delta \pi_t \end{bmatrix} \le \begin{bmatrix} 0.98 \\ 1.71 \end{bmatrix}$	$\begin{bmatrix} 3.12 & 2.49 \end{bmatrix} \begin{bmatrix} \Delta y_t \\ \Delta \pi_t \end{bmatrix}$	0.07 0.96
2	$\begin{bmatrix} 0.78 & 0.62 \\ -0.27 & -0.96 \\ 0.76 & 0.65 \\ 0.62 & 0.79 \end{bmatrix} \begin{bmatrix} \Delta y_t \\ \Delta \pi_t \end{bmatrix} \le \begin{bmatrix} -0.98 \\ 3.70 \\ -1.03 \\ -1.39 \end{bmatrix}$	-3.9	0.58 1.05
3	$\begin{bmatrix} 0.27 & 0.96 \end{bmatrix} \begin{bmatrix} \Delta y_t \\ \Delta \pi_t \end{bmatrix} \le -3.70$	-3.9 (Infeasible)	0.58 1.05
4	$\begin{bmatrix} -0.76 & -0.65 \\ -0.20 & -0.98 \\ 0.14 & 0.99 \end{bmatrix} \begin{bmatrix} \Delta y_t \\ \Delta \pi_t \end{bmatrix} \le \begin{bmatrix} 1.03 \\ 2.02 \\ -1.71 \end{bmatrix}$	$\begin{bmatrix} 3.15 & 2.70 \end{bmatrix} \begin{bmatrix} \Delta y_t \\ \Delta \pi_t \end{bmatrix} + 0.36$	0.07 0.96
5	$\begin{bmatrix} -0.62 & -0.79 \\ -0.13 & -0.99 \\ 0.20 & 0.98 \end{bmatrix} \begin{bmatrix} \Delta y_t \\ \Delta \pi_t \end{bmatrix} \le \begin{bmatrix} 1.39 \\ 4.42 \\ -2.02 \end{bmatrix}$	$\begin{bmatrix} 3.52 & 4.49 \end{bmatrix} \begin{bmatrix} \Delta y_t \\ \Delta \pi_t \end{bmatrix} + 4.05$	0.05 0.92
6	$\begin{bmatrix} -0.27 & -0.96 \\ 0.13 & 0.99 \end{bmatrix} \begin{bmatrix} \Delta y_t \\ \Delta \pi_t \end{bmatrix} \le \begin{bmatrix} 3.70 \\ -4.42 \end{bmatrix}$	$\begin{bmatrix} 5.55 & 19.6 \end{bmatrix} \begin{bmatrix} \Delta y_t \\ \Delta \pi_t \end{bmatrix} + 71.3$	0.00 0.58

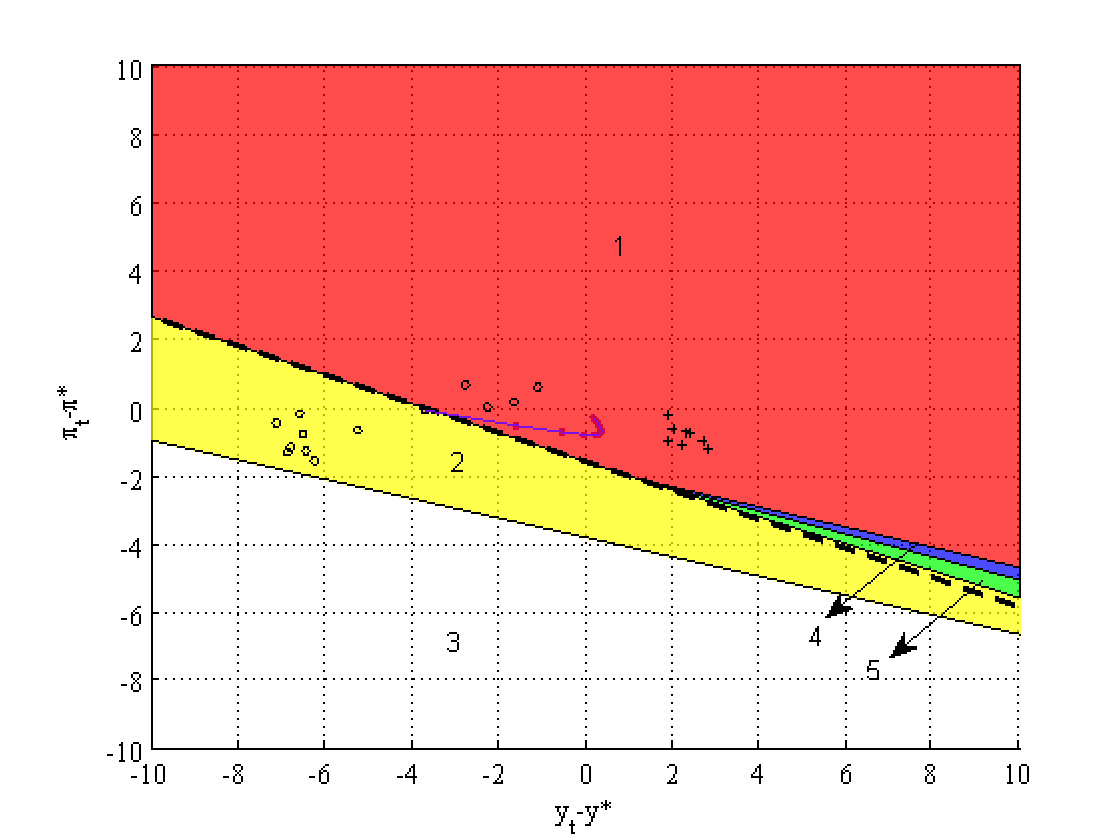

Figure 4.14. State space partition for $R = 0.55$ and $\lambda = 0.05$, corresponding rules are in Table 4.7, $\circ$ represents actual economy data points for period 08Q1-11Q1, $+$ represents actual economy data points for period 98Q1:99Q4, solid curve represent closed loop response from initial state (-3.7, 1.9), dashed line represents truncated solution of unconstrained case.

Table 4.7. mpMPC solution and state space partition for $R = 0.55$ and $\lambda = 0.05$

No.	Polytope bounds	Interest rate Δi_t	Closed-loop Eigenvalues
1	$\begin{bmatrix} -0.39 & -0.92 \\ -0.28 & -0.96 \end{bmatrix} \begin{bmatrix} \Delta y_t \\ \Delta \pi_t \end{bmatrix} \le \begin{bmatrix} 1.47 \\ 1.67 \end{bmatrix}$	$\begin{bmatrix} 1.03 & 2.44 \end{bmatrix} \begin{bmatrix} \Delta y_t \\ \Delta \pi_t \end{bmatrix}$	0.50 0.93
2	$\begin{bmatrix} 0.39 & 0.92 \\ -0.27 & -0.96 \\ 0.37 & 0.93 \end{bmatrix} \begin{bmatrix} \Delta y_t \\ \Delta \pi_t \end{bmatrix} \le \begin{bmatrix} -1.47 \\ 3.70 \\ -1.52 \end{bmatrix}$	-3.9	0.58 1.05
3	$\begin{bmatrix} 0.27 & 0.96 \end{bmatrix} \begin{bmatrix} \Delta y_t \\ \Delta \pi_t \end{bmatrix} \le -3.70$	-3.9 (Infeasible)	0.58 1.05
4	$\begin{bmatrix} -0.38 & -0.93 \\ -0.32 & -0.95 \\ 0.28 & 0.96 \end{bmatrix} \begin{bmatrix} \Delta y_t \\ \Delta \pi_t \end{bmatrix} \le \begin{bmatrix} 1.50 \\ 1.63 \\ -1.67 \end{bmatrix}$	$\begin{bmatrix} 1.13 & 2.77 \end{bmatrix} \begin{bmatrix} \Delta y_t \\ \Delta \pi_t \end{bmatrix} + 0.59$	0.50 0.92
5	$\begin{bmatrix} -0.37 & -0.93 \\ 0.32 & 0.95 \end{bmatrix} \begin{bmatrix} \Delta y_t \\ \Delta \pi_t \end{bmatrix} \le \begin{bmatrix} 1.52 \\ -1.63 \end{bmatrix}$	$\begin{bmatrix} 1.34 & 3.39 \end{bmatrix} \begin{bmatrix} \Delta y_t \\ \Delta \pi_t \end{bmatrix} + 1.65$	0.48 0.89

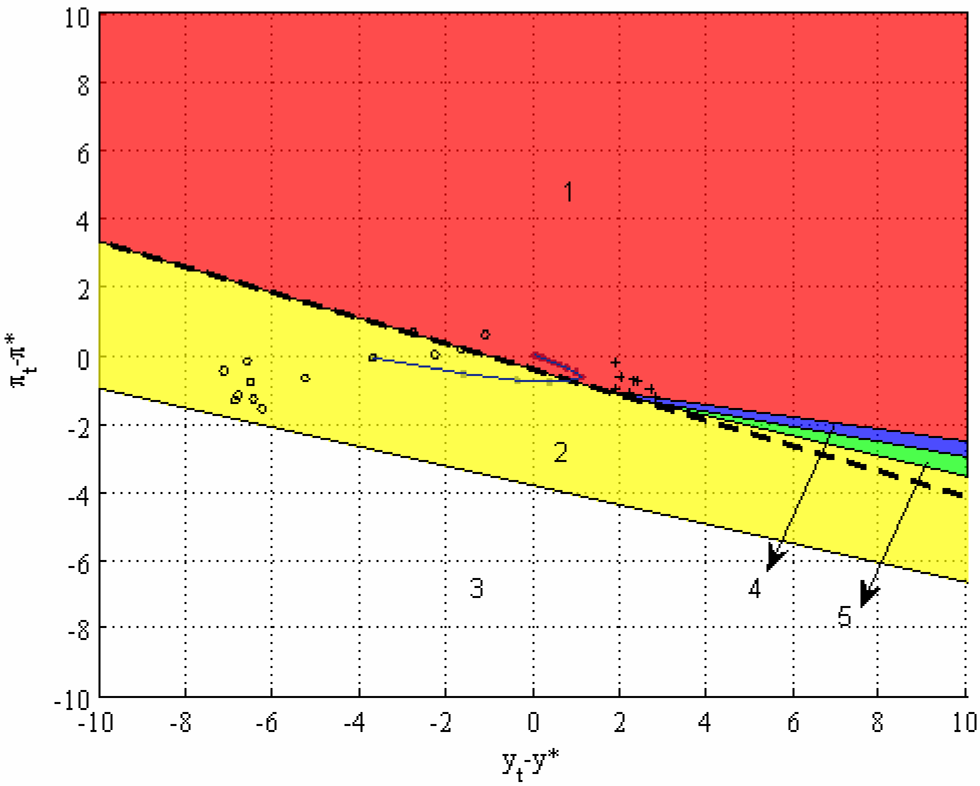

Figure 4.15. State space partition for $R = 0.07$ and $\lambda = 0.8$, corresponding rules are in Table 4.8, $\circ$ represents actual economy data points for period 08Q1-11Q1, $+$ represents actual economy data points for period 98Q1:99Q4, solid curve represent closed loop response from initial state (-3.7, 1.9), dashed line represents truncated solution of unconstrained case.

Table 4.8. mpMPC solution and state space partition for $R = 0.07$ and $\lambda = 0.8$

No.	Polytope bounds	Interest rate Δi_t	Closed-loop Eigenvalues
1	$\begin{bmatrix} -0.35 & -0.94 \\ -0.17 & -0.98 \end{bmatrix} \begin{bmatrix} \Delta y_t \\ \Delta \pi_t \end{bmatrix} \le \begin{bmatrix} 0.40 \\ 0.74 \end{bmatrix}$	$\begin{bmatrix} 3.39 & 9.09 \end{bmatrix} \begin{bmatrix} \Delta y_t \\ \Delta \pi_t \end{bmatrix}$	0.22 0.76
2	$\begin{bmatrix} 0.35 & 0.94 \\ -0.27 & -0.96 \\ 0.28 & 0.96 \\ 0.33 & 0.95 \end{bmatrix} \begin{bmatrix} \Delta y_t \\ \Delta \pi_t \end{bmatrix} \le \begin{bmatrix} -0.98 \\ 3.70 \\ -0.57 \\ -0.45 \end{bmatrix}$	-3.9	0.58 1.05
3	$\begin{bmatrix} 0.27 & 0.96 \end{bmatrix} \begin{bmatrix} \Delta y_t \\ \Delta \pi_t \end{bmatrix} \le -3.70$	-3.9 (Infeasible)	0.58 1.05
4	$\begin{bmatrix} -0.33 & -0.95 \\ -0.21 & -0.98 \\ 0.17 & 0.98 \end{bmatrix} \begin{bmatrix} \Delta y_t \\ \Delta \pi_t \end{bmatrix} \le \begin{bmatrix} 0.45 \\ 0.76 \\ -0.74 \end{bmatrix}$	$\begin{bmatrix} 3.65 & 10.6 \end{bmatrix} \begin{bmatrix} \Delta y_t \\ \Delta \pi_t \end{bmatrix} + 1.13$	0.21 0.72
5	$\begin{bmatrix} -0.28 & -0.96 \\ 0.21 & 0.98 \end{bmatrix} \begin{bmatrix} \Delta y_t \\ \Delta \pi_t \end{bmatrix} \le \begin{bmatrix} 0.57 \\ -0.76 \end{bmatrix}$	$\begin{bmatrix} 5.17 & 17.5 \end{bmatrix} \begin{bmatrix} \Delta y_t \\ \Delta \pi_t \end{bmatrix} + 6.48$	0.04 0.61

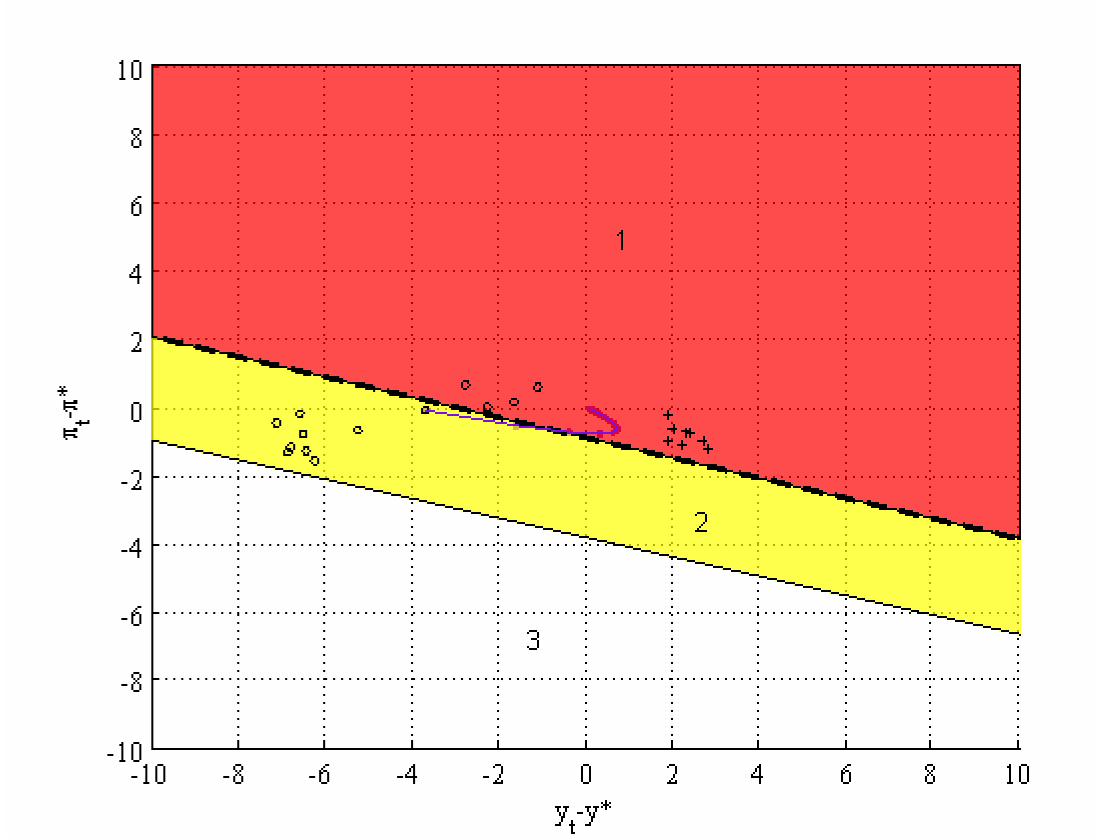

Figure 4.16. State space partition for $R = 0.55$ and $\lambda = 0.8$, corresponding rules are in Table 4.9, $\circ$ represents actual economy data points for period 08Q1-11Q1, $+$ represents actual economy data points for period 98Q1:99Q4, solid curve represent closed loop response from initial state (-3.7, 1.9), dashed line represents truncated solution of unconstrained case.

Table 4.9. mpMPC solution and state space partition for $R = 0.55$ and $\lambda = 0.8$

No.	Polytope bounds	Interest rate Δi_t	Closed-loop Eigenvalues
1	$\begin{bmatrix} -0.28 & -0.96 \end{bmatrix} \begin{bmatrix} \Delta y_t \\ \Delta \pi_t \end{bmatrix} \le 0.86$	$\begin{bmatrix} 1.29 & 4.36 \end{bmatrix} \begin{bmatrix} \Delta y_t \\ \Delta \pi_t \end{bmatrix}$	0.56 0.83
2	$\begin{bmatrix} 0.28 & 0.96 \\ -0.27 & -0.96 \end{bmatrix} \begin{bmatrix} \Delta y_t \\ \Delta \pi_t \end{bmatrix} \le \begin{bmatrix} -0.86 \\ 3.70 \end{bmatrix}$	-3.9	0.58 1.05
3	$\begin{bmatrix} 0.27 & 0.96 \end{bmatrix} \begin{bmatrix} \Delta y_t \\ \Delta \pi_t \end{bmatrix} \le -3.70$	-3.9 (Infeasible)	0.58 1.05

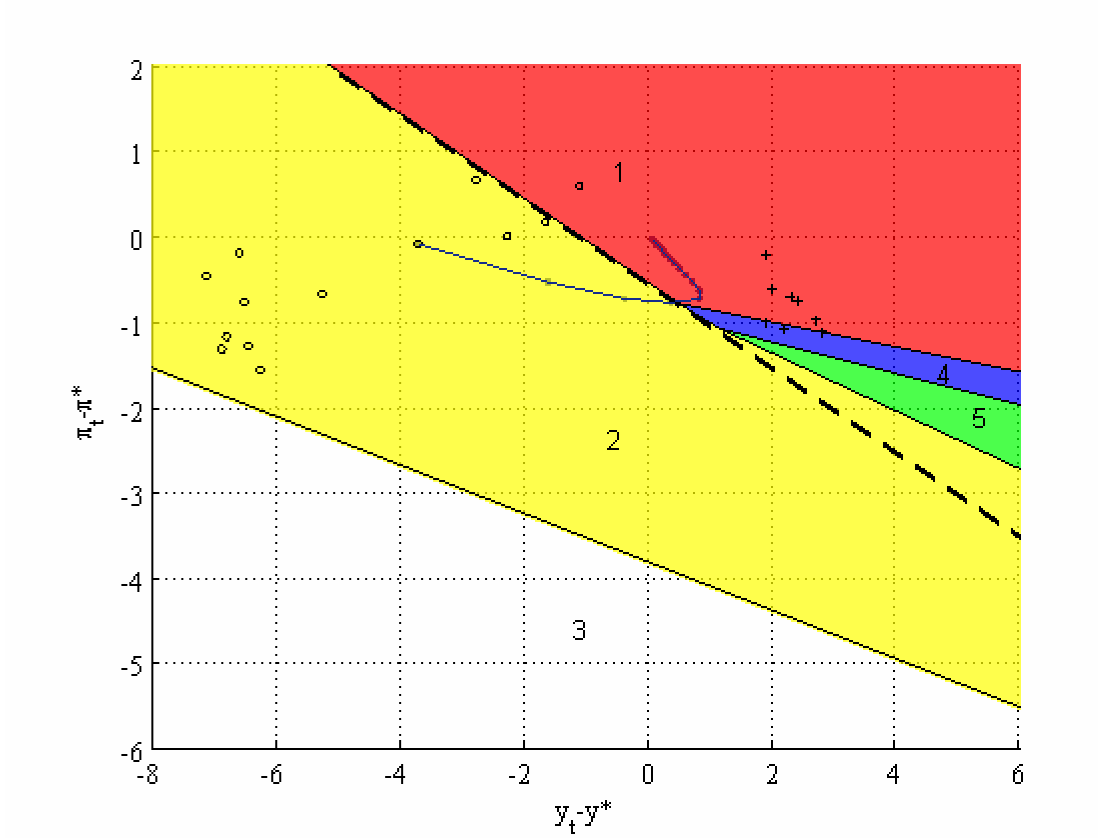

Figure 4.17. State space partition for $R = 0.07$ and $\lambda = 0.5$, corresponding rules are in Table 4.10, $\circ$ represents actual economy data points for period 08Q1-11Q1, $+$ represents actual economy data points for period 98Q1:99Q4, solid curve represent closed loop response from initial state (-3.7, 1.9), dashed line represents truncated solution of unconstrained case.

Table 4.10. mpMPC solution and state space partition for $R = 0.07$ and $\lambda = 0.5$

No.	Polytope bounds	Interest rate Δi_t	Closed-loop Eigenvalues
1	$\begin{bmatrix} -0.44 & -0.90 \\ 0.14 & -0.99 \end{bmatrix} \begin{bmatrix} \Delta y_t \\ \Delta \pi_t \end{bmatrix} \le \begin{bmatrix} 0.49 \\ 0.72 \end{bmatrix}$	$\begin{bmatrix} 3.51 & 7.11 \end{bmatrix} \begin{bmatrix} \Delta y_t \\ \Delta \pi_t \end{bmatrix}$	0.12 0.84
2	$\begin{bmatrix} 0.44 & 0.90 \\ -0.27 & -0.96 \\ 0.41 & 0.91 \\ 0.32 & 0.95 \end{bmatrix} \begin{bmatrix} \Delta y_t \\ \Delta \pi_t \end{bmatrix} \le \begin{bmatrix} -0.49 \\ 3.70 \\ -0.52 \\ -0.66 \end{bmatrix}$	-3.9	0.58 1.05
3	$\begin{bmatrix} 0.27 & 0.96 \end{bmatrix} \begin{bmatrix} \Delta y_t \\ \Delta \pi_t \end{bmatrix} \le -3.70$	-3.9 (Infeasible)	0.58 1.05
4	$\begin{bmatrix} -0.44 & -0.91 \\ -0.18 & -0.98 \\ 0.14 & 0.99 \end{bmatrix} \begin{bmatrix} \Delta y_t \\ \Delta \pi_t \end{bmatrix} \le \begin{bmatrix} 0.52 \\ 0.86 \\ -0.72 \end{bmatrix}$	$\begin{bmatrix} 3.67 & 8.26 \end{bmatrix} \begin{bmatrix} \Delta y_t \\ \Delta \pi_t \end{bmatrix} + 0.84$	0.12 0.81
5	$\begin{bmatrix} -0.32 & -0.95 \\ 0.18 & -0.98 \end{bmatrix} \begin{bmatrix} \Delta y_t \\ \Delta \pi_t \end{bmatrix} \le \begin{bmatrix} 0.66 \\ -0.86 \end{bmatrix}$	$\begin{bmatrix} 4.72 & 13.95 \end{bmatrix} \begin{bmatrix} \Delta y_t \\ \Delta \pi_t \end{bmatrix} + 5.82$	0.04 0.69

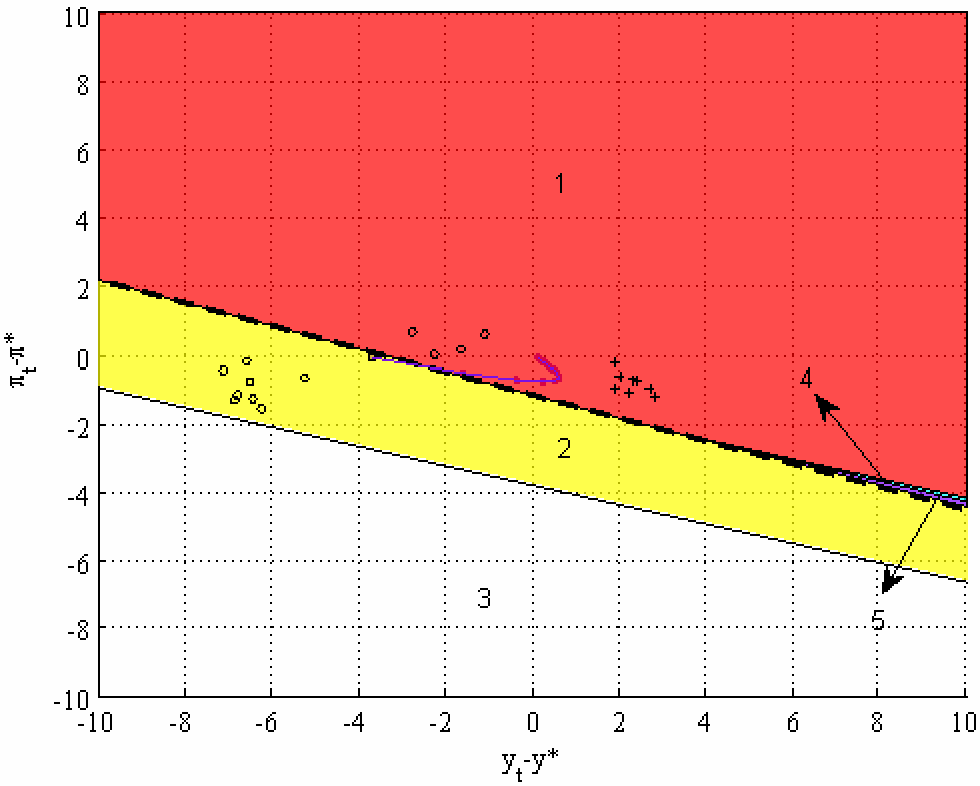

Figure 4.18. space partition for $R = 0.55$ and $\lambda = 0.5$, corresponding rules are in Table 4.11, $\circ$ represents actual economy data points for period 08Q1-11Q1, $+$ represents actual economy data points for period 98Q1:99Q4, solid curve represent closed loop response from initial state (-3.7, 1.9), dashed line represents truncated solution of unconstrained case.

Table 4.11. mpMPC solution and state space partition for $R = 0.55$ and $\lambda = 0.5$

No.	Polytope bounds	Interest rate Δi_t	Closed-loop Eigenvalues
1	$\begin{bmatrix} -0.31 & -0.95 \\ -0.29 & -0.96 \\ -0.27 & -0.96 \end{bmatrix} \begin{bmatrix} \Delta y_t \\ \Delta \pi_t \end{bmatrix} \leq \begin{bmatrix} 1.0 \\ 1.09 \\ 1.14 \end{bmatrix}$	$\begin{bmatrix} 1.21 & 3.71 \end{bmatrix} \begin{bmatrix} \Delta y_t \\ \Delta \pi_t \end{bmatrix}$	0.53 0.87
2	$\begin{bmatrix} 0.31 & 0.95 \\ -0.27 & -0.96 \\ 0.30 & 0.95 \end{bmatrix} \begin{bmatrix} \Delta y_t \\ \Delta \pi_t \end{bmatrix} \leq \begin{bmatrix} -1.00 \\ 3.70 \\ -1.04 \end{bmatrix}$	-3.9	0.58 1.05
3	$\begin{bmatrix} 0.27 & 0.96 \end{bmatrix} \begin{bmatrix} \Delta y_t \\ \Delta \pi_t \end{bmatrix} \leq -3.70$	-3.9 (Infeasible)	0.58 1.05
4	$\begin{bmatrix} -0.61 & -0.79 \\ 0 & -1 \\ 0 & 1 \end{bmatrix} \begin{bmatrix} \Delta y_t \\ \Delta \pi_t \end{bmatrix} \leq \begin{bmatrix} 2.03 \\ 4.51 \\ -2.99 \end{bmatrix}$	$\begin{bmatrix} 1.4 & 4.38 \end{bmatrix} \begin{bmatrix} \Delta y_t \\ \Delta \pi_t \end{bmatrix} + 0.8$	0.53 0.84
5	$\begin{bmatrix} -0.61 & -0.79 \\ 0 & -1 \\ 0 & 1 \end{bmatrix} \begin{bmatrix} \Delta y_t \\ \Delta \pi_t \end{bmatrix} \leq \begin{bmatrix} 2.03 \\ 4.51 \\ -2.99 \end{bmatrix}$	$\begin{bmatrix} 1.77 & 5.63 \end{bmatrix} \begin{bmatrix} \Delta y_t \\ \Delta \pi_t \end{bmatrix} + 2.23$	0.51 0.79

Further comparison of these figures reveals that the optimal rules follow an *asymmetric* pattern for small values of R (Figure 4.13, Figure 4.15, Figure 4.17), as has also been observed in a number of numerical studies with $R = 0$ (Orphanides and Wieland 2000; Kato and Nishiyama 2005; Williams 2006; Taylor and Williams 2010). However, this asymmetry practically disappears (i.e.,it would be observable only for unrealistically large output gaps) for large values of R (Figure 4.16, Figure 4.18), namely for very sluggish policies.

Specifically, for *negative output gap*, the resulting interest rate value is equal to either what a single corresponding Taylor-like rule would produce, if that value were positive, or zero when that same Taylor rule would produce a negative value. While it is obvious that a negative interest rate value produced by a Taylor rule cannot be implemented, what is shown from the preceding analysis is that *a zero value resulting from clipping the unconstrained Taylor rule value is optimal*. In addition, for *negative output gap*, when the interest rate is close to zero and future violations of the ZLB are anticipated, *no more aggressive action is needed; the same Taylor rule remains optimal.*

On the other hand, for *positive output gap* and *low inflation*, more interesting behavior is observed, namely a small number of piecewise linear rules result, corresponding to the linear polytopes numbered 4 and above. These rules become more aggressive as the interest rate approaches the ZLB. This behavior (*pre-emptiveness*) has also been observed in numerical studies (Kato and Nishiyama 2005; Taylor and Williams 2010, and references therein). However, in contrast to these numerical simulation studies, explicit rules are derived here, and these rules are (piecewise) linear rather than nonlinear.

4.7.2 Taylor rules with inertia form MPC with ZLB

For $S = 0.55$ and $\lambda = 0.5$, the resulting piece-wise linear policies and corresponding polytopes are shown in Table 4.12. The parameter space of mpMPC, which is now three-dimensional, is partitioned in 6 polytopes shown in Figure 4.19. Polytope 1 corresponds to no constraint being active and hence it produces a rule as in eqn. (4.41). In polytope 2 the ZLB is active, i.e.,the optimal policy is at zero. Polytopes 4, 5 and 6 entail rules that are different from the Taylor-like rule of polytope 1, in anticipation of future ZLB activation. The infeasibility polytope remains the same. From Table 4.12 and Figure 4.19 it can be concluded that in polytopes of low inflation and negative output gap, if the lagged interest rate $2 + 2\rho - 2\xi\phi_y + \alpha\xi(\phi_\pi - 1) > 0$ is high (polytopes 4 and 6), the optimal rule becomes less aggressive than the rule in the unconstrained case. However, for low $2 + 2\rho - 2\xi\phi_y + \alpha\xi(\phi_\pi - 1) > 0$, the optimal rule is just a truncation to zero of the unconstrained case, eqn. (4.41). Also, in polytope 5, characterized by low inflation, high output gap, and high $2 + 2\rho - 2\xi\phi_y + \alpha\xi(\phi_\pi - 1) > 0$, the optimal rule is more aggressive than the rule in the unconstrained case, eqn. (4.41). Therefore, an important conclusion is that for rules with inertia ($S > 0$), the optimal policy becomes asymmetrical with respect to both lagged interest rate and output gap for low inflation economic conditions.

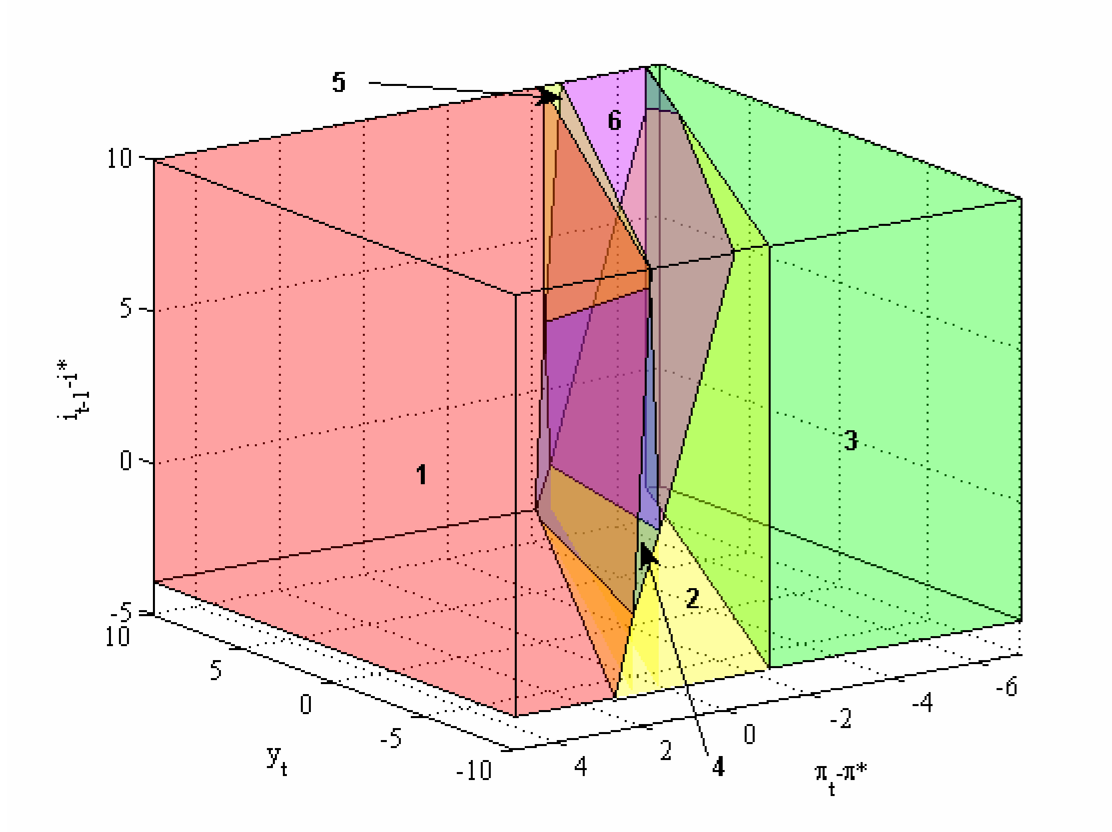

Figure 4.19. State-space partition for $S = 0.55$ and $\lambda = 0.5$; corresponding rules are in Table 4.12.

Table 4.12. mpMPC solution and state space partition for $S = 0.55$ and $\lambda = 0.5$

No.	Polytope bounds	Interest rate Δi_t	Closed-loop Eigenvalues
1	$\begin{bmatrix} -0.31 & -0.94 & -0.16 \\ -0.33 & -0.95 & -0.04 \\ -0.29 & -0.96 & 0.01 \end{bmatrix}\begin{bmatrix} \Delta y_t \\ \Delta \pi_t \\ \Delta i_{t-1} \end{bmatrix} \le \begin{bmatrix} 1.27 \\ 0.97 \\ 1.21 \end{bmatrix}$	$\begin{bmatrix} 0.96 & 2.88 & 0.48 \end{bmatrix}\begin{bmatrix} \Delta y_t \\ \Delta \pi_t \\ \Delta i_{t-1} \end{bmatrix}$	0.74 $0.59+0.20i$ $0.59-0.20i$
2	$\begin{bmatrix} 0.31 & 0.94 & 0.16 \\ -0.27 & -0.96 & 0 \\ 0.31 & 0.93 & 0.19 \\ 0.32 & 0.92 & 0.22 \end{bmatrix}\begin{bmatrix} \Delta y_t \\ \Delta \pi_t \\ \Delta i_{t-1} \end{bmatrix} \le \begin{bmatrix} -1.27 \\ 3.70 \\ -1.42 \\ -1.43 \end{bmatrix}$	-3.9	0.58 1.05 0
3	$\begin{bmatrix} 0.27 & 0.96 & 0 \end{bmatrix}\begin{bmatrix} \Delta y_t \\ \Delta \pi_t \\ \Delta i_{t-1} \end{bmatrix} \le -3.7$	-3.9 (Infeasible)	0.58 1.05 0
4	$\begin{bmatrix} -0.32 & -0.92 & -0.22 \\ -0.28 & -0.96 & 0.03 \\ 0.30 & 0.95 & 0.04 \end{bmatrix}\begin{bmatrix} \Delta y_t \\ \Delta \pi_t \\ \Delta i_{t-1} \end{bmatrix} \le \begin{bmatrix} 1.43 \\ 1.33 \\ -0.97 \end{bmatrix}$	$\begin{bmatrix} 0.63 & 1.88 & 0.44 \end{bmatrix}\begin{bmatrix} \Delta y_t \\ \Delta \pi_t \\ \Delta i_{t-1} \end{bmatrix} - 1.06$	0.87 $0.54+0.13i$ $0.54-0.13i$
5	$\begin{bmatrix} -0.31 & -0.95 & -0.05 \\ 0.29 & 0.96 & -0.01 \end{bmatrix}\begin{bmatrix} \Delta y_t \\ \Delta \pi_t \\ \Delta i_{t-1} \end{bmatrix} \le \begin{bmatrix} 0.89 \\ -1.21 \end{bmatrix}$	$\begin{bmatrix} 1 & 3 & 0.48 \end{bmatrix}\begin{bmatrix} \Delta y_t \\ \Delta \pi_t \\ \Delta i_{t-1} \end{bmatrix} + 0.16$	0.73 $0.59+0.21i$ $0.59-0.21i$
6	$\begin{bmatrix} -0.31 & -0.93 & -0.19 \\ -0.27 & -0.96 & 0.02 \\ 0.31 & 0.95 & 0.05 \\ 0.28 & 0.96 & -0.03 \end{bmatrix}\begin{bmatrix} \Delta y_t \\ \Delta \pi_t \\ \Delta i_{t-1} \end{bmatrix} \le \begin{bmatrix} 1.42 \\ 3.97 \\ -0.89 \\ -1.33 \end{bmatrix}$	$\begin{bmatrix} 0.71 & 2.1 & 0.43 \end{bmatrix}\begin{bmatrix} \Delta y_t \\ \Delta \pi_t \\ \Delta i_{t-1} \end{bmatrix} - 0.69$	0.85 $0.54+0.13i$ $0.54-0.13i$

4.7.3 Remarks on rules from MPC

The following can be observed in the results of sections 4.7.1 and 4.7.2.

- Polytope 1, where no constraint is active, grows in size with increasing R or S.
- The policy becomes sluggish and the size of polytopes 2, 4 and higher decreases as R or S increase.
- For any MPC formulation, situations may arise in which either a negative interest rate would be optimal (when the ZLB is not explicitly included in the optimization) or a stabilizing interest rate at or above the ZLB is not feasible (when the ZLB is explicitly included in the optimization). It can be shown (Appendix J) that for an economy model such as described by eqns. (4.4)-(4.7) the infeasibility polytope is characterized as the set of state values $\mathbf{x}_t$ that satisfy the inequality

$$\tilde{\mathbf{v}}_{\mathrm{u}}^{T}\mathbf{x}_t > \frac{\tilde{\mathbf{v}}_{\mathrm{u}}^{T}\mathbf{B}}{J_u - 1} i^* . \tag{4.54}$$

  It is clear that the state $\mathbf{x}_t$ may satisfy eqn. (4.54) fairly easily for economies with low i^*, i.e.,such economies at corresponding conditions run the risk of falling into the infeasibility polytope where a stabilizing interest rate above the ZLB may not exist. This situation has also been studied in literature numerically (e.g., Williams 2009).

- For $\mathbf{x}_t$ in a polytope such that a feasible MPC solution exists but not all of the corresponding closed-loop eignevalues are inside the unit disk, the state will definitely escape from that polytope and will enter one where stability is guaranteed. By contrast, for $\mathbf{x}_t$ in a polytope such that no feasible MPC solution exists and not all of the corresponding closed-loop eigenvalues are inside the unit disk, instability will persist. This is illustrated further in Figure 4.22, discussed below.

- It should be noted that entering into the polytope 2, where the ZLB is active, is an alarming situation, as the infeasibility polytope 3 seats next to this polytope. The longer the economy stays at ZLB, the higher the chance of getting into the infeasibility polytope (a case of liquidity trap) as a result of sudden adverse fluctuations in the economy. Similar observations have been made through numerical simulation (Reifschneider and Williams 2000).
- In Figure 4.13 through Figure 4.18 real-time economy data are plotted for 2008Q1:2011Q1. It is clear that from Figure 4.13, Figure 4.15 and Figure 4.17 ($R = 0.07$) that clipping to zero is optimal interest rate for nearly all economic points while in Figure 4.14, Figure 4.16 and Figure 4.18 ($R = 0.55$) more of the economic data indicate non-zero interest rate due to the policy rule being sluggish.

4.8 Closed-loop Simulations

4.8.1 Illustratiion of proposed approach

The first set of simulations serves to simply illustrate the effects of ZLB on the closed-loop system. Simulations are shown using the rules presented in Table 4.6 through Table 4.11, as well as the rules with inertia shown in Table 4.12 along with five additional rules with similar structure but different MPC weights R and S (not shown in Table 4.12 for brevity). For this set of simulations the economy is considered to be at $y = -3.7$ and $\pi = 1.9$ in year 1, corresponding to 2009Q1. The results are summarized in Figure 4.20 and Figure 4.21. The resulting sums of squared errors (discrepancies between actual and desired values) are summarized in Table 4.13 and Table 4.14.

Based on these simulation results, it is clear that for small values of R or S, optimal interest rate rules are aggressive and more likely to produce interest rate values at the ZLB when corresponding conditions arise. Conversely, increase in the values of R or S results in sluggish response, as expected.

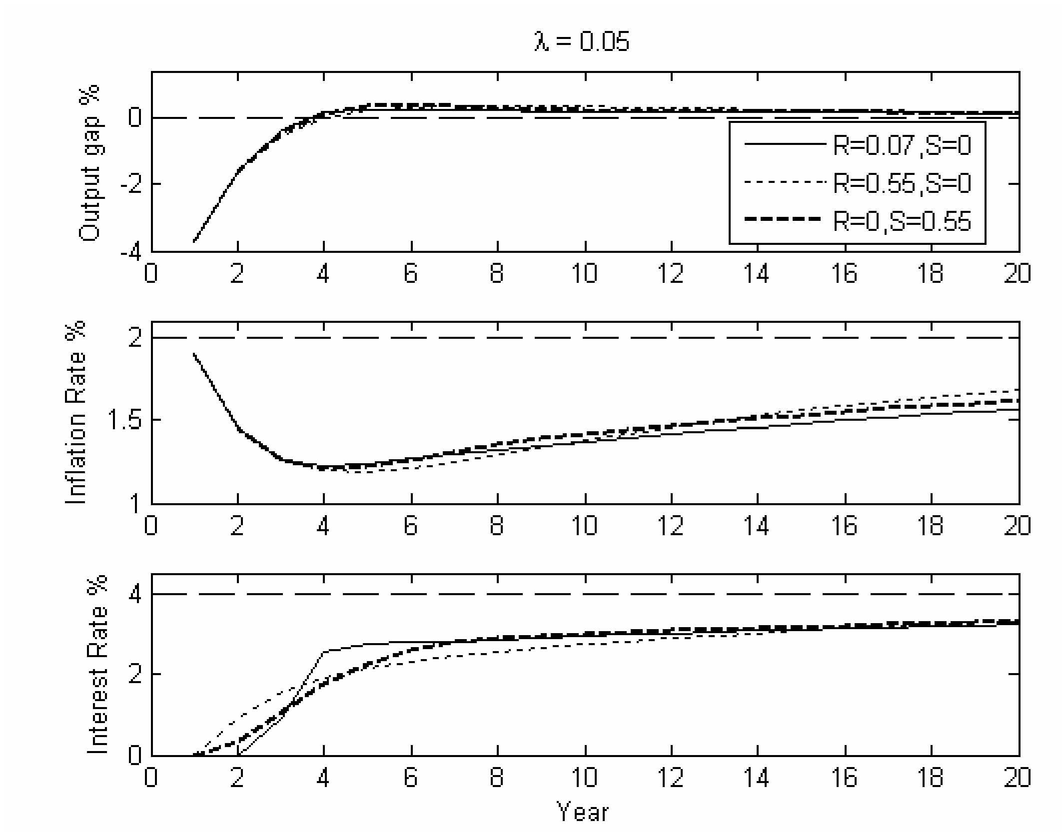

Figure 4.20. Closed-loop simulation for US economy (start point is 2009Q1) for $\lambda = 0.05$.

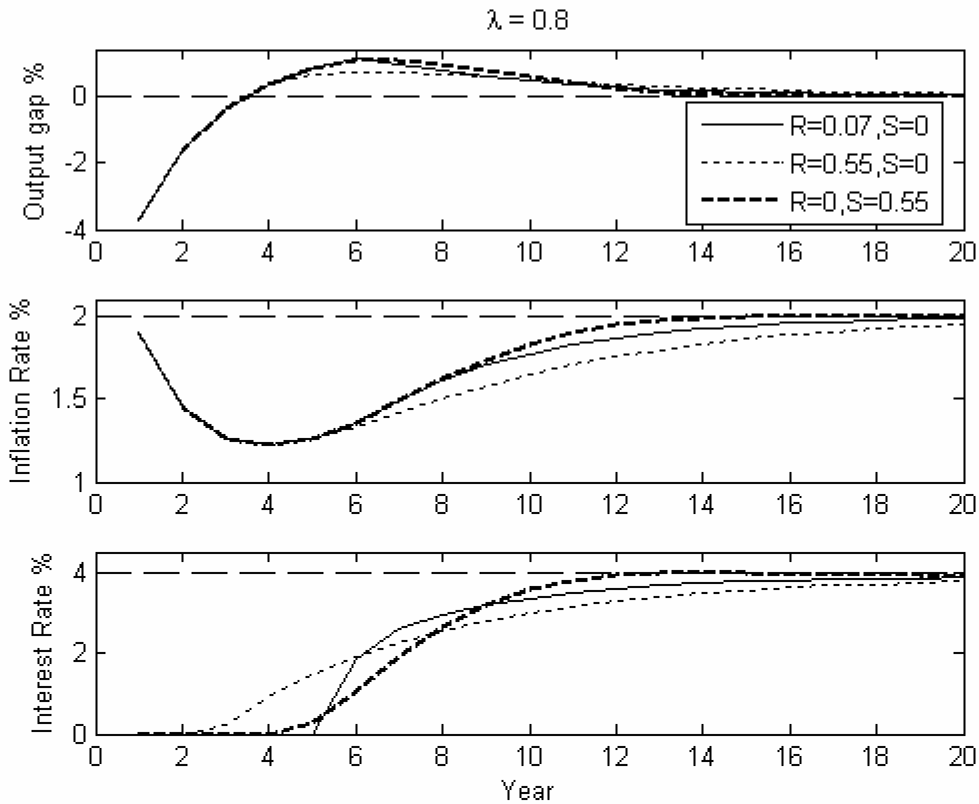

Figure 4.21. Closed-loop simulation for US economy (start point is 2009Q1) for $\lambda = 0.8$.

Table 4.13. Sum of squared errors for closed-loop simulations with $\lambda = 0.05$

	$S=0, R=0.07$	$S=0, R=0.55$	$S=0.07, R=0$	$S=0.55, R=0$
$\sum_{t=2}^{20} y_t^2$	3.30	4.12	3.29	3.65
$\sum_{t=2}^{20} (\pi_t - 2)^2$	7.21	6.69	7.22	6.52
$\sum_{t=1}^{19} (i_t - 3.9)^2$	54.5	53.2	54.4	54.3
$\sum_{t=1}^{19} (i_t - i_{t-1})^2$	3.63	1.52	3.32	1.54

Table 4.14. Sum of squared errors for closed-loop simulations with $\lambda = 0.8$

	$S=0, R=0.07$	$S=0, R=0.55$	$S=0.07, R=0$	$S=0.55, R=0$
$\sum_{t=2}^{20} y_t^2$	7.14	5.75	7.43	7.99
$\sum_{t=2}^{20} (\pi_t - 2)^2$	3.02	3.72	2.97	2.93
$\sum_{t=1}^{19} (i_t - 3.9)^2$	84.0	71.2	85.8	88.4
$\sum_{t=1}^{19} (i_t - i_{t-1})^2$	4.27	1.43	3.59	2.47

The second set of simulations illustrates a liquidity trap case. Figure 4.22, shows state-space partition for $R = 0.07$ and $\lambda = 0.5$. Two different initial conditions of the economy are considered. For the first case we let the initial point be $y_1 = -7.1$, $\pi_1 = 1.5$ (2009Q3), which lies in polytope 2 in Figure 4.22 and hence the corresponding optimal interest rate is zero. For the second case we let $y_1 = -7.1$, $\pi_1 = 0$, which lies inside the infeasibility polytope 3, namely no non-negative interest rate can stabilize the economy at that point. A zero interest rate alone results in an unstable closed loop. The only way to stabilize the closed loop would be through additional external stimulus. Given the fact that it is practically difficult to exactly quantify the polytope of liquidity trap, the central back should focus on external stimulus as soon as the ZLB is reached. Closed-loop simulations, the results of which are shown in

Figure 4.23, confirm the preceding assertions for both cases. It is also interesting to note that even though the interest rate in the first case is stabilizing, recovery of the economy is very slow due to the effect of ZLB (inflation stabilization, in particular, takes many years).

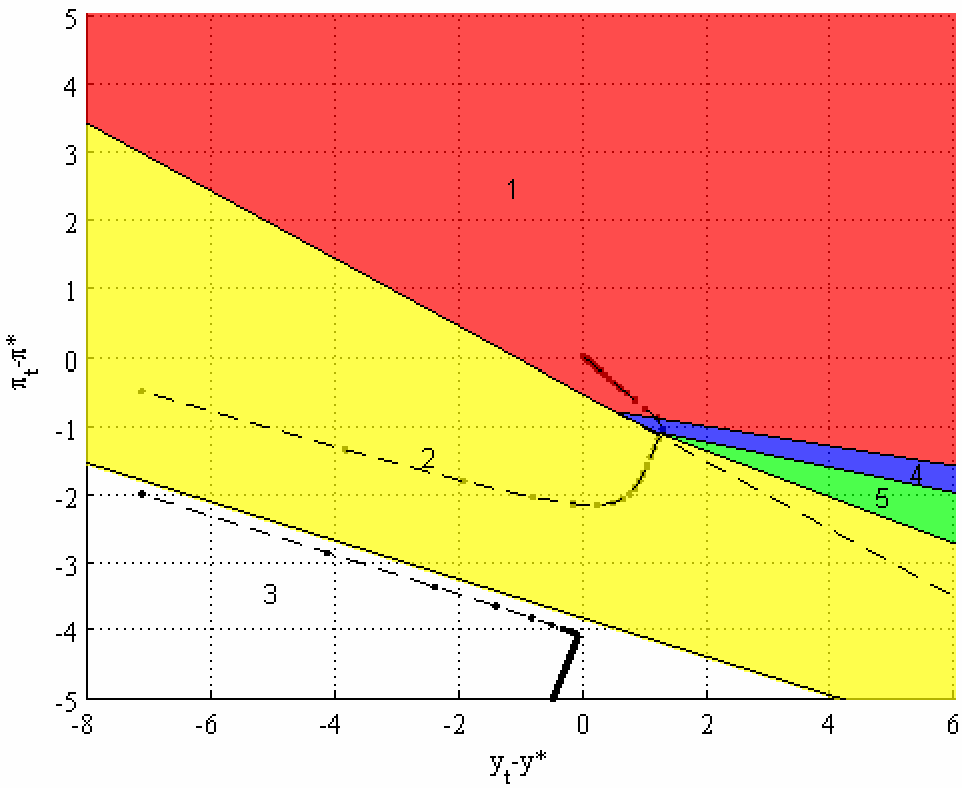

Figure 4.22. Closed-loop simulation for (y,π)=(-7.1, 1.5) 2009Q3 and (y,π)=(-7.0, 0) virtual point for $R = 0.07$, $\lambda = 0.5$. The later state lies in infeasibility polytope and no positive interest rate can stabilize the closed loop.

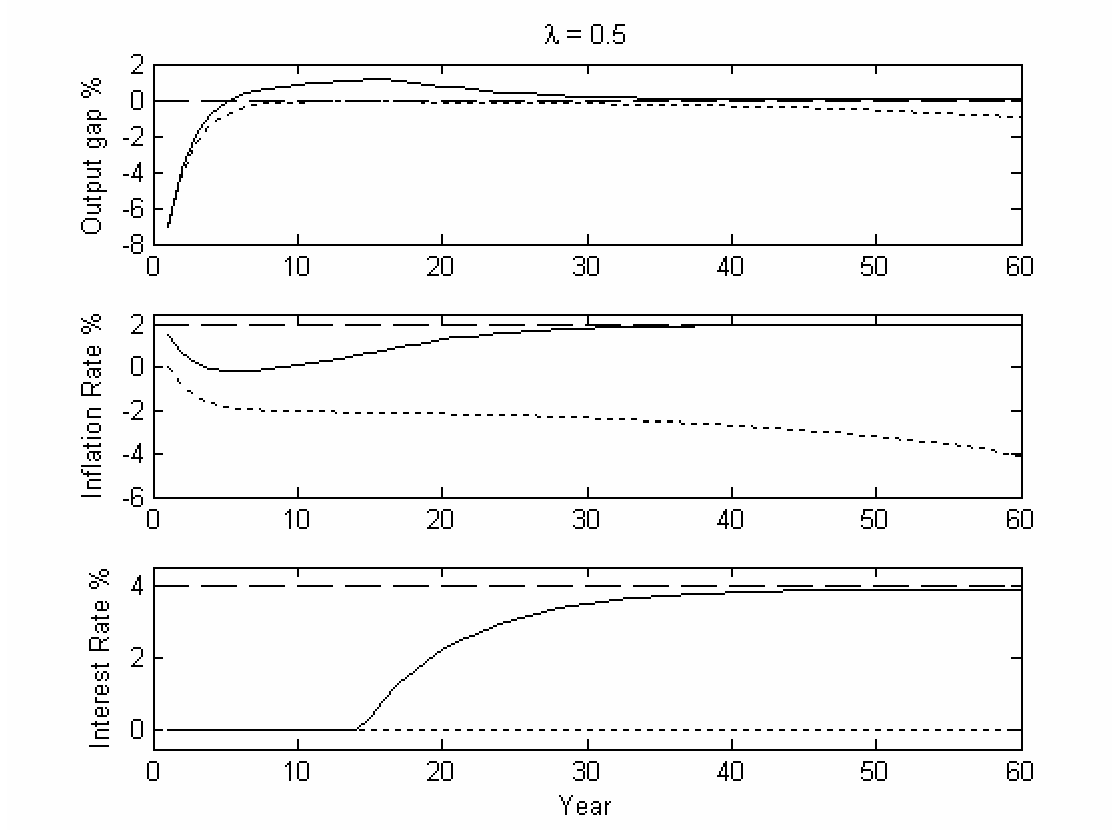

Figure 4.23. Closed-loop simulation for Figure 4.22.

4.8.2 Comparison with historical data

We use real-time data available to the central bank at the time of making a decision on the interest rate, for the period 1987Q4:2008Q4. For output gap we use Greenbook data over the period 1987Q4:2005Q4; for the remaining period we consider CBO data (Nikolsko-Rzhevskyy and Papell 2011). The real-time inflation data is also taken from the same publication.

We focus on the interest rate rule with inertia, eqn. (4.38), with $r^* = 1.9$ and $\pi^* = 2$. Since the coefficients ϕ_y, ϕ_π and ϕ_i are functions of the weights S and λ as given by eqns. (4.42)-(4.44), these weights and corresponding coefficients are estimated using regression to fit the historical data. Estimated values over the entire period of data are shown in Table 4.15. Figure 4.24 (and Figure 4.25) compares the interest rate resulting from fitting eqn. (4.38) to the interest rate implemented, as well as to the interest rate suggested by the standard Taylor rule (eqn. (4.1) with $\phi_y = 0.5$, $\phi_\pi = 1.5$), and by the Taylor rule with values fitted over the entire period of data examined (eqn. (4.1) with $\phi_y = 0.77$, $\phi_\pi = 2.0$). It is clear that the inertial rule captures the central bank decisions better, as also demonstrated by the residuals shown in Figure 4.26.

Table 4.15. Inertial Policy estimation for US interest rate rule based on real-time data. Standard deviations are reported in brackets.

	Period	S	λ	ϕ_y	ϕ_π	ϕ_i	$\phi_\pi + \phi_i$
	1987Q4:2008Q4	0.83(0.23)	0.09(0.03)	0.29	0.71	0.62	1.33
1	1987Q4:1999Q4	1.1(0.43)	0.10(0.06)	0.24	0.67	0.64	1.31
2a	2000Q1:2004Q4	0.15(0.08)	-0.07(0.03)	0.66	0.13	0.47	0.60
2b	2000Q1:2004Q4	0.3	0	0.48	0.60	0.55	1.15
3	2005Q1:2008Q4	0.44(0.26)	0.16(0.1)	0.53	1.25	0.55	1.80

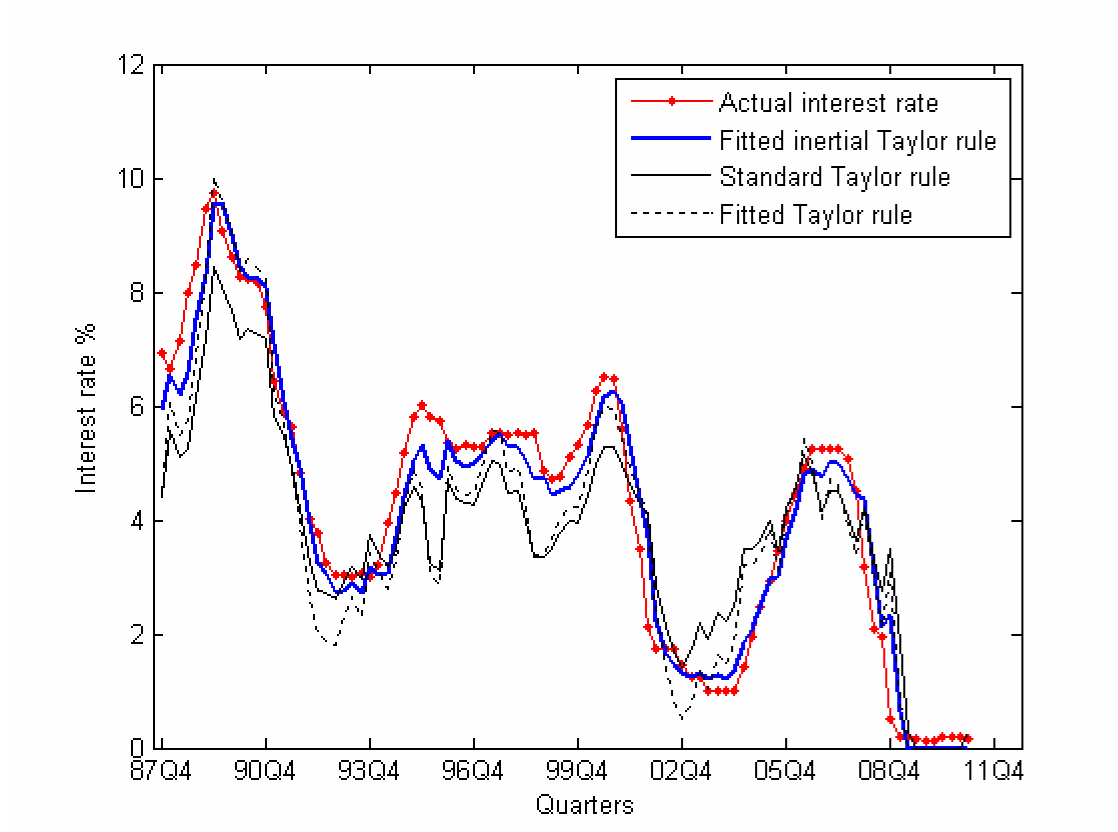

Figure 4.24. Federal funds rate, standard Taylor rule, fitted inertial and fitted Taylor rules (fitting period 1987Q4: 2008Q4) for period 1987Q4: 2011Q1. Note that the interest rate reduction in 2008 suggested by the inertial Taylor rule is more drastic than that suggested by the standard Taylor rule. Note also that the actual interest rate over the period 2002-2005 is captured fairly well by the inertial Taylor rule, while the standard Taylor rule produces significantly larger values, as has been studied extensively by Taylor (Taylor 2009).

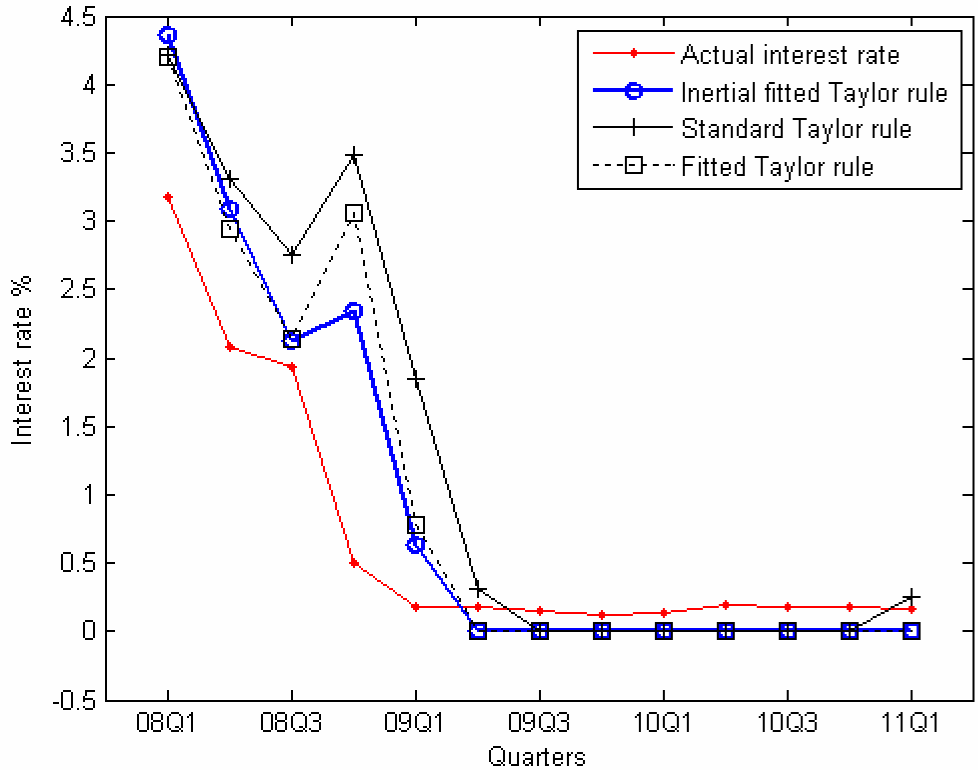

Figure 4.25. Magnified view of Figure 4.24 when interest rates are near zero.

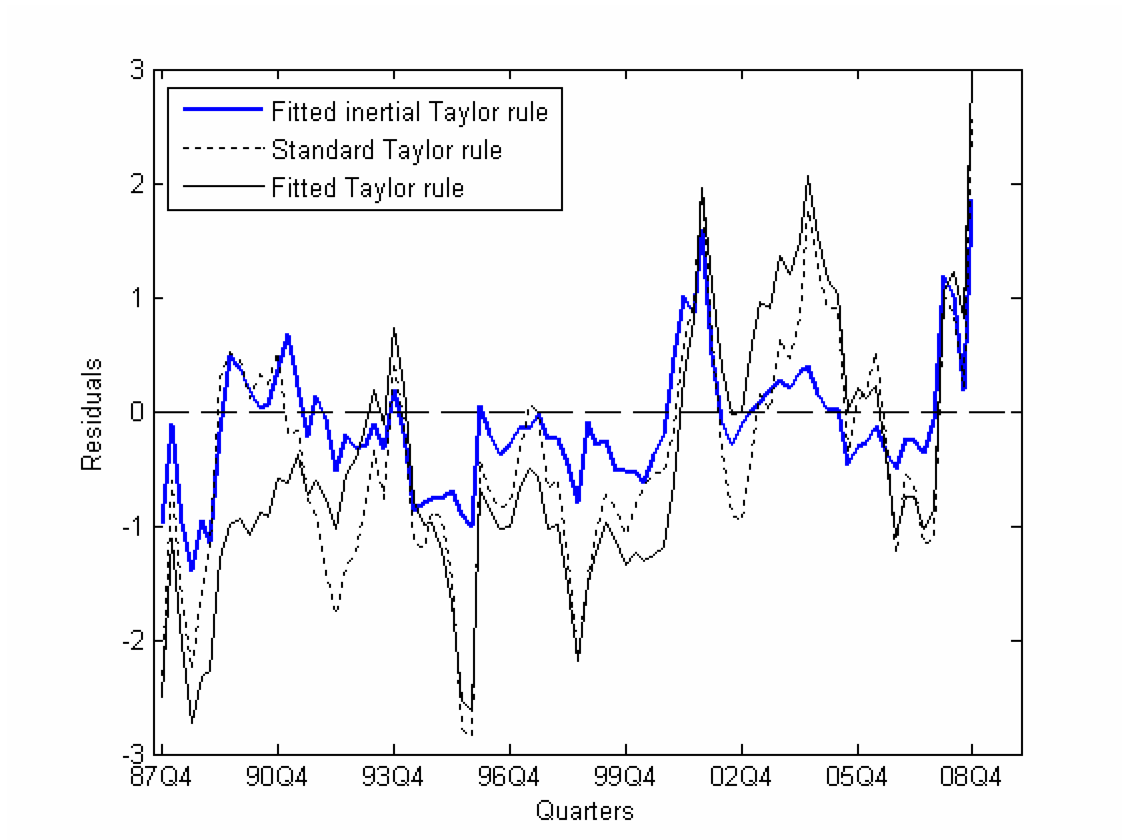

Figure 4.26. Residuals for policies in Figure 4.24 for fitting period 1987Q4: 2008Q4

It is also interesting to examine whether additional insight may be gained by fitting data over short periods for which large residuals result from fitting the entire data set. One such period with large residuals is 2000Q1:2004Q4. Table 4.15 (line 2a) suggests that this period may be problematic, in that the corresponding inertial rule, if applicable, is not stabilizing, i.e.,the fitted value of $\phi_\pi + \phi_i$ is greater than 1, thus violating the closed-loop stability condition in eqn. (4.47). In fact, it is dubious whether the same objective as on the average was used over that period, since the value of λ fitted over that period is negative, hence unacceptable. Constrained fitting (i.e., enforcing $0 \le \lambda \le 1$) produces parameter values that do correspond to a stabilizing rule (Table 4.15, line 2b) but nonetheless places all emphasis on output gap (growth). The actual policy implemented over that period and its role on stimulating over-expansion of the economy has been the subject of intense discussion (Taylor 2009).

4.9 Conclusions

The main issue addressed in this work is the effect of zero lower bound on the optimal interest rate determined by a central bank. We address this issue in a multi-parametric model predictive control (mpMPC) framework, which allows the derivation of explicit feedback rules even when inequality constraints are present. Application of this framework to a simple model of the US economy produced a number of Taylor-like rules, depending on the form and parameter values in the objective function employed by MPC. The results suggest that a small number of simple Taylor-like rules can be applied at each time, depending on the state of the economy. However, it was also shown that simply setting to zero negative interest rates produced by unconstrained Taylor rules is optimal in situations of negative output gap, as happened recently. Furthermore, it was observed, as has been noted elsewhere, that rules with inertia appear to better capture past decisions by the Central bank. Such rules have been systematically derived here by considering penalties on the rate of interest rate change in the MPC objective function.

CHAPTER 5

CONCLUSIONS AND FUTURE DIRECTIONS

The main results of this research work and the scope for future work are summarized below:

First part of this research work has demonstrated how linear control can be designed for a nonlinear industrial process. A theoretical framework is developed for controller design for a nonlinear process with input disturbances. Main result of this work is a stability criterion for open loop stable nonlinear process which is given by

$$\left\|(N-L)Q\right\|_{\Delta E} < 1. \qquad (5.1)$$

Eqn. (5.1) has similar expression as developed by (Eker and Nikolaou 2000; Nikolaou and Misra 2003) for robust controller synthesis. However, it has been found that size of set E also play significant role to govern the stability of closed loop which was not found to be critical in earlier research. An iterative computational approach is presented here to calculate $\left\|(N-L)Q\right\|_{\Delta E}$. A simulation case study has been shown for an industrial NOx reduction unit which is required to operate in rich fuel conditions. The proposed framework is used to gain useful insight into linear controller design. The key for linear controller design is that (a) control has to be tight enough (i.e., the controller gain should be large enough) to ensure that the process does not escape far from the desired set-point trajectory and reversal of the steady-state gain is not realized, hence closed-loop is stable, and (b) control must not be too tight (i.e., the controller gain should not be too high) to avoid potential problems such as instability and lack of robustness. Therefore present study put an emphasis that excessive detuning of linear controller should be avoided and detuning is limited by nonlinearity of process. The work presented here can be extended in a number of ways, to address issues such as the following:

- How does the proposed approach perform on multivariable systems?
- Can closed-loop performance be improved appreciably by automatically detecting in real time when aggressive or sluggish control action can be taken and by adapting controller action accordingly?
- Could nonlinear controller design provide appreciable performance improvements and be robust enough for practical use in the absence of a detailed nonlinear model of the controlled process?

In second part the focus is an industrial process which suffers with bottlenecking of level control in three tanks in series. It has been found that conventional feedback scheme is not able to provide desired control performance. To debottleneck the system, a new control scheme is proposed based on multivariate control structure and it is designed in such a way so that at the same time inventory capacity of all tanks can be utilized to reject sinusoidal or step disturbances. The scheme basically transforms a system of tanks in series into a single tank of larger inventory and hence provides additional flexibility to reject disturbance and achieving flow attenuation. The control scheme can easily be extended to N tank in series as given by eqn. (3.18). Control tuning charts are prepared based on tank level constraints for the step and sinusoidal disturbances. Computer simulations have verified the control performance of proposed scheme is better than conventional feedback scheme. Finally proposed control scheme has been implemented in real plant and much better control performance was reported. Further, an effort has been made to derive the optimal control structure based on numerical optimization which minimizes the desired control objective. The formuletd minimization porblom is non convex in nature and the solution to the optimization problem is diffucult to obtain. Finally, feedforward action is also included in proposed scheme. It has been found that in general proposed scheme is much easier to tune and has better performance for sinusoidal disturbances of various frequencies in compare to conventional feedback feedforward scheme.

In third part an effort has been made to derive optimal interest rate rules when interest rates determined by a central bank are subject to a zero lower bound. Particularly these questions are answered, (a) how a zero lower bound on interest rate affects the optimal interest rate rule, (b) can interest rate rules be interpreted as a linear rule similar to Taylor rule in presence of ZLB constraint, (c) how interest rate rule coefficients depend on various weights in central bank's objective function. Earlier research works have tried to address these questions on ad-hoc basis or as a solution to optimization problem with the help of dynamic programming. In this research work answers to these questions are addressed in mpMPC framework which allows the derivation of explicit feedback rules even when inequality constraints are present. An application to proposed framework is shown using a linear dynamic model of US economy.

The investigations with mpMPC have revealed that when economy is near to ZLB, interest rate rule can deviate from the solution of unconstrained case in anticipation that future interest rates can be constrained. On one side large negative output gap results in "zero" as optimal interest rate rule and another side in case of positive output gap we observe interest rate rule becomes more aggressive than unconstrained case. mpMPC results in explicit rules which are small in number and follow the same form as Taylor rule eqn (4.36). Such rules help policy makers to understand how to adopt interest rate when economy is near ZLB. As discussed (Williams 2009) that ad-hoc rules suffers with practical problem that public may get confused. mpMPC is systematic way to derive optimal rules and hence eliminate possibility of confusion. Further, the present work also creates the basis for the some of the ad-hoc rules (various truncation rules) being optimal for some particular choice of weights in optimization problem.

The mpMPC frame-work provides explicit interest rate rules which create a link between weights in objective function and resulted interest rate rules. The investigations with actual interest rate applied by central bank have revealed that there is a significant amount of inertia present in the interest rate rules adopted by central bank. It is found that interest rates are not changed in aggressive manner expect in recent few years when economy reached near ZLB (Table 4.15). This suggests that central bank operates in dual mode, i.e., it has long term and short term objectives. In case of emergency if central bank realizes that inflation or output gap need to be stabilized they modify their preference based on their choice (more weight on output or inflation or interest rate smoothing). It is evident that mpMPC provides a practical framework for central bank to determine how to modify (eqns. (4.25) and (4.26); eqns. (4.42)-(4.44)) Taylor rules based on policy preference and presence of ZLB.

A number of issues touched in this work warrant further investigation, such as the following:

- The inverse problem: Given a suggested Taylor-like rule, what objective function, as in eqn. (4.11), is minimized? A promising approach is suggested in section 4.3.1.5.

- Robust stability and performance: There is a vast body of work in the automatic control community addressing the robustness issue, namely how a controller performs when the model assumed in controller design has quantifiable uncertainty.
- Modeling and selection of controlled variables: Should the pair output gap and inflation be the main focus or could variables such unemployment (Orphanides and Williams 2007) be central in controlling an economy?
- Policy adaptation: The main attractiveness of a fixed rule is its simplicity and predictability (Williams 2009). However, such a rule may become sub-optimal over time, as the economy or disturbance models change (Orphanides 2003). Can a fixed rule be replaced by a fixed rule adaptation policy that maintains robustness?

We hope to address the above issues in forthcoming publications.

REFERENCES

Adam, K. and R. M. Billi (2007). "Discretionary monetary policy and the zero lower bound on nominal interest rates." Journal Of Monetary Economics **54**(3): 728-752.

Allgöwer , F. (1996). Definition and computation of a nonlinearity measure. Proceedings of Nonlinear Control System Design Symposium, Pergamon,Oxford,UK.

Balakotaiah, V. and D. Luss (1985). "Input-Multiplicity In Lumped-Parameter Systems." Chemical Engineering Communications **39**(1-6): 309-322.

Ball, L. (1999). "Efficient Rules for Monetary Policy." International Finance **2**: 63–83.

Bayer (2008). Personal Communication. Baytown, TX.

Boyd, S., L. El Ghaoui, E. Feron, and V. Balakrishnan (1994). Linear Matrix Inequalities in System and Control Theory, Society for Industrial and Applied Mathematics (SIAM).

CBO (2011). Budget And Economic Outlook: Fiscal Years 2011 To 2021. C. B. Office.

Cheung, T. F. and W. L. Luyben (1979). "LIQUID-LEVEL CONTROL IN SINGLE TANKS AND CASCADES OF TANKS WITH PROPORTIONAL-ONLY AND PROPORTIONAL-INTEGRAL FEEDBACK CONTROLLERS." Industrial & Engineering Chemistry Fundamentals **18**(1): 15-21.

Cheung, T. F. and W. L. Luyben (1980). "NON-LINEAR AND NON-COVENTIONAL LIQUID-LEVEL CONTROLLERS." Industrial & Engineering Chemistry Fundamentals **19**(1): 93-98.

Chidambaram, M. and G. P. Reddy (1996). "Nonlinear control of systems with input and output multiplicities." Computers & Chemical Engineering **20**(3): 295-299.

Chmielewski, D. and V. Manousiouthakis (1996). "On constrained infinite-time linear quadratic optimal control." Systems & Control Letters **29**(3): 121-129.

Clarida, R., J. Gali and M. Gertler (2000). "Monetary policy rules and macroeconomic stability: Evidence and some theory." Quarterly Journal Of Economics **115**(1): 147-180.

Darby, M. L. and M. Nikolaou (2007). "A parametric programming approach to moving-horizon state estimation." Automatica **43**(5): 885-891.

Dash, S. K. and L. B. Koppel (1989). "Sudden Destabilization Of Controlled Chemical Processes." Chemical Engineering Communications **84**: 129-157.

Davig, T. and E. M. Leeper (2007). "Generalizing the Taylor Principle." American Economic Review **97**(3): 607-635.

Desoer, C. A. and R. W. Liu (1982). "Global parametrization of feedback systems with nonlinear plants." Systems & Control Letters **1**(4): 249-251.

Desoer, C. A. and M. Vidyasagar (1975). Feedback Systems: Input-Output Properties, Academic Press.

Desoer, C. A. and Y.-T. Wang (1980). "Foundations of Feedback Theory for Nonlinear Dynamical Systems." IEEE Trans. Circ. Syst. **CAS-27**(2): 104-123.

Edward P. Gatzke, E. S. M., Chung Wang and Francis J. Doyle III (2000). "Model Based Control of a Four-Tank System." Computers and Chemical Engineering **24**: 1503-1509.

Eker, S. A. and M. Nikolaou (2000). "Linear Control of Nonlinear Systems - The Interplay between Nonlinearity and Feedback." AICHE Journal **48**(9): 1957-1980.

Eker, S. A. and M. Nikolaou (2002). "Linear control of nonlinear systems: Interplay between nonlinearity and feedback." AIChE Journal **48**(9): 1957-1980.

Fuhrer, J. C. and B. F. Madigan (1997). "Monetary policy when interest rates are bounded at zero." Review Of Economics And Statistics **79**(4): 573-585.

Garcia, C. E. and M. Morari (1982). "Internal model control: 1. a unifying review and some new results." Ind. Eng. Chem. Process Des. Dev. **24**: 308-323.

Genceli, H. and M. Nikolaou (1993). "ROBUST STABILITY ANALYSIS OF CONSTRAINED L(1)-NORM MODEL-PREDICTIVE CONTROL." Aiche Journal **39**(12): 1954-1965.

Giannoni, M. P. and M. Woodford (2002). Optimal Interest rate Rules: I. General Theory NBER Working Paper Series.

Giannoni, M. P. and M. Woodford (2003). "How forward-looking is optimal monetary policy?" Journal Of Money Credit And Banking **35**(6): 1425-1469.

Golbert, J. and D. R. Lewin (2004). "Model-based control of fuel cells: (1) Regulatory control." Journal of Power Sources **135**(1-2): 135-151.

Goodfriend, M. (1991). Interest rates and the conduct of monetary policy Carnegie-Rochester Conference Series on Public Policy, Elsevier. **34:** 7-30.

Grieder, P., F. Borrelli, F. Torrisi and M. Morari (2004). "Computation of the constrained infinite time linear quadratic regulator." Automatica **40**(4): 701-708.

Helbig, A., W. Marquardt and F. Allgower (2000). "Nonlinearity measures: definition, computation and applications." Journal of Process Control **10**: 113-123.

Hunt, B. and D. Laxton (2003). The zero-interest rate floor and its implications for monetary policy in Japan. Japan's Lost Decade: Policies for Economic Revival. T. Callen and J. D. Ostry. Washington, DC, International Monetary Fund**:** 179–205.

Jones, W. P. and R. P. Lindstedt (1988). "GLOBAL REACTION SCHEMES FOR HYDROCARBON COMBUSTION." Combustion and Flame **73**(3): 233-249.

Judd, J. P. and G. D. Rudebusch (1998). Taylor's Rule and the Fed: 1970–1997. Federal Reserve Bank of San Francisco Economic Review. **3:** 3-16.

Jung, T., Y. Teranishi and T. Watanabe (2005). "Optimal monetary policy at the zero-interest-rate bound." Journal Of Money Credit And Banking **37**(5): 813-835.

Karra, S. and M. N. Karim (2010). Extended SBX-RCGA Neural Network-Based Multi-Model Predictive Control for Wastewater Neutralization Process. AIChE Annual Meeting, Paper No: 197g, Salt Lake City, UT.

Kato, R. and S. I. Nishiyama (2005). "Optimal monetary policy when interest rates are bounded at zero." Journal Of Economic Dynamics & Control **29**(1-2): 97-133.

Khalil, H. K. (2002). Nonlinear Systems. Upper Saddle River, New Jersey, Prentice Hall.

Kim, J. P., Schnell, U., Scheffknecht, G. (2008). "Comparison of different global reaction mechanisms for mild combustion of natural gas." Combustion Science and Technology **180**: 565-592.

Konnov, A. A., J. N. Zhu, J. H. Bromly and D. K. Zhang (2004). "Noncatalytic partial oxidation of methane into syngas over a wide temperature range." Combustion Science and Technology **176**(7): 1093-1116.

Koppel, L. B. (1982). "Input Multiplicities In Non-Linear, Multivariable Control-Systems." Aiche Journal **28**(6): 935-945.

Ljung, L. (1999). System Identification: Theory for the User, Prentice Hall.

Luyben, W. L. and P. S. Buckley (1977). "PROPORTIONAL-LAG LEVEL CONTROLLER." instrumentation technology **24**(12): 65-68.

Ma, K. M., H. Valdes-Gonzalez, and I. D. L. Bogle (2010). "Process design in SISO systems with input multiplicity using bifurcation analysis and optimisation." Journal Of Process Control **20**(3): 241-247.

Maciejowski, J. (2000). Predictive Control with Constraints, Prentice Hall.

McDonald, K. A., T. J. McAvoy and A. Tits (1986). "OPTIMAL AVERAGING LEVEL CONTROL." Aiche Journal **32**(1): 75-86.

Morari, M. and E. Zafiriou (1989). Robust Process Control, Prentice-Hall.

Muske, K. R. and J. B. Rawlings (1993). "Linear model predictive control of unstable processes." Journal of Process Control **3**(2): 85-96.

Muske, K. R. and J. B. Rawlings (1993). "Model predictive control with linear models." AIChE Journal **39**(2): 262-287.

Nakov, A. (2008). "Optimal and Simple Monetary Policy Rules with Zero Floor on the Nominal Interest Rate." International Journal of Central Banking **4**(2): 73-127.

Nikolaou, M. (1993). When is Nonlinear Dynamic modeling necessary? Proceedings of the American Control Conference, San Francisco,CA.

Nikolaou, M. (1997). Computer-Aided Process Engineering in the Snack Food Industry. Fifth International Conference on Chemical Process Control. J. C. Kantor, C. E. García and B. Carnahan. Tahoe City, CA, CACHE-AIChE. **93:** 61-69.

Nikolaou, M. and Manousiouthakis (1989). " Hybrid Approach to Nonlinear System Stability and Performance." AICHE **35**(4): 559-572.

Nikolaou, M. and P. Misra (2003). "Linear control of nonlinear processes: recent developments and future directions." Computers & Chemical Engineering **27**(8-9): 1043-1059.

Nikolsko-Rzhevskyy, A. and D. H. Papell (2011). Taylor's Rule versus Taylor Rules.

Orphanides, A. (2003). "Monetary policy evaluation with noisy information." Journal Of Monetary Economics **50**(3): 605-631.

Orphanides, A. and V. Wieland (2000). "Efficient monetary policy design near price stability." Journal Of The Japanese And International Economies **14**(4): 327-365.

Orphanides, A. and J. C. Williams (2007). "Robust monetary policy with imperfect knowledge." Journal Of Monetary Economics **54**(5): 1406-1435.

Pearson, R. K. (2003). "Selecting nonlinear model structures for computer control." Journal of Process Control **13**(1): 1-26.

Pistikopoulos, E. N., V. Dua, N. A. Bozinis, A. Bemporad and M. Morari (2000). "On-line optimization via off-line parametric optimization tools." Computers & Chemical Engineering **24**(2-7): 183-188.

Qin, S. and T. Badgwell (2000). An overview of nonlinear model predictive control applications. Nonlinear Predictive Control.

Rawlings, J. B. and D. Q. Mayne (2009). Model Predictive Control: Theory and Design, Nob Hill Publishing.

Razon, L. F. and R. A. Schmitz (1987). "MULTIPLICITIES AND INSTABILITIES IN CHEMICALLY REACTING SYSTEMS - A REVIEW." Chemical Engineering Science **42**(5): 1005-1047.

Reifschneider, D. and J. C. Williams (2000). "Three lessons for monetary policy in a low-inflation era." Journal Of Money Credit And Banking **32**(4): 936-966.

Rivera, D. E., M. Morari and S. Skogestad (1986). "INTERNAL MODEL CONTROL .4. PID CONTROLLER-DESIGN." Industrial & Engineering Chemistry Process Design and Development **25**(1): 252-265.

Rotemberg, J. J. and M. Woodford (1997). An optimization-based econometric framework for the evaluation of monetary policy. Nber Macroeconomics Annual 1997. Cambridge, M I T Press. **12:** 297-+.

Sbarbaro, D. and R. Ortega (2007). "Averaging level control: An approach based on mass balance." Journal of Process Control **17**(7): 621-629.

Scokaert, P. O. M. and J. B. Rawlings (1998). "Constrained linear quadratic regulation." Ieee Transactions on Automatic Control **43**(8): 1163-1169.

Shin, J., J. Lee, S. Park, K. K. Koo and M. Lee (2008). "Analytical design of a proportional-integral controller for constrained optimal regulatory control of inventory loop." Control Engineering Practice **16**(11): 1391-1397.

Singh, A. and M. Nikolaou (2009). Controller Design for Processes with Unmeasured Disturbances Changing the Steady-State Gain Sign AIChE Annual Meeting, Nashville,TN.

Singh, A. and M. Nikolaou (2011). Simple and Improved Level Control Scheme for Tanks In Series. Spring Meeting, AICHE,(117d), Chicago, IL.

Sistu, P. B. and B. W. Bequette (1995). "MODEL-PREDICTIVE CONTROL OF PROCESSES WITH INPUT MULTIPLICITIES." Chemical Engineering Science **50**(6): 921-936.

Smith, G. P., Golden, D. M., Frenklach, M., Moriarty, N. W., Eiteneer, B., Goldenberg, M., Bowman, C. T., Hanson, R. K., Song, S., Gardiner, W. C., Jr., Lissianski, V. V., Qin, Z. (1999). GRI-Mech 3.0.

Stack, A. J. and F. J. Doyle (1997). "The optimal control structure: An approach to measuring control-law nonlinearity." Computers & Chemical Engineering **21**(9): 1009-1019.

Taylor, J. B. (1993). Discretion versus policy rules in practice. Carnegie-Rochester Conference Series on Public Policy 39, North-Holland.

Taylor, J. B. (2009). Getting off track: how government actions and interventions caused, prolonged, and worsened the financial crisis. Stanford, CA, Hoover Institution Press.

Taylor, J. B. and J. C. Williams (2010). "Simple and Robust Rules for Monetary Policy." Federal Reserve Bank of San Francisco Working Paper Series(http://www.frbsf.org/publications/economics/papers/2010/wp10-10bk.pdf).

Taylor, J. B. and J. C. Williams (2010). Simple and Robust Rules for Monetary Policy. Federal Reserve Bank of San Francisco Working Paper Series.

Tsang, W. and R. F. Hampson (1986). "CHEMICAL KINETIC DATABASE FOR COMBUSTION CHEMISTRY .1. METHANE AND RELATED-COMPOUNDS." Journal of Physical and Chemical Reference Data **15**(3): 1087-1279.

Vidyasagar, M. (1985). Control System Synthesis : A Factorization Approach, MIT Press.

Vidyasagar, M. (1993). Nonlinear systems analysis. Englewood Cliffs, N.J., Prentice Hall.

Vuthandam, P., H. Genceli and M. Nikolaou (1995). "PERFORMANCE BOUNDS FOR ROBUST QUADRATIC DYNAMIC MATRIX CONTROL WITH END CONDITION." Aiche Journal **41**(9): 2083-2097.

Willems, J. (1971). "The Analysis of Feedback Systems."

Williams, J. C. (2006). Monetary Policy in a Low Inflation Economy with Learning. Proceedings of the Bank of Korea International Conference, Seoul:Bank of Korea.

Williams, J. C. (2009). "Heeding Daedalus: Optimal Inflation and the Zero Lower Bound." Brookings Papers on Economic Activity: 1-49.

Williams, J. C. (2009). "Heeding Daedalus: Optimal Inflation and the Zero Lower Bound." Brookings Papers On Economic Activity(2): 1-49.

Woodford, M. (1999). "Optimal monetary policy inertia." Manchester School **67**: 1-35.

Woodford, M. (2001). "The Taylor Rule and Optimal Monetary Policy." The American Economic Review **91**(2): 232-237.

Woodford, M. (2003). Interest and Prices, Princeton University Press.

APPENDICES

Appendix A. Background on nonlinear operators (Willems 1971) (Desoer and Vidyasagar 1975)

The norm and incremental norm of a nonlinear operator $N:\ U \to Y$ over a set $V \subseteq U$ are defined as,

$$\|N\|_V = \sup_{\substack{u\in V \\ u\neq 0}} \frac{\|Nu\|}{\|u\|}, \tag{A.1}$$

and

$$\|N\|_{\Delta V} = \sup_{\substack{u_1,u_2\in V \\ u_1\neq u_2}} \frac{\|Nu_1 - Nu_2\|}{\|u_1 - u_2\|}, \tag{A.2}$$

respectively. The norm function considered here for the right-hand sides of above two equations defined on the spaces U and Y is

$$\|x\| \mathrel{\hat{=}} \begin{cases} \int_S \|x(t)\|^p \, dt & \text{if } p \geq 1 \\ \underbrace{\sup}_{t\in S} \|x(t)\| & \text{if } p = \infty \end{cases}, \tag{A.3}$$

where $\|x(t)\|$ denotes any norm of the vector $x(t)$. In present work norms are calculated for $p = 2$.

An operator $N:\ U \to Y : u \mapsto y = Nu$ is finite-gain stable if there exists a constant $k < \infty$, such that,

$$\|y\| \leq k\|u\|. \tag{A.4}$$

Appendix B. Proof of Theorem 1

For the closed-loop structure shown in Figure 2.6, it is clear that

$$\begin{aligned} e_1 &= u_1 - (y_2 - y_L) \\ &= u_1 - Ne_2 + LS_1Qe_1 \\ &= u_1 - Ne_2 + LS_1Qe_1 - NS_1Qe_1 + NS_1Qe_1 \\ &= u_1 - N\left(S_2u_2 + S_1Qe_1\right) - (N-L)S_1Qe_1 + NS_1Qe_1 \\ &\Rightarrow \end{aligned}$$

$$\begin{aligned} \|e_1\| &= \left\|u_1 - N\left(S_2u_2 + S_1Qe_1\right) - (N-L)S_1Qe_1 + NS_1Qe_1\right\| \\ &\le \|u_1\| + \|(N-L)S_1Qe_1\| + \left\|NS_1Qe_1 - N\left(S_2u_2 + S_1Qe_1\right)\right\| \\ &\le \|u_1\| + \left\|\left(N-L\right)S_1Q\right\|\|e_1\| + \|N\|_{\Delta U}\left\|S_1Qe_1 - \left(S_2u_2 + S_1Qe_1\right)\right\| \\ &\Rightarrow \end{aligned}$$

$$\left(1 - \left\|\left(N-L\right)S_1Q\right\|\right)\|e_1\| \le \|u_1\| + \|N\|_{\Delta U}\|S_2u_2\|. \tag{B.1}$$

If

$$\gamma \mathrel{\hat{=}} \left\|\left(N-L\right)S_1Q\right\| < 1, \tag{B.2}$$

then the above eqn. (B.1) implies

$$\|e_1\| \le \frac{\|u_1\| + \|N\|_{\Delta U}\|u_2\|}{1-\gamma}. \tag{B.3}$$

Using the above inequality and the fact that $e_2 = S_2u_2 + S_1Qe_1$ (Figure 2.6) it follows immediately that

$$\begin{aligned} \|e_2\| &= \|S_2u_2 + S_1Qe_1\| \\ &\le \|u_2\| + \|Qe_1\| \\ &\le \|u_2\| + \|Q\|\|e_1\| \qquad , \\ &\le \|u_2\| + \|Q\|\frac{\|u_1\| + \|N\|_{\Delta U}\|u_2\|}{1-\gamma} \\ &= \frac{\|Q\|}{1-\gamma}\|u_1\| + \left(1 + \|Q\|\frac{\|N\|_{\Delta U}}{1-\gamma}\right)\|u_2\| \end{aligned} \tag{B.4}$$

where the linear operator Q is assumed to be stable.

Together, eqns. (B.3) and (B.4) imply that the closed loop is finite-gain stable.

Appendix C. Justification of control scheme

The transfer functions from F_{in} to F_1 and F_2 are

$$G_{\text{in}\to 1} = \frac{A_1 s(\tau_{\text{I},1} s + 1)}{\frac{A\tau_{\text{I},1}}{-K_{c,1}} s^2 + \tau_{\text{I},1} s + 1}, \tag{C.1}$$

and

$$G_{\text{in}\to 2} = G_{\text{in}\to 1} \frac{A_2 s(\tau_{\text{I},2} s + 1)}{\frac{A\tau_{\text{I},2}}{-K_{c,2}} s^2 + \tau_{\text{I},2} s + 1}, \tag{C.2}$$

respectively. The corresponding frequency responses have high-frequency asymptotes $-K_{c,1}$ and $K_{c,1}K_{c,2}$, with break frequencies $\sqrt{\frac{A_1\tau_{\text{I},1}}{-K_{c,1}}}$ and $\left\{\sqrt{\frac{A_1\tau_{\text{I},1}}{-K_{c,1}}}, \sqrt{\frac{A_2\tau_{\text{I},2}}{-K_{c,2}}}\right\}$, respectively. For $-K_{c,1} \approx -K_{c,2} \approx 1$ fluctuations in the disturbance F_{in} create comparable high-frequency fluctuations in F_1 and F_2.

Appendix D. Control design of RLCs

Controller design for first RLC

Refering to Figure 3.6 closed-loop for first RLC is given by,

$$\begin{aligned} As\Delta\tilde{L}_1(s) &= \Delta F_{\mathrm{in}}(s) - \Delta F_1(s) \\ &= \Delta F_{\mathrm{in}}(s) + K_1(s)\left(\Delta\tilde{L}_2(s) - Y_1\Delta\tilde{L}_1(s)\right). \\ \Delta\tilde{L}_1(s) &= \frac{\Delta F_{\mathrm{in}}(s)}{As + Y_1K_1(s)} + \frac{K_1(s)\Delta\tilde{L}_2(s)}{As + Y_1K_1(s)} \end{aligned} \tag{D.1}$$

Let us assume that $\tilde{L}_3 \approx Y_2\tilde{L}_2$ and $\Delta L_3' \approx \Delta L_3 (= \Delta\tilde{L}_3)$. Using eqn. (D.1) and eqn. (3.20) yields,

$$\Delta\tilde{L}_1(s) \approx \frac{\eta As + K_3(s) + \dfrac{K_1(s)}{Y_2}}{\left(\eta As + K_3(s)\right)\left(As + Y_1K_1(s)\right)}\Delta F_{\mathrm{in}}(s), \tag{D.2}$$

$$\frac{\Delta\tilde{L}_1(s)}{\Delta\tilde{L}_3(s)} \approx \frac{\left(\eta As + K_3(s) + K_1(s)/Y_2\right)}{\left(As + Y_1K_1(s)\right)}. \tag{D.3}$$

At steady state ampltitude ratio of $\Delta\tilde{L}_1$ to $\Delta\tilde{L}_3$ is given by

$$\begin{aligned} \left\|\frac{\Delta\tilde{L}_1(s)}{\Delta\tilde{L}_3(s)}\right\| &= \frac{\left\|\eta A\omega j + K_{c,3} + \dfrac{K_{c,3}}{\tau_{\mathrm{I},3}\omega j} + \dfrac{K_{c,1}}{Y_2} + \dfrac{K_{c,1}}{Y_2\tau_{\mathrm{I},1}\omega j}\right\|}{\left\|A\omega j + Y_1K_{c,1} + \dfrac{Y_1K_{c,1}}{\tau_{\mathrm{I},1}\omega j}\right\|} \\ &= \frac{\left\|\left(K_{c,3} + \dfrac{K_{c,1}}{Y_2}\right) + \left(\eta A\omega - \left(\dfrac{K_{c,3}}{\tau_{\mathrm{I},3}\omega} + \dfrac{K_{c,1}}{Y_2\tau_{\mathrm{I},1}\omega}\right)\right)j\right\|}{\left\|Y_1K_{c,1} + \left(A\omega - \dfrac{Y_1K_{c,1}}{\tau_{\mathrm{I},1}\omega}\right)j\right\|}. \end{aligned} \tag{D.4}$$

If

$$K_{c,3} \ll \frac{K_{c,1}}{Y_2}, \tag{D.5}$$

$$A\omega \ll \frac{Y_1 K_{c,1}}{\tau_{\mathrm{I},1}\omega}, \tag{D.6}$$

and

$$\eta A\omega \ll \frac{K_{c,1}}{Y_2 \tau_{\mathrm{I},1}\omega}, (\tau_{\mathrm{I},1} \ll \tau_{\mathrm{I},3}), \tag{D.7}$$

are satisfied eqn. (D.4) can be approximated by

$$\begin{aligned}\left\|\frac{\Delta\tilde{L}_1(s)}{\Delta\tilde{L}_3(s)}\right\| &= \left\|\frac{\left(\eta As + K_3(s) + K_1(s)/Y_2\right)}{\left(As + Y_1K_1(s)\right)}\right\| \\ &\approx \left\|\frac{K_1(s)/Y_2}{Y_1K_1(s)}\right\| \\ &= \frac{1}{Y_1Y_2}\end{aligned} \quad . \tag{D.8}$$

Thus eqn. (D.5)-(D.7) are tuning rules for first RLC.

Controller design for seond RLC

Refering to Figure 3.6 closed-loop for second RLC is given by

$$\begin{aligned}As\Delta\tilde{L}_2(s) &= \Delta F_1(s) - \Delta F_2(s) \\ &= -K_1(s)\left(\Delta\tilde{L}_2(s) - Y_1\Delta\tilde{L}_1(s)\right) + K_2(s)\left(\Delta\tilde{L}_3(s) - Y_2\Delta\tilde{L}_2(s)\right) \\ &= -\left(K_1(s) + Y_2K_2(s)\right)\Delta\tilde{L}_2(s) + K_1(s)Y_1\Delta\tilde{L}_1(s) + K_2(s)\Delta\tilde{L}_3(s)\end{aligned} \quad . \tag{D.9}$$

Using eqn. (D.1) and (D.9) yields,

$$\frac{\Delta\tilde{L}_2(s)}{\Delta\tilde{L}_3(s)} = \frac{\dfrac{K_1(s)Y_1}{As + Y_1K_1(s)}\dfrac{\Delta F_{\mathrm{in}}(s)}{\Delta\tilde{L}_3(s)} + K_2(s)}{\left(As + K_1(s) + Y_2K_2(s) - \dfrac{Y_1K_1^2(s)}{As + Y_1K_1(s)}\right)} \tag{D.10}$$

With the assumption that $\Delta L_3' \approx \Delta L_3 (= \Delta\tilde{L}_3)$, using eqn. (3.20),

$$\frac{\Delta\tilde{L}_2(s)}{\Delta\tilde{L}_3(s)} \approx \frac{\left(\eta As + K_3(s)\right)K_1(s)Y_1 + \left(As + Y_1K_1(s)\right)K_2(s)}{\left(As + Y_1K_1(s)\right)\left(As + K_1(s) + Y_2K_2(s)\right) - Y_1K_1^2(s)}. \tag{D.11}$$

The amplitude ratio of $\Delta\tilde{L}_2$ to $\Delta\tilde{L}_3$ is given by

$$\left\|\frac{\Delta\tilde{L}_2(s)}{\Delta\tilde{L}_3(s)}\right\| \approx \frac{\left\|\left(K_{c,3} + K_{c,2}\right) + \left(\eta A\omega - \frac{K_{c,3}}{\tau_3\omega} - \frac{K_{c,2}}{\tau_{\mathrm{I},2}\omega}\right)j\right\|\left\|Y_1K_{C_1}(\omega j)\right\|}{\left\|\left(Y_1K_{c,1} + \left(A\omega - \frac{Y_1K_{c,1}}{\tau_{\mathrm{I},1}\omega}\right)j\right)\left(K_{c,1} + Y_2K_{c,2} + \left(A\omega - \frac{K_{c,1}}{\tau_{\mathrm{I},1}\omega} - \frac{Y_2K_{c,2}}{\tau_{\mathrm{I},2}\omega}\right)j\right) - Y_1K_1^2(\omega j)\right\|}. \tag{D.12}$$

If $A\omega \ll \frac{Y_1K_{c,1}}{\tau_{\mathrm{I},1}\omega}$ which is same as eqn. (D.6) and

$$K_{c,3} \ll K_{c,2}, \tag{D.13}$$

$$\eta A\omega \ll \frac{K_{c,2}}{\tau_{\mathrm{I},2}\omega}, (\tau_{\mathrm{I},2} \ll \tau_{\mathrm{I},3}), \tag{D.14}$$

$$A\omega - \frac{K_{c,1}}{\tau_{\mathrm{I},1}\omega} \ll \frac{Y_2K_{c,2}}{\tau_{\mathrm{I},2}\omega}, \tag{D.15}$$

are satisfied, the amplitude ratio of $\Delta\tilde{L}_2$ to $\Delta\tilde{L}_3$ is given by

$$\begin{aligned}\left\|\frac{\Delta\tilde{L}_2(s)}{\Delta\tilde{L}_3(s)}\right\| &\approx \frac{\left\|K_{c,1} + \frac{K_{c,1}}{\tau_{\mathrm{I},1}\omega j}\right\|\left\|Y_1K_1(\omega j)\right\|}{\left\|\left(Y_1K_{c,1} + \frac{Y_1K_{c,1}}{\tau_{\mathrm{I},1}\omega j}\right)\left(K_{c,1} + \frac{K_{c,1}}{\tau_{\mathrm{I},1}\omega j} + Y_2\left(K_{c,2} + \frac{K_{c,2}}{\tau_{\mathrm{I},2}\omega j}\right)\right) - Y_1K_1^2(\omega j)\right\|} \\ &= \frac{\left\|K_1(\omega j)\right\|\left\|Y_1K_1(\omega j)\right\|}{\left\|Y_1K_1(\omega j)\left(K_1(\omega j) + Y_2K_2(\omega j)\right) - Y_1K_1^2(\omega j)\right\|} \\ &= \frac{1}{Y_2}\end{aligned} \tag{D.16}$$

Thus eqn. (D.13)-(D.15) are tuning rules for second RLC.

Appendix E. mpMPC formulation for Taylor rules

Based on the optimization function in eqn. (4.11) and the method discussed in Muske and Rawlings (1993) with discount factor β, the terminal penalty weight matrix $\bar{\mathbf{Q}}$ is

$$\bar{\mathbf{Q}} = \sum_{i=0}^{\infty} \mathbf{A}^{T^i} \beta^i \mathbf{Q} \mathbf{A}^i . \tag{E.1}$$

Since the unstable mode is constrained to be zero at time $k+N$, it follows that

$$\bar{\mathbf{Q}} = \tilde{\mathbf{v}}_s \sum \tilde{\mathbf{v}}_s^T . \tag{E.2}$$

where

$$\Sigma = \frac{\mathbf{v}_s^T Q \mathbf{v}_s}{1-\beta J_s^2} . \tag{E.3}$$

From eqns. (E.2) and (E.3) it follows that

$$\bar{\mathbf{Q}} = \frac{\mathbf{v}_s^T \mathbf{Q} \mathbf{v}_s}{1-\beta J_s^2} \tilde{\mathbf{v}}_s \tilde{\mathbf{v}}_s^T . \tag{E.4}$$

Further, eqn. (4.14) along with eqn. (4.15) results in

$$u_{t+m-1|t} = \mathbf{a}_m^T \mathbf{x}_t + \mathbf{b}_m^T \mathbf{u}_m , \tag{E.5}$$

where

$$\mathbf{a}_m^T = \frac{-\tilde{\mathbf{v}}_{\mathrm{u}}^T \mathbf{A}^N}{\tilde{\mathbf{v}}_{\mathrm{u}}^T \left(\mathbf{A}^{N-m}\mathbf{B} + ... + \mathbf{AB} + \mathbf{B} \right)} , \quad \mathbf{b}_m^T = \frac{-\tilde{\mathbf{v}}_{\mathrm{u}}^T \left[\mathbf{A}^{m-2}\mathbf{B} ..., \mathbf{AB}, \mathbf{B} \right]}{\tilde{\mathbf{v}}_{\mathrm{u}}^T \left(\mathbf{A}^{N-m}\mathbf{B} + ... + \mathbf{AB} + \mathbf{B} \right)} \tag{E.6}$$

and the optimization variable $\mathbf{u}_m$ contains the first $m-1$ elements of $\mathbf{u}$.

Using eqns. (4.12) and (4.15) for the case when $k > m$ yields

$$\hat{\mathbf{x}}_{t+k|t} = \mathbf{A}^k x_t + \sum_{\ell=1}^{m-1} \mathbf{A}^{k-\ell} \mathbf{B} u_{t+\ell-1|t} + \left(\sum_{\ell=m}^{k} \mathbf{A}^{k-\ell} \mathbf{B} \right) u_{t+m-1|t} . \tag{E.7}$$

Using eqns. (E.5) and (E.7) yields

$$\hat{\mathbf{x}}_{t+k|t} = \mathbf{f}_{k,\ell}\mathbf{x}_t + \sum_{\ell=1}^{m-1} \mathbf{h}_{k,\ell} u_{t+\ell-1|t} \,, \tag{E.8}$$

where

$$\mathbf{h}_{k,\ell} = \begin{cases} \left(\mathbf{A}^{k-\ell} + b_\ell \left(\sum_{\ell=m}^{k} \mathbf{A}^{k-\ell} \right) \right) \mathbf{B} & k \geq m, \ell \leq k \\ \mathbf{A}^{k-\ell}\mathbf{B} & k < m, \ell \leq k \\ 0 & k < m, \ell > k \end{cases} , \tag{E.9}$$

$$\begin{aligned} \mathbf{f}_k &= \left[\mathbf{f}_{k,1} \ldots\ldots \mathbf{f}_{k,m-1} \right] \in \Re^{2\times(m-1)} \\ \mathbf{f}_{k,\ell} &= \begin{cases} \mathbf{A}^k + \sum_{\ell=m}^{k} \mathbf{A}^{k-l}\mathbf{B}\mathbf{a}^T & \text{for } k \geq m \\ \mathbf{A}^k & \text{for } k < m \end{cases} , \end{aligned} \tag{E.10}$$

$$\mathbf{h}_k = \left[\mathbf{h}_{k,1} \ldots\ldots \mathbf{h}_{k,m-1} \right] \in \Re^{(m-1)\times(m-1)} . \tag{E.11}$$

Substituting eqns (E.8)-(E.11) into eqn. (4.11) with $S = 0$ yields eqn. (4.22).

The solution to eqn. (4.22) is

$$\mathbf{u}_m = -\mathbf{H}^{-1}\mathbf{F}^T\mathbf{x}_t \,. \tag{E.12}$$

where

$$\mathbf{H} = \sum_{k=1}^{N-1} \mathbf{h}_k^T \beta^k \mathbf{Q} \mathbf{h}_k + \mathbf{h}_N^T \beta^N \bar{\mathbf{Q}} \mathbf{h}_N + R^2 \left(\frac{\beta^{m-1} - \beta^N}{1-\beta} \mathbf{b}\mathbf{b}^T + \mathbf{D}_R \right), \tag{E.13}$$

$$\mathbf{D}_R \mathrel{\hat{=}} \operatorname{diag}\begin{bmatrix} 1 & \beta & . & . & \beta^{m-2} \end{bmatrix}, \tag{E.14}$$

$$\mathbf{F} = \left(\sum_{k=1}^{N-1} \mathbf{f}_k^T \beta^k \mathbf{Q} \mathbf{h}_k \right) + \mathbf{f}_N^T \beta^N \bar{\mathbf{Q}} \mathbf{h}_N + R^2 \frac{\beta^{m-1} - \beta^N}{1-\beta} \mathbf{a}\mathbf{b}^T \,. \tag{E.15}$$

Appendix F. Closed-loop stability for Taylor rule

The standard Taylor rule can be written as

$$u_t = \mathbf{c}^T \mathbf{x}_t \,, \tag{F.1}$$

where $\mathbf{c}^T \triangleq \begin{bmatrix} \phi_y & \phi_\pi \end{bmatrix}$.

The characteristic equation for the matrix $\mathbf{A}_{\mathrm{CL}}$ in eqn. (4.28) is given by

$$f(\mu) \triangleq \mu^2 - \left(1 + \rho + \alpha\xi - \xi\phi_y - \alpha\xi\phi_\pi\right)\mu + \left(\rho - \xi\phi_y\right), \tag{F.2}$$

where μ is an eigenvalue of the matrix $\mathbf{A}_{\mathrm{CL}}$. For closed-loop stability the eigenvalues of the matrix $\mathbf{A}_{\mathrm{CL}}$ should lie inside the unit disk, which is guaranteed (by the Jury-Routh–Hurwitz stability criterion) if and only if

$$2 + 2\rho - 2\xi\phi_y + \alpha\xi(\phi_\pi - 1) > 0 \,, \tag{F.3}$$

$$1 - \rho + \xi\phi_y - \alpha\xi(\phi_\pi - 1) > 0 \,, \tag{F.4}$$

$$\alpha\xi(\phi_\pi - 1) > 0 \,. \tag{F.5}$$

Given that $\alpha\xi > 0$, eqn. (F.5) is satisfied if and only if $\phi_\pi > 1$.

Appendix G. mpMPC formulation for Taylor rules with inertia

Using the equality constraints in Appendix E, the ZLB constraint given in eqn. (4.16) can be written as,

$$\mathbf{G}\mathbf{u}_m \leq \mathbf{w} + \mathbf{E}\mathbf{x}_t\,, \tag{G.1}$$

where $\mathbf{G} \hat{=} \begin{bmatrix} -\mathbf{I} \\ -\mathbf{b}^T \end{bmatrix}$; $\mathbf{I}$ is the identity matrix in $\Re^{(m-1)\times(m-1)}$; $\mathbf{w} \hat{=} \begin{bmatrix} i^* & \cdots & i^* \end{bmatrix}^T \in \Re^m$;

$\mathbf{E} = \begin{bmatrix} \mathbf{\Theta} \\ \mathbf{a}^T \end{bmatrix}$; $\mathbf{\Theta} = \begin{bmatrix} 0 & \cdots & 0 \\ 0 & \cdots & 0 \end{bmatrix}^T \in \Re^{(m-1)\times 2}$. Therefore, the optimization problem eqn. (4.22) subject to the constraint eqn. (G.1) can be formulated as

$$\min_{\mathbf{z}} \frac{1}{2}\mathbf{z}^T\mathbf{H}\mathbf{z}\,, \tag{G.2}$$

$$\mathbf{G}\mathbf{z} \leq \mathbf{w} + \mathbf{D}\mathbf{x}_t\,, \tag{G.3}$$

where $\mathbf{z} \hat{=} \mathbf{u}_m + \mathbf{H}^{-1}\mathbf{F}^T\mathbf{x}_t$, $\mathbf{D} \hat{=} \mathbf{E} + \mathbf{G}\mathbf{H}^{-1}\mathbf{F}^T$.

Appendix H. mpMPC formulation for Taylor rules with inertia

Adopting the same approach as shown in Appendix E, a similar kind of expression for the optimization problem set-up in eqn. (4.11) can be derived when $S > 0$ as

$$\min_{\mathbf{u}_m}\left[\frac{1}{2}\mathbf{u}_m^T\tilde{\mathbf{H}}\mathbf{u}_m + \tilde{\mathbf{x}}_t^T\tilde{\mathbf{F}}\mathbf{u}_m + \frac{1}{2}\tilde{\mathbf{x}}_t^T\tilde{\mathbf{Y}}\tilde{\mathbf{x}}_t\right], \tag{H.1}$$

where,

$$\tilde{\mathbf{x}}_t \triangleq \begin{bmatrix}\Delta y_t \\ \Delta\pi_t \\ \Delta u_{t-1}\end{bmatrix}, \tag{H.2}$$

$$\begin{aligned}\tilde{\mathbf{H}}_{m-1\times m-1} = &\sum_{k=1}^{N-1}\mathbf{h}_k^T\beta^k\mathbf{Q}\mathbf{h}_k + \mathbf{h}_N^T\beta^N\bar{\mathbf{Q}}\mathbf{h}_N + \\ &S^2\left(\beta^{m-1}\left(\mathbf{b}-\mathbf{b}_0\right)\left(\mathbf{b}-\mathbf{b}_0\right)^T + \beta^{N-1}\mathbf{b}\mathbf{b}^T + \mathbf{S}_0\right)\end{aligned}, \tag{H.3}$$

where $\mathbf{b}_0 = \begin{bmatrix}0 & \cdots & 0 & 1\end{bmatrix}^T \in \Re^{m-1}$, $\mathbf{S}_0 \in \Re^{(m-1)\times(m-1)}$ is given by,

$$\mathbf{S}_0 \triangleq \left[s_{i,j}\right]\begin{cases} s_{i,j} = \beta^{i-1}\left(1+\beta\right), i = j, i \neq m-1 \\ s_{i,j} = \beta^{m-2}, i = j, i = m-1 \\ s_{i,j} = -\beta, \left|i-j\right| = 1 \\ s_{i,j} = 0, \left|i-j\right| > 1 \end{cases}, \tag{H.4}$$

and

$$\tilde{\mathbf{F}}_{3\times m-1} = \begin{bmatrix}\left(\sum_{k=1}^{N-1}\mathbf{f}_k^T\mathbf{Q}\mathbf{h}_k\right) + \mathbf{f}_N^T\bar{\mathbf{Q}}\mathbf{h}_N + S^2\left[\beta^{m-1}\mathbf{a}\left(\left(\mathbf{b}-\mathbf{b}_0\right)^T + \beta^{N-1}\mathbf{b}^T\right)\right] \\ -S^2, \underbrace{0.......0}_{m-2}\end{bmatrix}. \tag{H.5}$$

When there is no inequality constraint, the solution to eqn. (H.1) is given by

$$\mathbf{u}_m = -\tilde{\mathbf{H}}^{-1}\tilde{\mathbf{F}}^T\tilde{\mathbf{x}}_t\,. \tag{H.6}$$

ZLB constraint given by eqn. (4.16) is equivalent to,

$$\mathbf{G}\mathbf{u}_m \le \mathbf{w} + \tilde{\mathbf{E}}\tilde{\mathbf{x}}_t \,, \tag{H.7}$$

where $\tilde{\mathbf{E}} = \begin{bmatrix} \mathbf{E} & \mathbf{E}_0 \end{bmatrix}$ and $\mathbf{E}_0 = \begin{bmatrix} 0 & \cdots & 0 \end{bmatrix}^T \in \Re^m$. Eqns. (H.1) and (H.7) can be formulated as,

$$\min_{\tilde{\mathbf{z}}} \frac{1}{2} \tilde{\mathbf{z}}^T \tilde{\mathbf{H}} \tilde{\mathbf{z}} \,, \tag{H.8}$$

$$\mathbf{G}\tilde{\mathbf{z}} \le \mathbf{w} + \tilde{\mathbf{D}}\tilde{\mathbf{x}}_t \,, \tag{H.9}$$

where $\tilde{\mathbf{z}} \mathrel{\hat{=}} \mathbf{u}_m + \tilde{\mathbf{H}}^{-1}\tilde{\mathbf{F}}^T\tilde{\mathbf{x}}_t$, $\tilde{\mathbf{D}} \mathrel{\hat{=}} \tilde{\mathbf{E}} + \mathbf{G}\tilde{\mathbf{H}}^{-1}\tilde{\mathbf{F}}^T$. Eqn. (H.8) and inequality constraints eqn. (H.9) are used for mpMPC formulation to derive explicit inertia-based Taylor rules with ZLB constraints.

Appendix I. Closed-loop stability for inertial Taylor-like rule

The interest rate rule is

$$u_t = \phi_i u_{t-1} + \mathbf{c}^T \mathbf{x}_t \,, \tag{I.1}$$

The characteristic equation for the matrix $\tilde{\mathbf{A}}_{CL}$ is given by

$$\begin{aligned}\tilde{f}(\mu) \triangleq{}& \mu^3 - \left(1+\rho-\xi\phi_y+\phi_i\right)\mu^2 \\ &+\left(\rho-\xi\phi_y+\left(1+\rho\right)\phi_i-\alpha\xi\left(1-\phi_\pi\right)\right)\mu-\left(\rho-\alpha\xi\right)\phi_i\end{aligned}\,. \tag{I.2}$$

Closed-loop stability is guaranteed (by the Jury-Routh–Hurwitz stability criterion) if and only if

$$2+2\phi_i+2\rho(1+\phi_i)-2\xi\phi_y-\alpha\xi(1+\phi_i-\phi_\pi)>0\,, \tag{I.3}$$

$$4-4\rho\phi_i+\alpha\xi(1+3\phi_i-\phi_\pi)>0\,, \tag{I.4}$$

$$2-2\phi_i+2\rho(-1+\phi_i)+2\xi\phi_y+\alpha\xi(1-3\phi_i-\phi_\pi)>0\,, \tag{I.5}$$

$$\alpha\xi(\phi_\pi+\phi_i-1)>0\,, \tag{I.6}$$

$$\begin{aligned}&-8\left(\left(\alpha\xi\phi_i\right)^2+\left(\rho\phi_i-1\right)\left(1-\rho+\rho\phi_i\right)-\phi_i+\xi\phi_y\right) \\ &+\alpha\xi\left(\left(1-2\rho\right)\phi_i^2+\phi_i\left(1+\rho-\xi\phi_y\right)+\phi_\pi-1\right)>0\end{aligned}\,, \tag{I.7}$$

Appendix J. Infeasibility polytope

The model decomposition of $\mathbf{A}$ is represented by,

$$\mathbf{A} = \mathbf{V}\mathbf{J}\mathbf{V}^{-1} = \left[\begin{array}{c:c} \mathbf{v}_{\mathrm{u}} & \mathbf{v}_{\mathrm{s}} \end{array}\right] \begin{bmatrix} J_{\mathrm{u}} & 0 \\ 0 & J_{\mathrm{s}} \end{bmatrix} \begin{bmatrix} \tilde{\mathbf{v}}_{\mathrm{u}}^T \\ \hdashline \tilde{\mathbf{v}}_{\mathrm{s}}^T \end{bmatrix} \tag{J.1}$$

where

$$J_u = \frac{1+\rho+\sqrt{(1-\rho)^2+4\alpha\xi}}{2} > 1 \tag{J.2}$$

$$J_{\mathrm{s}} = \frac{1+\rho-\sqrt{(1-\rho)^2+4\alpha\xi}}{2} < 1 \tag{J.3}$$

Eqns. (J.1) and (4.8) imply

$$\mathbf{V}^{-1}\hat{\mathbf{x}}_{t+k|t} = \sum_{\ell=0}^{k-1} \mathbf{J}^{\ell}\mathbf{V}^{-1}\mathbf{B}u_{t+k-\ell-1|t} + \mathbf{J}^{k}\mathbf{V}^{-1}\mathbf{x}_t \tag{J.4}$$

From eqn. (J.4) stable and unstable modes can be treated separately. In terms of the unstable mode

$$\tilde{\mathbf{v}}_{\mathrm{u}}^T\hat{\mathbf{x}}_{t+k|t} = \sum_{\ell=0}^{k-1} J_u^{\ell}\, \tilde{\mathbf{v}}_{\mathrm{u}}^T\mathbf{B}u_{t+k-\ell-1|t} + J_u^{k}\, \tilde{\mathbf{v}}_{\mathrm{u}}^T\mathbf{x}_t \tag{J.5}$$

If $\mathbf{x}_t$ lies in the polytope of attraction, then

$$\lim_{k\to\infty} \tilde{\mathbf{v}}_{\mathrm{u}}^T\hat{\mathbf{x}}_{t+k|t} = 0 \tag{J.6}$$

and

$$\tilde{\mathbf{v}}_{\mathrm{u}}^T\mathbf{x}_t = -J_u^{-k}\sum_{\ell=0}^{k-1} J_u^{\ell}\, \tilde{\mathbf{v}}_{\mathrm{u}}^T\mathbf{B}u_{t+k-\ell-1|t} \tag{J.7}$$

since $-u_{t+k-\ell-1|t} \le i*$.

The polytope of attraction is given by

$$\tilde{\mathbf{v}}_{\mathrm{u}}^{T}\mathbf{x}_{t} \leq \lim_{k\to\infty}\left(\sum_{\ell=0}^{\ell=k-1} J_{u}^{\ell-k}\right)\tilde{\mathbf{v}}_{\mathrm{u}}^{T}\mathbf{B}i^{*} \Rightarrow \tilde{\mathbf{v}}_{\mathrm{u}}^{T}\mathbf{x}_{t} \leq \frac{\tilde{\mathbf{v}}_{\mathrm{u}}^{T}\mathbf{B}}{J_{u}-1}i^{*}. \tag{J.8}$$

Hence the infeasibility polytope is characterized by,

$$\tilde{\mathbf{v}}_{\mathrm{u}}^{T}\mathbf{x}_{t} > \frac{\tilde{\mathbf{v}}_{\mathrm{u}}^{T}\mathbf{B}}{J_{u}-1}i^{*}. \tag{J.9}$$

Similarly, in the case of inertial policy the above exercise can be repeated and the counterpart of eqn. (J.8) can be derived.